MASARYK UNIVERSITY
Faculty of Science
Department of Mathematics and Statistics

Statistical inference for stochastic point processes with application on neuronal data

Ph.D. Dissertation

Kamil Rajdl

Supervisor: doc. RNDr. Petr Lánský, DrSc. Brno 2017

Bibliographic entry

Author:	Mgr. Bc. Kamil Rajdl Faculty of Science, Masaryk University Department of Mathematics and Statistics
Title of Dissertation:	Statistical inference for stochastic point processes with application on neuronal data
Degree Programme:	Mathematics
Field of Study:	Probability, statistics and mathematical modeling
Supervisor:	doc. RNDr. Petr Lánský, DrSc. Faculty of Science, Masaryk University Department of Mathematics and Statistics
Academic Year:	2016/2017
Number of Pages:	106
Keywords:	Stochastic processes, point processes, neural models, analysis of neural data, variability measures of point processes, neural coding, Fano factor, Stein's model, Shannon entropy

Bibliografický záznam

Autor:	Mgr. Bc. Kamil Rajdl Přírodovědecká fakulta, Masarykova univerzita Ústav matematiky a statistiky
Název práce:	Statistická analýza bodových procesů a aplikace na jednotkovou aktivitu neuronu
Studijní program:	Matematika
Studijní obor:	Pravděpodobnost, statistika a matematické modelování
Školitel:	doc. RNDr. Petr Lánský, DrSc. Přírodovědecká fakulta, Masarykova univerzita Ústav matematiky a statistiky
Akademický rok:	2016/2017
Počet stran:	106
Klíčová slova:	Stochastické procesy, bodové procesy, modely neuronu, analýza neuronových dat, míry variability bodových procesů, neuronové kódování, Fano factor, Steinův model, Shannonova entropie

Abstract

This thesis consists of two main parts. In the first part, we briefly present the mathematical theory and tools used in the text and an introduction to neural modeling. The second part consists of four papers devoted to study of variability and randomness in neural models. One of the most often used measures of variability of neural spike trains, Fano factor, is studied and two new measures are created. Some new properties of Fano factor are derived and an optimization procedure of its estimator with respect to the length of the observation window is proposed. The new measures focus on generalization of Fano factor and on application of Shannon entropy as a measure of randomness. The influence of the variability of neural input on its output is also explored. For this purpose, the Stein's neural model is generalized assuming pooled renewal input.

Abstrakt

Tato dizertační práce se skládá ze dvou hlavních částí. V první části stručně uvádíme v textu dále používané matematické prostředky a úvod do neuronového modelování. Druhá část se pak skládá se čtyř odborných článků věnujících se především studiu variability a náhodnosti v neuronových modelech. Je zde studována jedna z nejčastěji používaných měr variability posloupností neuronových impulsů, Fano factor, a vytvořeny dvě míry nové. Pro Fano factor jsou odvozeny nové vlastnosti a navržena metoda optimalizace jeho odhadu vzhledem k délce pozorovacího okna. Nové míry se zaměřují na zobecnění Fano factoru a využití Shannonovy entropie jako míry náhodnosti. Zkoumán je také vliv variability vstupu neuronu na jeho výstup. K tomuto účelu je zobecněn Steinův model tak, že je jeho vstup popsán pomocí součtu procesů obnovy.

Acknowledgements

I would like to express my sincere gratitude to my supervisor doc., RNDr. Petr Lánský, DrSc. for his helpful advices, patience and all the support and encouragement I received during my doctoral studies.

Brno, March 2017

Contents

Introduction

The mathematical and statistical aim of this theses is analysis of stochastic point processes. These processes describe sequences of times, which mostly represent occurrence of certain identical events. The range of applications of point processes is thus very wide, there are many fields where such data emerges (e.g. description of accidents, natural disasters, creation of particles in chemical reactions, passage of vehicles, transmission of some messages in human communication, etc. [2, 39, 45, 77]). Nevertheless, in this theses, we focus mainly on their utilization to study data arising in neuroscience, where the role of point processes is prominent.

One of the most important questions in neuroscience is how is information transferred and processed in the nervous system. It is widely accepted that information is transferred using the sequences of impulses (spike trains) which are transmitted among neurons. As the spikes are very similar from the point of view of size shape and duration, information has to be coded only using the times of their occurrence and the spike trains can be suitably modeled as point processes. Nevertheless, the specific details of the mechanism, mainly the method of coding, is still not completely clear [24, 30, 64]. The most basic concept of coding is rate coding, it assumes that information is coded by the spike rate (defined for example as the number of spikes fired in a time unit) [24, 35]. It is very likely that the rate contains a lot of the transferred information, however, probably not all of it. That comes from the fact that even with a fixed rate spike trains can be very various. Codes which reflect also some rate-independent behavior, given by specific positions of the spikes, are called temporal codes. It is hardly possible that information is coded by the exact positions of all the individual spikes, but the response of a neuron can be surely influenced by some rate-independent characteristics.

Probably the most simple concept of temporal coding is variability coding [54, 56]. It unites all the rate-independent behavior into one term – variability, described by a variability measure. Variability measures and their estimation from experimental data create an important part of analysis of neural spike trains. Even if the variability does not directly transfer information,

its characterization is important for spike trains classification, to distinguish various neurons or firing regimes. To measure the variability, various quantities have been proposed and used [27, 34, 49, 50, 51, 58, 68, 71], nevertheless, there is not a universal measure suitable in all possible situations. Often, there might not be even any suitable, as their estimation is problematic, mainly with limited data [17, 54]. Another important area concerning neural variability is its influence on behavior of neurons, as to transfer information using variability neurons have to be able to register and reflect it.

In this thesis we focus on the mentioned issues – variability measures of points processes (with focus on neural spike trains), their estimation and study of variability processing in neurons. The aim is to create results which can help in analysis of variability of neural spike trains and improve understanding of influence of variability in the nervous system. Our results are presented in four papers which create the main part of this thesis. A more detailed overview of these papers and contained results can be found in Chapter 3. We present also an introduction to theory of point processes, necessary mathematical concepts and methods (Chapter 1) and introduction to neural models (Chapter 2).

Mathematical notations

Ω	sample space
$\mathcal{A}$	event space
P	probability function
$\mathbb{N}, \mathbb{Z}, \mathbb{R}$	natural numbers, integers, real numbers
$Y(t)$	random process
$N(t)$	counting process
X_i	time of the i-th event
T_i	length of the i-th inter-event interval
$\mathrm{E}(X)$	mean of random variable X
$\mathrm{Var}(X)$	variance of random variable X
$\lambda(t)$	intensity of a counting process
$\mathrm{d}h(t)/\mathrm{d}t$	derivative of $h(t)$ with respect to t
$f(t)$	probability density of inter-event intervals
$f_k(t)$	probability density of time up to the k-th event
$F(t)$	cumulative distribution function of inter-event intervals
$N_e(t)$, $N_o(t)$	equilibrium and ordinary counting renewal process
$\lambda_e(t)$, $\lambda_o(t)$	intensity of equilibrium and ordinary renewal process
$\mathcal{L}\{g\}, \tilde{g}(s)$	Laplace transform of a function g
CV	coefficient of variation
$\mathrm{FF}(t)$	Fano factor
$\Gamma(x)$	gamma function
$S(t)$	shot noise process
$w(x)$	shot noise response function
$WN(t)$	white noise with unit variance
$W(t)$	standard Wiener process
$\lfloor x \rfloor$	floor function
$\lceil x \rceil$	ceiling function

List of publications

Main publications

I. K. Rajdl and P. Lansky. Fano Factor Estimation. *Math. Biosci. Eng.*, 11(1):105–123, 2014.

II. K. Rajdl and P. Lansky. Stein's neuronal model with pooled renewal input. *Biol. Cybern.*, 109(3):389–399, 2015.

III. K. Rajdl and P. Lansky. Shot-noise Fano factor. *Phys. Rev. E*, 92(5):052135, 2015.

IV. K. Rajdl, P. Lansky and L. Kostal. Entropy factor for randomness quantification in neuronal data. *Neural Networks*, under revision.

Other publications

V. J. Hon, T. Martinek, K. Rajdl and M. Lexa. Triplex: an R/Bioconductor package for identification and visualization of potential intramolecular triplex patterns in DNA sequences. *Bioinformatics*, 29(15):1900–1, 2013.

VI. K. Rajdl, A. Farda, P. Stepanek and P. Zahradnicek. Testing a statistical forecasting model of electric energy consumption for two regions in the Czech Republic. In O. Urban, M. Sprtova and K. Klem. Global Change: A Complex Challenge, Conference Proceedings, Brno: Global Change Research Centre, 2015, 178–181.

VII. M. Trnka, J. E. Olesen, K. C. Kersebaum, R. P. Rotter, R. Brazdil, J. Eitzinger, S. Jansen, A. O. Skjelvag, P. Peltonen-Sainio, P. Hlavinka, J. Balek, H. Eckersten, A. Gobin, V. Vuceti, A. Dalla Marta, S. Orlandini, V. Alexandrov, D. Semeradova, P. Stepanek, E. Svobodova and K. Rajdl. Changing regional weather-crop yield relationships across Europe between 1901 and 2012. *Climate Res.*, 70(2–3):179–193, 2016.

VIII. P. Stepanek, P. Zahradnicek, A. Farda, P. Skalak, M. Trnka, J. Meitner and K. Rajdl. Projection of drought-inducing climate conditions in the Czech Republic according to Euro-CORDEX models. *Climate Res.*, 70(2–3):195–214, 2016.

Chapter 1

Mathematical background

The mathematical framework used in this thesis for description and analysis of neural models is presented in this chapter. We focus mainly on stochastic processes, which form the basis of neuronal modeling. The theory of stochastic processes can be found in more detail for example in [11, 12, 13, 31, 53, 59, 82]. Not all the mathematical and statistical background is described, mainly the fundamentals of the probability theory and related terms and methods are assumed to be known, e.g. the definition and meaning of a random variable, probability density function, statistical moments of a random variable, probability space, convolution, Laplace transform and its inversion, etc. A description of these terms can be found in standard mathematical textbooks.

1.1 Introduction to stochastic processes

Definition 1.1. Let $(\Omega, \mathcal{A}, P)$ be a probability space, $I \subseteq \mathbb{R}$. A set of random variables $\{Y(t),\, t \in I\}$ defined on $(\Omega, \mathcal{A}, P)$ is called a random process.

Remark 1. Two main variants of random processes can be distinguished according to the character of the set I – random process with discrete time ($I \subseteq \mathbb{Z}$) and random process with continuous time ($I = [a, b]$, $-\infty \leq a < b \leq \infty$). If it is not necessary to specify the set I, we denote the random process only as $Y(t)$. A random process can be seen as a function of two variables $t \in I$ and $\omega \in \Omega$. For a fixed ω, $Y(t)$ is a real-valued function of t called a trajectory.

Definition 1.2. Let us have identical events occurring at random times $X_k \geq 0$, $k \in \mathbb{N}$, which create a strictly increasing sequence. Next, let $N(t)$

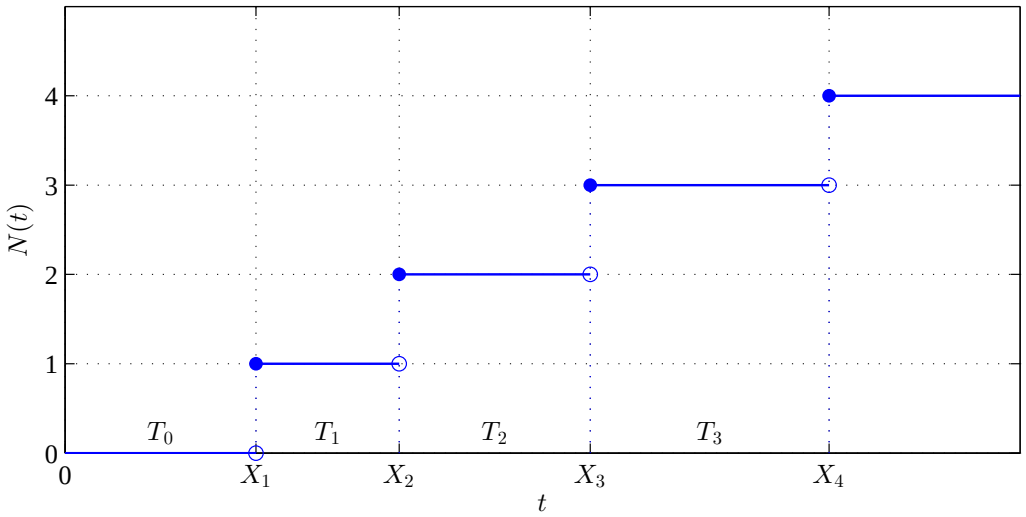

Fig. 1.1: The trajectory of a counting process with events occurred at times X_1, X_2, X_3 and X_4.

be the number of events occurred in $(0, t]$. Then $\{N(t), t \geq 0\}$ is a random process with continuous time called a counting process.

Remark 2. It is not necessary to define the values X_k, $k \in \mathbb{N}$, as times of certain events, but it is the most natural possibility.

Remark 3. The trajectory of a counting process is a piecewise constant function with unit jumps at times of the single events. For an illustration of such a trajectory see Fig. 1.1.

Remark 4. The full description of a counting process is given by both the sequence of times X_k or the sequence of (inter-event) intervals $T_k = X_{k+1} - X_k$, $k = 0, 1, \ldots$, $X_0 = 0$. These two approaches are connected by relationships

$$N(t) < k \iff X_k > t, \quad k = 1, 2, \ldots, \tag{1.1}$$

and

$$X_k = T_0 + T_1 + \ldots + T_{k-1}, \quad k = 1, 2, \ldots \tag{1.2}$$

Remark 5. The counting process is also called a point process, mainly if it is understood as the sequence of times X_k, $k = 1, 2, \ldots$, instead of as the process $N(t)$.

Definition 1.3. Let $N(t)$ be a counting process, function $\lambda : \mathbb{R} \to \mathbb{R}$ defined as

$$\lambda(t) = \frac{\mathrm{dE}(N(t))}{\mathrm{d}t}, \ t \geq 0, \tag{1.3}$$

is called an intensity of $N(t)$.

Remark 6. The probability of occurrence of an event in an interval $[t, t+\Delta t)$ is approximately $\lambda(t)\Delta t$, for a small $\Delta t > 0$. Function (1.3) thus represents the intensity of the process even in the intuitive sense of the word – the larger the intensity is at a time t, the more probable is the occurrence of an event near t.

Definition 1.4. Let $X(t)$, $t \geq 0$, $X(0) = x_0$, be a random process and $\theta > x_0$. Random variable

$$T_\theta = \inf\{t, X(t) \geq \theta\}, \tag{1.4}$$

is then called a first passage time (of threshold θ).

Remark 7. The first passage time (FPT) represents the time when a random process $X(t)$ reaches a threshold θ for the first time. It has an important significance in neural modeling.

1.2 Renewal processes

Definition 1.5. Let $N(t)$ be a counting process, $X_k \geq 0$, $k \in \mathbb{N}$, the times of the single events and $X_0 = 0$. If the random variables $T_k = X_{k+1} - X_k$, $k = 0, 1, 2, \ldots$, are independent and identically distributed (i.i.d.), $N(t)$ is called a renewal process.

A renewal process is a model of occurrence of discrete events which assumes that the time of the occurrence of every event depends only on the time that passed since the last event, not on the previous run of the process. The time intervals between the successive events have equal probability distribution, they correspond to the same random variable. We denote this random variable as T, its cumulative distribution function as $F(t)$ and probability density as $f(t)$.

According to Definition 1.5 the random variable T describes also the length of the interval from time zero (e.g. start of the observation) to the first event. It can be assumed if the time zero corresponds also to an event (not counted by the process $N(t)$). Nevertheless, sometimes it is not suitable to use this assumption. Often, in an experiment, the start of the observation of some events is unrelated to the sequence of the events – it can be seen as "fully random". A renewal process with this property is called an equilibrium renewal process. The time up to the first event has in this case generally a different probability distribution from T. Let us denote the corresponding

random variable as T_0, the cumulative distribution function as $F_0(t)$ and the probability density as $f_0(t)$. It holds [11]

$$f_0(t) = \frac{1 - F(t)}{\mathrm{E}(T)}. \tag{1.5}$$

Remark 8. To distinguish between various types of renewal processes, the process from Definition 1.5 is usually called an ordinary renewal process. Except from the ordinary and equilibrium renewal processes, modified renewal process is also defined. It is a renewal process where the probability distribution of the time up to the first event, $F_0(t)$, is defined arbitrarily, according to the modeled situation. Notation $N_o(t)$ and $\lambda_o(t)$ is used for the counting process and the intensity corresponding to an ordinary renewal process and analogously notation $N_e(t)$ and $\lambda_e(t)$ is used for an equilibrium renewal process.

Remark 9. It is possible to derive relationship (1.5) based on an ordinary renewal process whose true origin is located in "infinite distance" before the time zero. This way the necessary independence of the sequence of events and the time zero is achieved [29].

One of the most important goals in study of renewal processes is to reveal the relationship of T and $N(t)$ and their properties. A common situation is such that the process is defined by a probability distribution of T and the distribution of $N(t)$, thus the functions

$$p_n(t) = P(N(t) = n),\ t \geq 0,\ n = 0, 1, \ldots,$$

are of interest. Despite the relative simplicity of renewal processes, the distribution of $N(t)$ is mostly impossible to express analytically in a closed form, numerical calculations have to be often used to obtain some specific values.

The first step from T to $N(t)$ is derivation of the probability distribution of X_k, the time of occurrence of the k-th event. Let us denote its probability density by $f_k(t)$ and cumulative distribution function by $F_k(t)$. As X_k is a sum of independent random variables, $f_k(t)$ can be expresses as gradual convolution of the single densities ($f_0(t)$ and $(k-1)$ times $f(t)$). Working directly with the convolution is difficult, however, the corresponding relationships can be more suitably expressed using the Laplace transform, which is for a continuous function $g : [0, \infty) \to \mathbb{R}$ given by equation

$$\mathcal{L}\{g\}(s) = \int_0^\infty e^{-st} g(t) \mathrm{d}t. \tag{1.6}$$

Sometimes we use notation $\tilde{g}(s)$ instead of $\mathcal{L}\{g\}(s)$. The Laplace transform of $f_k(t)$ is then [29]

$$\tilde{f}_k(s) = \tilde{f}_0(s)(\tilde{f}(s))^{k-1} \tag{1.7}$$

for an equilibrium renewal process and

$$\tilde{f}_k(s) = (\tilde{f}(s))^k \tag{1.8}$$

for an ordinary renewal process. The function $f_k(t)$ can be thus calculated by the inverse Laplace transform, $\mathcal{L}^{-1}$, of relationships (1.7) and (1.8). Nevertheless, for most of the standard probability distributions of T, it cannot be transformed into a closed form and have to be calculated numerically.

The connection between X_k and $N(t)$ follows from obvious relationships

$$P(N(t) \geq k) = P(X_k \leq t) = F_k(t),\ t \geq 0,\ k = 1, 2, \ldots \tag{1.9}$$

and

$$\begin{aligned} P(N(t) = k) &= P(N(t) \geq k) - P(N(t) \geq k+1) \\ &= F_k(t) - F_{k+1}(t),\ t \geq 0,\ k = 1, 2, \ldots \end{aligned} \tag{1.10}$$

Considering moreover equations (1.7) and (1.8), a link from T to $N(t)$ arises. These relationships can be further transformed into some specific more tractable formulas for properties of $N(t)$ based on $f(t)$, e.g. [29]

$$P(N_e(t) = 0) = \mathcal{L}^{-1}\left\{\frac{1}{s} - \frac{1 - \tilde{f}(s)}{\mathrm{E}(T)s^2}\right\}(t), \tag{1.11}$$

$$P(N_e(t) = n) = \mathcal{L}^{-1}\left\{\frac{(1 - \tilde{f}(s))^2(\tilde{f}(s))^{n-1}}{s^2\mathrm{E}(T)}\right\}(t),\ n \in \mathbb{N}, \tag{1.12}$$

$$P(N_o(t) = 0) = \mathcal{L}^{-1}\left\{\frac{1 - \tilde{f}(s)}{s}\right\}(t), \tag{1.13}$$

$$P(N_o(t) = n) = \mathcal{L}^{-1}\left\{\frac{(1 - \tilde{f}(s))(\tilde{f}(s))^n}{s}\right\}(t),\ n \in \mathbb{N}, \tag{1.14}$$

$$\mathrm{E}(N_e(t)) = \frac{t}{\mathrm{E}(T)}, \tag{1.15}$$

$$\mathcal{L}\{\mathrm{E}(N_o)\}(s) = \frac{\tilde{f}(s)}{s(1 - \tilde{f}(s))}, \tag{1.16}$$

$$\lambda_e(t) = \frac{1}{\mathrm{E}(T)}, \tag{1.17}$$

$$\mathcal{L}\{\lambda_o\}(s) = \frac{\tilde{f}(s)}{1 - \tilde{f}(s)}, \tag{1.18}$$

$$\lim_{t\to\infty} \lambda_o(t) = \lambda_e(t) = \frac{1}{\mathrm{E}(T)}. \tag{1.19}$$

Even with a known probability density function of T, these formulas have to be mostly solved numerically, especially the Laplace transform of $f(t)$ and the potential inverse Laplace transforms. For some probability distributions of T, e.g. gamma or inverse Gaussian, the Laplace transforms of $f(t)$ exist in closed forms, simplifying the calculations. There is also one important distribution of T, exponential, for which the formulas transform to closed forms. The mentioned distributions are described in more detail later.

Except for formulas of the previous type, some asymptotic approximations of properties of $N(t)$ are useful, e.g. [11]

$$\mathrm{Var}(N_e(t)) \approx \frac{\mathrm{Var}(T)}{\mathrm{E}^3(T)}t + \frac{1}{2}\left(1 + \frac{\mathrm{Var}(T)}{\mathrm{E}^2(T)}\right)^2 - \frac{1}{3}\frac{\mathrm{E}(T^3)}{\mathrm{E}^3(T)}, \quad \text{for } t \to \infty. \tag{1.20}$$

From equation (1.15) we can see that for an equilibrium renewal process the mean number of events occurred in an interval of a length t is directionally proportional to t. The proportionality constant is

$$\lambda = \frac{1}{\mathrm{E}(T)}. \tag{1.21}$$

This value is also directly the intensity of an equilibrium renewal process at an arbitrary time $t > 0$. The intensity is a basic characteristic of a renewal process. Other important characteristics of renewal processes are characteristics describing their variability. Two of the most often used are coefficient of variation,

$$\mathrm{CV} = \frac{\sqrt{\mathrm{Var}(T)}}{\mathrm{E}(T)}, \tag{1.22}$$

and Fano factor,

$$\mathrm{FF}(t) = \frac{\mathrm{Var}(N(t))}{\mathrm{E}(N(t))}, \quad t > 0. \tag{1.23}$$

Coefficient of variation represents the variability of the lengths of inter-event intervals, on the other hand, Fano factor describes the variability of numbers of events in time window of a certain length. Thus, while CV is a constant for a given process, Fano factor is a function of t. Because of this fact, the value

$$\mathrm{FF} = \lim_{t\to\infty} \mathrm{FF}(t) \tag{1.24}$$

is often used as a simpler variability characteristic based on numbers of events. It is sometimes directly denoted as Fano factor, instead of function (1.23). The values CV and FF are connected by relationship [11]

$$\mathrm{FF} = \mathrm{CV}^2, \tag{1.25}$$

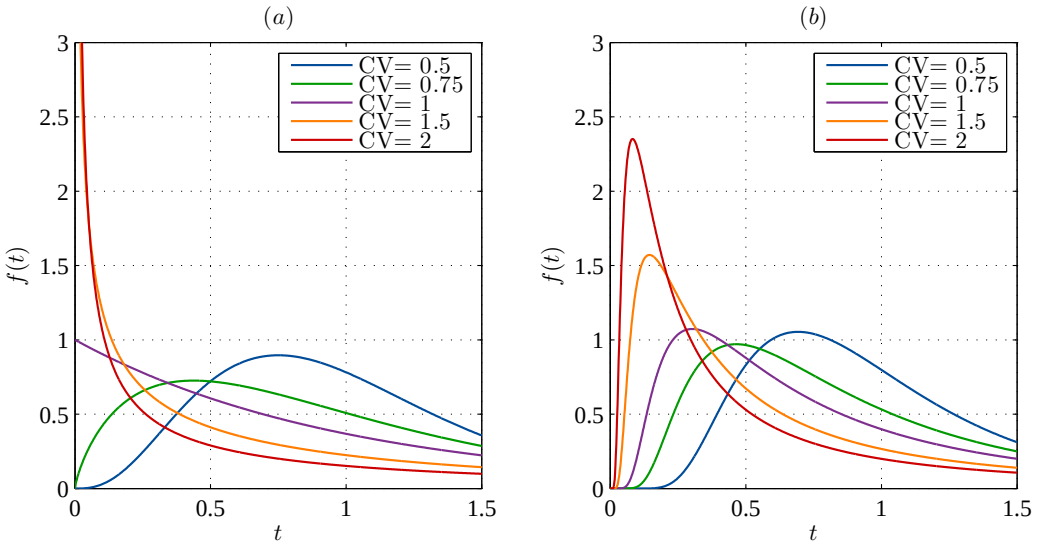

Fig. 1.2: The probability density of gamma (a) and inverse Gaussian (b) distributions with $\mathrm{E}(T) = 1$ and for various values of CV. The gamma density for $\mathrm{CV} = 1$ is also the probability density of exponential distribution.

which holds for any renewal process (however, it does not hold for a general counting process).

Next we describe some examples of renewal processes (distributions of T) which are useful to model some real phenomena. We focus mainly on distributions often used in neuroscience to describe sequences of neural spikes.

1.2.1 Poisson process

Poisson process is probably the most important and most often used point process. It is a renewal process with exponential distribution of T. Its density is

$$f(t) = \lambda e^{-\lambda t}, \quad t \geq 0,\ \lambda > 0, \tag{1.26}$$

where parameter λ corresponds directly to relationship (1.21). Probability density (1.26) is illustrated in Fig. 1.2(a) (line for $\mathrm{CV} = 1$).

A specific property of the Poisson process is memorylessness. The future course of the process is independent even from the time that passed since the last event (not only from the course of the process up to the previous event), thus it is independent from the complete history of the process. It yields the fact that the ordinary and equilibrium variants of this process are equal, e.g.

$$\lambda_o(t) = \lambda_e(t) = \frac{1}{\mathrm{E}(T)}. \tag{1.27}$$

Poisson process is the only renewal process fulfilling this relationship. As mentioned earlier the corresponding distribution of $N(t)$ can be expressed in a closed form, it is the well know Poisson distribution,

$$P(N(t) = n) = \frac{(\lambda t)^n e^{-\lambda t}}{n!},\ t \geq 0,\ n = 0, 1, \ldots \tag{1.28}$$

The importance of Poisson process comes also from the fact that it emerges as a limit in some asymptotic theorems, stating convergence of sum (superposition) of some "'sparse"' processes (events). It makes Poisson process important among point processes similarly as normal distribution is important among random variables. An important example of such a theorem is presented in Section 1.3.

It can be easily obtained that $\mathrm{CV} = 1$ and $\mathrm{FF}(t) = 1$, $t > 0$, the variability of this process is thus independent from λ, from the point of view of both of the characteristics. Next, using some direct calculations, it is possible to express the density of the time up to the k-th event explicitly,

$$f_k(t, \lambda) = \frac{\lambda^k t^{k-1} e^{-\lambda t}}{(k-1)!}, \quad t \geq 0,\ \lambda > 0,\ k \in \mathbb{N}. \tag{1.29}$$

This probability distribution is called an Erlang distribution. Let us note that parameter λ does not equal to the reciprocal value of the mean of this distribution.

1.2.2 Gamma process

A gamma process is a renewal process where T has a gamma probability distribution. Its density,

$$f(t; \alpha, k) = \frac{\alpha^k t^{k-1} e^{-\alpha t}}{\Gamma(k)}, \quad t \geq 0,\ \alpha > 0,\ k > 0, \tag{1.30}$$

is illustrated in Fig. 1.2:(a). Gamma distribution is a generalization of Erlang distribution (1.29) for non-integer k ($k > 0$). It can be also understood as a generalization of Poisson distribution, since density (1.30) with $k = 1$ is density of an exponential distribution. It holds

$$\lambda = \frac{\alpha}{k},\ \mathrm{CV}^2 = \mathrm{FF} = \frac{1}{k}, \tag{1.31}$$

however, $\mathrm{FF}(t)$ cannot be expressed in a closed form.

1.2.3 Inverse Gaussian process

An inverse Gaussian (IG) process is a renewal process where T has inverse Gaussian (IG) distribution. Its density is

$$f(t;\mu,\nu) = \sqrt{\frac{\nu}{2\pi t^3}} \exp\left\{-\frac{\nu(t-\mu)^2}{2\mu^2 t}\right\}, \quad t \geq 0,\ \mu > 0,\ \nu > 0, \tag{1.32}$$

which is illustrated in Fig. 1.2(b). It holds

$$\lambda = \frac{1}{\mu},\ \mathrm{CV}^2 = \mathrm{FF} = \frac{\mu}{\nu}, \tag{1.33}$$

while, as well as for a gamma process, $\mathrm{FF}(t)$ cannot be expressed in a closed form.

1.3 Sum of renewal processes

A very important process in neuronal modeling is a counting process created as a sum of independent renewal processes. Its description and some properties are presented here.

Let us have n generally various independent renewal processes $N_i(t)$, $i = 1,\ldots,n$, and define their sum

$$N(t) = \sum_{i=1}^{n} N_i(t),\ t > 0. \tag{1.34}$$

This process describes the total number of events occurred up to a time $t \geq 0$ in all the renewal processes, its trajectory is thus a simple sum of the trajectories of the single processes. From the point of view of the sequences of times, the final sequence contains all the times of all the events from all the processes (see Fig. 1.3). In this sense the term superposition of processes is often used instead of sum of processes. Let us note, that is not necessary to restrict the sum to renewal processes. The same way, it is possible to define a sum of arbitrary counting processes.

In a general case, determination of the type or properties of process (1.34) is not easy. The sum is not a renewal process, not even when all the renewal processes are same (with the exception of sum of Poisson processes, which creates also a Poisson process). Mainly, the independence of the lengths of the inter-event intervals between the single events is violated. It is possible to obtain easily at least the moment characteristics of process (1.34) (e.g. the mean or variance). They equal to the sum of the corresponding characteristics of the single processes.

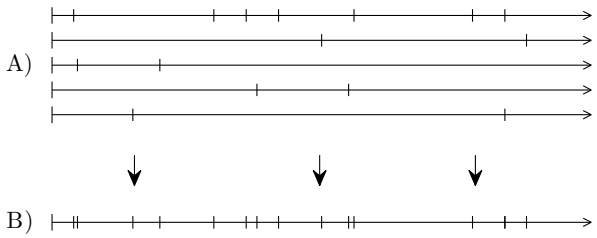

Fig. 1.3: Sum (superposition) of sequences of events.

Theorem 1.1. *Let $f(t)$ be the a probability density function of a positive, continuous random variable T and $\lambda = 1/\mathrm{E}(T)$. For every $n \in \mathbb{N}$, let us define independent and identical equilibrium renewal processes $N_1(t)$, $N_2(t), \ldots,$ $N_n(t)$ with probability density of inter-event intervals*

$$f_n(t) = \frac{1}{n} f\left(\frac{t}{n}\right). \tag{1.35}$$

Next, let $N(t,n)$ be the sum of processes $N_1(t)$, $N_2(t), \ldots, N_n(t)$ and $g(t)$, $t \geq 0$, its probability density function. Then

$$\lim_{n\to\infty} g(t) = \lambda e^{-\lambda t}, \ t \geq 0. \tag{1.36}$$

Theorem 1.1 describes the behavior of a sum of renewal processes with increasing number of summed processes. Specifically, it states that the sum of equal renewal processes converges to a Poisson process. A key part of this theorem is condition (1.35), which ensures a scaling of time such that the intensity of the sum remains constant, equal to λ. Without this scaling the convergence to Poisson process is not fulfilled [41]. For proof of Theorem 1.1 (even in a more general version) see [31].

1.4 Shot noise process

Another important random process used in neural modeling is process called shot noise. Its brief description is presented here. More details can be found for example in [53].

Definition 1.6. Let $X_k \geq 0$, $k \in \mathbb{N}$, be a strictly increasing sequence of random times, $\{N(t), t \geq 0\}$ the corresponding counting process and $w(x)$

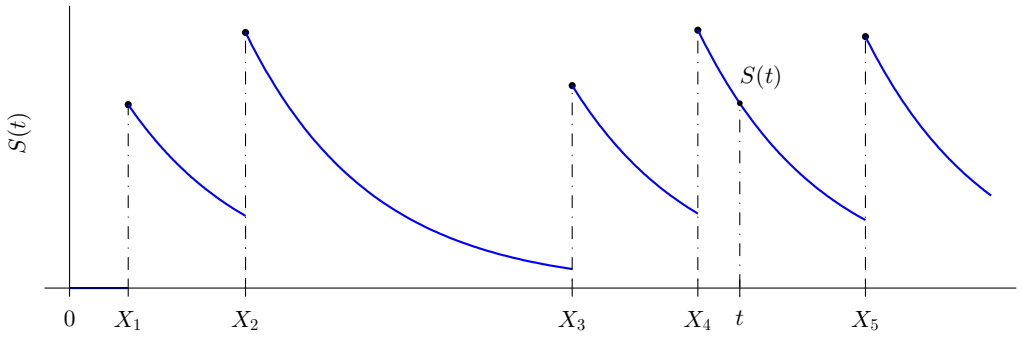

Fig. 1.4: An example of trajectory of a shot noise process with response function of type (1.38) for events occurred at times X_1, X_2, X_3, X_4 and X_5.

a real-valued function defined on $[0, \infty)$. A random process defined by relationship

$$S(t) = \begin{cases} \sum_{k=1}^{N(t)} w(t - X_k), & N(t) \geq 1, \\ 0, & \text{otherwise}, \end{cases} \tag{1.37}$$

is called a shot noise.

Shot noise process can be understood as a generalization of a counting process. In case of a counting process, every event causes permanent increase of the value of the process by one. On the other hand, the course of a shot noise process is given by the function $w(x)$ (response function), which determines the influence of every event on the trajectory. The most often used response function is the decreasing exponential,

$$w(x) = e^{-x/\tau}, \ x \geq 0, \tag{1.38}$$

where $\tau > 0$ (time constant) influences the rate of decrease. In Fig 1.4, there is an illustration of a shot noise process (1.37) with response function (1.38). This process can be interpreted as a counting process where the events are being forgotten in time. Some other types of the response functions are sometimes studied, e.g. power-law functions [57]. Note that for $w(x) = 1$, $x \geq 0$, shot noise process equals to the corresponding counting process.

Beside others, the properties of $S(t)$ are influenced by the character of the underlying sequence of time. Of course, any point process can be used to model this sequence, however, most commonly a Poisson process is considered. Poisson distributed times are even often directly part of definition of shot noise process. In connection with response function (1.38) we obtain

the most important type of shot noise process,

$$S_P(t) = \begin{cases} \sum_{k=1}^{N(t)} e^{-\frac{t-X_k}{\tau}}, & N(t) \geq 1, \\ 0, & \text{otherwise}, \end{cases} \tag{1.39}$$

where X_k, $k \in \mathbb{N}$, correspond to a Poisson process with intensity λ. Some properties can be derived for this process in closed forms, e.g. [72],

$$\mathrm{E}(S_P(t)) = \lambda\tau(1 - e^{-t/\tau}), \tag{1.40}$$

$$\mathrm{Var}(S_P(t)) = \frac{\lambda\tau}{2}(1 - e^{-2t/\tau}), \tag{1.41}$$

however, properties of some more complex variants of shot noise process are mostly complicated to analytically explore. We study some more general variants of this process in Publication III.

1.5 Diffusion processes

Among the random processes important in neuroscience belong also the diffusion processes. Contrary to the previously mentioned processes, they are not used to describe discrete events, but a continuous quantity, which stochastic part is influenced by a random process called white noise.

Definition 1.7. A random process $\{X(t),\, t \geq 0\}$ is called a (Gaussian) white noise, if for any $t_1 \geq 0$, $t_2 \geq 0$, $t_1 \neq t_2$, the random variables $X(t_1)$ and $X(t_2)$ are uncorrelated and for any $t \geq 0$ the random variable $X(t)$ has normal distribution with zero mean and variance $\sigma^2 > 0$. White noise with unit variance is denoted $WN(t)$.

Definition 1.8. A random process $\{W(t),\, t \geq 0\}$ is called a standard Wiener process, if it holds

(a) $W(0) = 0$,

(b) for any $0 \leq t_1 < t_2 < t_3 < t_4$ the random variables $W(t_2) - W(t_1)$ and $W(t_4) - W(t_3)$ are independent,

(c) for any $0 \leq t_1 < t_2$ the random variable $W(t_2) - W(t_1)$ has normal distribution with zero mean and variance $t_2 - t_1$.

Definition 1.9. Let $\{W(t),\, t \geq 0\}$ be a standard Wiener process, $\sigma > 0$, $x_0 \in \mathbb{R}$, $\lambda \in \mathbb{R}$. Then random process

$$X(t) = x_0 + \lambda t + \sigma W(t), \quad t \geq 0, \tag{1.42}$$

is called a Wiener process with drift.

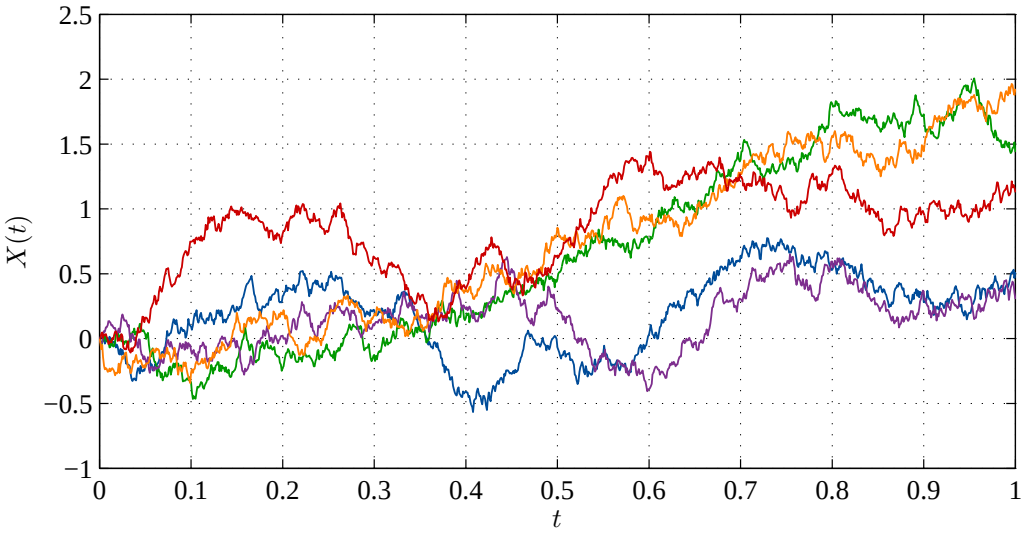

Fig. 1.5: Several examples of trajectories of Wiener process with drift with parameters $x_0 = 0, \lambda = 1, \sigma = 1$.

Wiener process (with drift) is a basic diffusion process, it is a process with continuous time and continuous trajectories (for illustration of its trajectories see Fig. 1.5). White noise and Wiener process are closely related. Wiener process can be understood as the integral of a white noise and conversely white noise as the derivative of a Wiener process. However, this idea is not rigorously correct, as the trajectories of a Wiener process are not differentiable with unit probability. This mechanism creates the core of the stochastic differential equations, which solutions are diffusion processes.

One of the reasons of importance of diffusion processes is that they can be used to approximate some other processes with discontinuous trajectories, which is called a diffusion approximation. For example, let us assume two Poisson processes, $N_1(t)$ and $N_2(t)$, and define a random process

$$Y(t) = aN_1(t) - bN_2(t),\ a > 0,\ b > 0.$$

The trajectory of process $Y(t)$ is thus a piecewise constant function with up and down jumps of size a and b. It can be shown that with decreasing values of a and b and increasing intensity of the Poisson processes $Y(t)$, converges in distribution to a Wiener process with drift [83]. Similarly, diffusion approximations can be constructed for other processes, e.g. for a combination of shot noise processes, which leads to another well-known and important diffusion process called Ornstein–Uhlenbeck process [72].

For a Wiener process with drift, it is possible to derive the distribution

of FPT in an explicit form. Specifically, the first passage time of a threshold $\theta > x_0$ has IG distribution with parameters [10]

$$\mu = \frac{\theta - x_0}{\lambda}, \quad \nu = \frac{(\theta - x_0)^2}{\sigma^2}, \tag{1.43}$$

under the condition that the threshold is reached in a finite time. On the other hand, e.g. for the Ornstein–Uhlenbeck process there is no a closed form of the FPT.

Chapter 2

Mathematical models in neurobiology

An introduction to mathematical models in neurobiology is presented in this chapter, more details can be found for example in [24, 30, 82].

2.1 Structure and functions of neurons

Neurons are the basic units of the nervous system, they are connected into a very dense network (in an adult human brain there are approximately $86 \cdot 10^9$ neurons connected by $10^{14} - 10^{15}$ junctions [24]) and their main function is transmission and preservation of information. There are various types of neurons, but a typical one consists of three parts – dendrites, a body and an axon (see Fig. 2.1). Simply put, these parts represent input, processing and output devices. Using the dendrites neuron receives signals from other neurons, they are "processed" in the body and based on the processing output signals are generated and sent to other neurons through the axon. The place where two neurons are connected is called a synapse. Accordingly, the sender is called a presynaptic neuron and the receiver is called a postsynaptic neuron. The neuronal signals are short electric impulses with amplitude approximately 100 mV and duration 1–2 ms, there are almost no differences between two impulses and they are also called action potentials or spikes [24].

The inside of a neuron is separated from the outside by a cytoplasmic membrane, this membrane creates a border of two environments with different concentration of ions, there is thus a difference between the potential inside and outside. This difference is called the membrane potential. When there are no impulses being received by the neuron (for a sufficiently long time), the value of the membrane potential is approximately -65 mV (resting

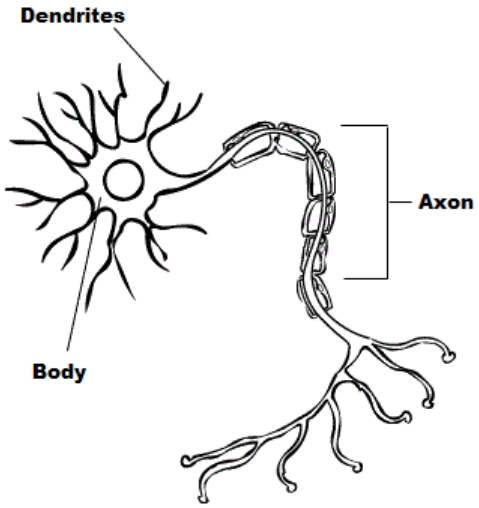

Fig. 2.1: The basic structure of a neuron.

value). However, it is being changed by the incoming spikes, these changes can be both positive (excitation pulses) or negative (inhibition pulses). These changes are not permanent, the membrane potential spontaneously returns to the resting value. If the potential reaches a certain value (threshold) the neuron generates an output spike and the potential decreases under the resting values, to which it subsequently returns. If there are other pulses being received by the neuron, this mechanism is repeated and a sequence of output spikes (spike train) is generated.

Even if the intensity of the input is high, the time intervals between successive spikes cannot be arbitrarily short. The spikes are always separated by a time interval of a certain minimal length, which is called a refractory period. The term relative refractory period is also established, to denote the time interval in which generation of a spike is unlikely (but possible).

2.2 Basic neuronal models

The presented description of neurons and their behavior can be summed up so that a neuron works as an input–output device which transforms an input spike train into an output spike train. A formal mathematical model of a single neuron can be thus separated into two parts, a model of the input and a model of the transformation mechanism. The aim of the models is mostly description of the character of the corresponding output.

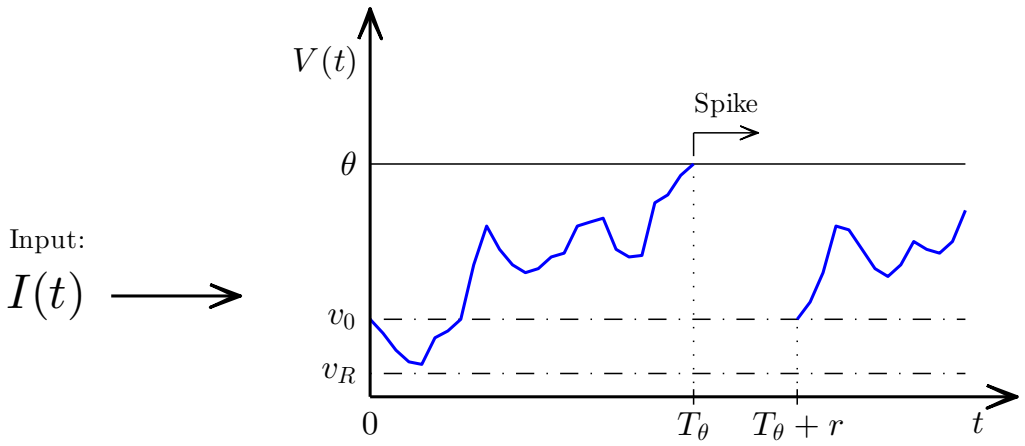

Fig. 2.2: A neural input to output transformation scheme.

The basis of the most of the neuronal models is the transformation of the given input to membrane potential until the threshold is reached, after which a spike is generated. Some of these models are described in this chapter, while the following notation is used (see a schematic illustration in Fig. 2.2). A function $I(t)$ represents the input received by a neuron at a time $t \geq 0$, it can describe both a continuous or discrete signal. In the second case, the pulses can be formally defined as a sum of Dirac δ-functions. Next, $V(t)$ denotes the value of the membrane potential at a time $t \geq 0$, $\theta \in \mathbb{R}$ denotes the threshold, $v_R \in \mathbb{R}$ the resting value and $v_0 \leq \theta$ an initial value of the potential at the time zero. As it was mentioned, as soon as $V(t)$ reaches θ a spike is generated. The time interval (T_θ) from the time zero up to this moment corresponds to the FPT from Definition 1.4, thus

$$T_\theta = \inf\{t \geq 0;\, V(t) \geq \theta\}. \tag{2.1}$$

Neuronal models focus often directly on description of the FPT (e.g. in dependence on the character of the input, parameters of the model, etc.), in that case it is not necessary to define the behavior of the model for time $t > T_\theta$. However, the model can continue and generate a sequence of impulses. Then we will assume that immediately after T_θ the value of $V(t)$ is returned to v_0, after which there is a time interval of length $r \geq 0$ (representing the refractory period) where any input is ignored. This mechanism continues and an output sequence is generated. The character of the ISIs can be both constant (the intervals have equal length or, in the case of stochastic models, the same probability distribution) or variable. The specific situation depends on the assumed model, mostly on its input.

2.2.1 Models of neuronal input

The models of neuronal input can be approximately divided into two groups, models of a discrete input and models of a continuous input. From the point of view of the true behavior of neurons, the discrete models, describing discrete times of the input spikes, are more realistic. However, even a continuous signal can be in certain situations a suitable description of the input [38, 61, 62]. The first example of such situations are controlled experiments in which the input (continuous) voltage is artificially supplied. The second example of such a case is input of a relatively large intensity, when the discrete character fades and a continuous signal can be a sufficiently precise approximation.

The most basic model of a continuous input is a constant voltage $\lambda > 0$, thus $I(t) = \lambda$. Such a model is often extended by a random component represented by the white noise, $I(t) = \lambda + WN(t)$. As $I(t)$, it is possible to use, according to the modeled situation, an arbitrary function or random process. For a discrete description of the neural input, there is also a wide range of possibilities, from simple deterministic sequences to complex stochastic processes. The most often used model of spike trains is clearly a Poisson process. One of the reasons is its relative simplicity, allowing derivation of many explicit results. Nevertheless, the more important reason is the fact that a Poisson process can be often considered to well approximate the real input. This assumption is based on Theorem 1.1, stating convergence of a sum of renewal process to a Poisson process, as neuronal input can be seen as a sum of many spike trains, coming from many neurons.

2.2.2 Perfect-integrator models

A basic type of models of the mechanism which transforms the input to output spike trains are the perfect-integrator models. They suppose that the input is transformed by a simple integration of the function $I(t)$. The value of $V(t)$ at a time $0 \leq t \leq T_\theta$ is thus given by relationship

$$V(t) = v_0 + \int_0^t I(s)\mathrm{d}s. \tag{2.2}$$

Due to the simplicity of this relationship, it is often possible to explicitly derive the value or probability distribution of T_θ. Let us present several examples.

a) *A constant continuous input signal*, $I(t) = \lambda$, $\lambda > 0$.

   In this case, it is possible to simply obtain the (deterministic) value of FPT, $T_\theta = (\theta - v_0)/\lambda$.

b) *A continuous input signal with constant deterministic component combined with white noise,* $I(t) = \lambda + \sigma WN(t)$, $\lambda > 0$, $\sigma > 0$.

For $0 \leq t \leq T_\theta$ we obtain $V(t) = v_0 + \lambda t + \sigma W(t)$, thus a Wiener process with a drift. According to Section 1.5, the random variable T_θ has an inverse Gaussian distribution.

c) *A Poisson process.*

Let us suppose that the input corresponds to a Poisson process representing times of spikes with a constant amplitude $a > 0$, thus a sequence of impulses with independent and exponentially distributed ISIs. The amplitudes of the pulses are summed up to reaching the value θ, for which $k = \lceil (\theta - v_0)/a \rceil$ spikes are necessary. The value T_θ thus corresponds to the waiting time for the k-th event in a Poisson process, which has an Erlang distribution, thus also a gamma distribution.

2.2.3 Leaky-integrator models

The leaky-integrator models eliminate probably the largest drawback of the perfect-integrator models – neglecting of the spontaneous return of the membrane potential to the resting value. In the leaky-integrator models, this effect is embedded to the model using an assumption that the rate of the return to the resting potential is directly proportional to difference $V(t) - v_r$ with the proportionality constant $1/\tau$, where $\tau > 0$ is called a time constant. This assumption yields a differential equation for $V(t)$, $0 \leq t \leq T_\theta$,

$$\frac{\mathrm{d}V}{\mathrm{d}t} = -\frac{V(t) - v_R}{\tau} + I(t),\ V(0) = v_0. \tag{2.3}$$

Let us present several specific variants of this model in dependence on $I(t)$.

a) *A constant continuous input signal,* $I(t) = \lambda$, $\lambda > 0$.

It is possible to find an explicit solution of equation (2.3)

$$V(t) = v_0 e^{-\frac{t}{\tau}} + (v_R + \lambda\tau)(1 - e^{-\frac{t}{\tau}}),\ t \geq 0. \tag{2.4}$$

The solution is an increasing function converging to $v_R + \lambda\tau$, reaching the threshold is thus possible only if $\theta < v_R + \lambda\tau$, then

$$T_\theta = \tau \ln \frac{v_R + \lambda\tau - v_0}{v_R + \lambda\tau - \theta}.$$

Let us note that model given by equation (2.3) with a general deterministic function $I(t)$ is called a Lapicque model, model given by equation (2.4) is thus its basic variant.

b) *A continuous input signal with a constant deterministic component combined with white noise,* $I(t) = \lambda + \sigma WN(t)$, $\lambda > 0$, $\sigma > 0$.

Combination of the leaky-integrator mechanism and this input yields membrane potential corresponding to an Ornstein-Uhlenbeck process. It is a very often used model of the membrane potential [14, 60], however, both the probability density and the cumulative distribution functions of the random variable T_θ are not known in an explicit form. They are mostly studied using some numerical simulations.

c) *A point process.*

In the case of input described by discrete pulses (mostly a Poisson process), the trajectory of the membrane potential has a shape of a function with jumps of a certain value, between which it returns to the resting value v_R by an exponential rate. The membrane potential thus corresponds to a shot noise process. An important extension of this model is situation when we consider also negative jumps (inhibition pulses). Such a model is called Stein's model [74].

Chapter 3

Overview of the published results

Publication I: Fano Factor Estimation

In this paper, we study one of the most often used measures of variability of neural spike trains – Fano factor. It is a quantity which was firstly proposed to measure the fluctuations of the produced number of ion pairs in a volume of gas [21]. Nevertheless, it is now often used to measure (among others) variability of neural spike trains [20, 22, 27]. Fano factor is defined as the variance to mean ratio of numbers of spikes in an observation window of a certain length, t. Such a characteristic is easy to use, which is clearly one of the reasons of its popularity, however, it has to be interpreted carefully as its value generally strongly depends on the length of the observation window [49]. When estimating Fano factor, the aim is mostly to obtain the limit value for infinitely long observation window, to remove the dependence on t. That yields a need to use as large t as possible. On the other hand, there are also some reasons to use a short window, e.g. a lack of data or an effort to capture the instantaneous variability on a short scale. To be able to optimally balance between these two contradictory requirements, it is necessary to know some theoretical properties of Fano factor for some suitable models of spike trains.

A very often used model of sequences of spikes is a renewal process, which assumes that the ISIs are independent and identically distributed positive continuous random variables. Among the most useful distributions of ISIs belong gamma and inverse Gaussian distributions [23, 37, 40, 50, 51, 52, 69]. Nevertheless, note that a renewal process is not always a suitable model of the neural spike trains [3, 8, 66]. It is well known that for renewal processes the value of Fano factor starts in unit value (for $t \to 0$) and converges to CV^2

(for $t \to \infty$), where CV, coefficient of variation, is another very often used variability measure, defined as the standard deviation to mean of interspike intervals (ISIs) ratio [11]. However, the specific dependence on t and thus even the choice of the optimal window is not fully clear.

To clarify these issues, we study estimation of Fano factor for renewal processes. In the first part of the paper, we derive some its new properties and in the second part we propose a procedure of selecting of the length of the observation window with the aim on minimizing the mean square error of standard Fano factor estimator when estimating from a segmented single spike train. Estimation from repeated trials is also explored, focusing on determination of the accuracy of the standard estimators of CV and Fano factor in various situations. From the derived properties, let us mention the effect of a refractory period. We show that both a relative and absolute refractory periods cause an initial decrease of the value of Fano factor, independently of the true variability of the spike trains, which has to be strongly taken into account while using a very short window. This effect was earlier observed in experimental data in [78], but according to our knowledge it has not yet been explained analytically.

Publication II: Stein's neuronal model with pooled renewal input

In this paper, we explore the influence of variability of input of a neuron on character of its output. Neural input is mostly described by a Poisson process, the reason comes from the fact that sum (superposition) of suitably scaled renewal processes converges to a Poisson process with increasing number of the processes. As a renewal process is a standard model of a single spike train and input of a neuron is created by many spike trains, it is reasonable to assume that the input can be well approximated by a Poisson process. However, such an assumption rejects the possibility of variability coding, as all the rate-independent variability is neglected in the Poissonian approximation. Therefore, we explore the precision of this approximation with the aim to determine whether the variability of the input spike trains can influence behavior of a neuron.

For this study we use a famous and often used neuronal model – Stein's model [6, 26, 72, 73, 74, 82]. Note that there are also some its more complex modifications [5, 16, 28, 48, 63, 81]. Standardly, it is studied with a Poissonian input and in that case the rate and variability coding cannot be separated [35, 36, 70]. The insufficiency of this approach was observed in

in-vivo data in [15] and some more general variants of the input were studied e.g. in [7, 18, 25, 42, 44, 65]. Firstly, we thus generalize this model by assuming input described by pooled independent and identical renewal processes. Secondly, we compare the behavior of this model in dependence on CV of the single inputs, representing their variability, and on number of the inputs with behavior of Stein's model with a Poissonian input. We use two criteria – character of the neuronal membrane potential and character of the neuronal output. Both of the criteria show that the Poissonian approximation can be insufficient. Even for a realistic number of inputs (e.g. 10000) there are some significant differences in behavior of the models. It is thus possible that the input variability influences the response of neuron and variability coding cannot be rejected.

Publication III: Shot-noise Fano factor

Fano factor is a useful measure of variability of neural spike trains, however, it might be considered to be too simple. Mainly, it probably does not measure the variability the way neurons can register it (if they can register it). The problem is in the used window, which assumes that every spike is reflected either fully or not at all – in dependence on whether the spike is inside or outside of the window. A more realistic approach, corresponding to the leaky-integrator mechanism, could be that the influence of spikes decreases with increasing time that passed since their arrival. Based on this idea, we have proposed a new variability measure in this paper. This measure can be seen as a generalization of Fano factor where the spikes are weighted using a smooth (response) function. From a mathematical point of view, it is the variance to mean ratio of a linearly filtered point process, often called shot noise [12, 53]. We study the measure under the standard assumption that the spike trains follow a renewal process, derive some of its properties and compare them with the properties of Fano factor. Specifically, we focus on the measure with the response function in form of a decreasing exponential, which seems to be the most important case, as an exponential spontaneous decrease of membrane potential is often assumed [24]. As the proposed measure can be used in any situation when dealing with data in form of a sequence of discrete points, we do not restrict the publication only to the neuronal point of view. Analogous data arise e.g. when studding natural disasters (earthquakes, fires) [77, 79, 80], chemical reactions [4, 9], or many other phenomena [1, 32, 55, 86].

Even if the measure is more complex than Fano factor, some of the derived formulas describing its behavior are simpler than the Fano factor alternatives and they can be used to make inferences about the local character of exper-

imental data. There is also another application of the theoretical results. They can be used when processing data that we assume to be directly realizations of a shot-noise process. Such data arise in many situations, e.g. in study of traffic noise [45, 85], river flows [39] or (for our purpose most importantly) the neural membrane potential [72]. For such situations we use our results to propose a CV estimator of the underlying renewal process.

Publication IV: Entropy factor for randomness quantification in neuronal data

The term variability is usually used as a general term to denote the intensity independent behavior of the spike trains (or other phenomena). However, there is a similar but not equivalent term which should be distinguished – randomness. The difference between the variability and randomness can be well seen from the fact that even a deterministic (non-random) process can be variable. To measure the randomness there is a suitable quantity – Shannon entropy [67], which is very often used in neuroscience [46, 47, 75, 76, 84]. Based on it, some randomness measures were proposed and thoroughly studied [33, 34, 35], however, the focus is given only to randomness of ISIs. As neurons more likely register the numbers of spikes than the actual lengths of the interspike intervals, it is natural to extend the randomness measures even to the numbers. In this paper we therefore propose such a measure, entropy factor. It is defined as the ratio of Shannon entropy of numbers of spikes in an observation window to Shannon entropy of a counting Poisson process with the same rate. This way we obtain a measure which is a close analogy to Fano factor, with the difference that is uses the Shannon entropy instead of the variance.

We derive some properties of the proposed measure for renewal processes and compare them with the properties of Fano factor. We show that there are some significant differences between these measures and thus it cannot be assumed that they both provide the same information about the rate-independent behavior of spike trains. Mainly, Fano factor better reflects the variability for long observation windows, while entropy factor provides most information about the randomness for relatively short observation windows (which could correspond to windows used by neurons). There is also highly non-monotonic dependence of the entropy factor on CV, creating another difference from Fano factor. Finally, we compared the theoretical properties of the new measure with the behavior deduced from experimental data – records of spontaneous firing of olfactory receptor neurons in rats [19].

Bibliography

[1] C. Anteneodo, R. D. Malmgren & D. R. Chialvo, Poissonian bursts in e-mail correspondence, *Eur. Phys. J. B*, 75:389–394, 2010.

[2] T. Aoki, T. Takaguchi, R. Kobayashi & R. Lambiotte, Input-output relationship in social communications characterized by spike train analysis, *Phys. Rev. E*, 94:042313, 2016.

[3] O. Avila-Akerberg & M. J. Chacron, Nonrenewal spike train statistics: causes and functional consequences on neural coding, *Exp. Brain Res.*, 210:353–371, 2011.

[4] A. C. Barato & U. Seifert, Universal Bound on the Fano Factor in Enzyme Kinetics, *J. Phys. Chem. B*, 119:6555–6561, 2015.

[5] A. N. Burkitt, Balanced neurons: analysis of leaky integrate-and-fire neurons with reversal potentials, *Biol. Cybern.*, 85:247–255, 2001.

[6] A. N. Burkitt, A review of the integrate-and-fire neuron model: I. Homogeneous synaptic input, *Biol. Cybern.*, 95:1–19, 2006.

[7] A. N. Burkitt, A review of the integrate-and-fire neuron model: II. Inhomogeneous synaptic input and network properties, *Biol. Cybern.*, 95:97–112, 2006.

[8] M. J. Chacron, A. Longtin & L. Maler, Negative interspike interval correlations increase the neuronal capacity for encoding time-dependent stimuli, *J. Neurosci.*, 21:5328–5343, 2001.

[9] S. Chaudhury, Poisson Indicator and Fano Factor for Probing Dynamic Disorder in Single-Molecule Enzyme Inhibition Kinetics, *J. Phys. Chem.*, 118:10405–10412, 2014.

[10] R. S. Chhikara & J. L. Folks, *The inverse Gaussian distribution: Theory, methodology, and aplications*, Marcel Dekker, New York, 1989.

[11] D. R. Cox, *Renewal Theory*, Methuen & Co., London, 1962.

[12] D. R. Cox & V. Isham, *Point processes*, University Press, Cambridge, 1980.

[13] D. R. Cox & P. A. W. Lewis, *The Statistical Analysis of Series of Events*, Chapman & Hall, London, 1966.

[14] J. Cupera, Diffusion Approximation of Neuronal Models Revisited, *Math. Biosci. Eng.*, 11:11–25, 2014.

[15] M. Deger & M. Helias, Statistical properties of superimposed stationary spike trains, *J. Comput. Neurosci.*, 32:443–463, 2012.

[16] A. Di Crescenzo & B. Martinucci, Analysis of a stochastic neuronal model with excitatory inputs and state-dependent effects, *Math. Biosci.*, 209:547–563, 2007.

[17] S. Ditlevsen & P. Lansky, Firing variability is higher than deduced from the empirical coefficient of variation, *Neural. Comput.*, 23:1944–1966, 2011.

[18] F. Droste & B. Lindner, Integrate-and-fire neurons driven by asymmetric dichotomous noise, *Biol. Cybern.*, 108:825–843, 2014.

[19] P. Duchamp-Viret, L. Kostal, M. Chaput, P. Lansky & J. P. Rospars, Patterns of Spontaneous Activity in Single Rat Olfactory Receptor Neurons Are Different in Normally Breathing and Tracheotomized Animals, *Eur. J. Neurosc.*, 10:2690–2696, 2005.

[20] U. T. Eden & M. A. Kramer, Drawing inferences from fano factor calculations, *J. Neurosci. Methods*, 190:149–152, 2010.

[21] U. Fano, Ionization Yield of Radiations. II. The Fluctuations of the Number of Ions, *Phys. Rev.*, 72:26–29, 1947.

[22] F. Farkhooi, M. F. Strube-Bloss & M. P. Nawrot, Serial correlation in neural spike trains: Experimental evidence, stochastic modeling, and single neuron variability, *Phys. Rev. E*, 79:021905, 2009.

[23] K. Fisch, T. Schwalger, B. Lindner, A. V. M. Herz & J. Benda, Channel Noise from Both Slow Adaptation Currents and Fast Currents Is Required to Explain Spike-Response Variability in a Sensory Neuron, *J. Neurosci.*, 32:17332–17344, 2012.

[24] W. Gerstner & W. M. Kistler, *Spiking Neuron Models*, Cambridge University Press, Cambridge, 2002.

[25] L. Gomez, R. Budelli, R. Saa, M. Stiber & J. P. Segundo, Pooled spike trains of correlated presynaptic inputs as realizations of cluster point processes, *Biol. Cybern.*, 92:110–127, 2005.

[26] N. Hohn & A. N. Burkitt, Shot noise in the leaky integrate-and-fire neuron, *Phys. Rev. E*, 63:031902, 2001.

[27] C. Hussar & T. Pasternak, Trial-to-trial variability of the prefrontal neurons reveals the nature of their engagement in a motion discrimination task, *P. Natl. Acad. Sci. USA*, 107:21842–21847, 2010.

[28] P. Jahn, R. W. Berg, J. Hounsgaard & S. Ditlevsen, Motoneuron membrane potentials follow a time inhomogeneous jump diffusion process, *Phys. Rev. E*, 63:031902, 2011.

[29] W. S. Jewell, The properties of recurrent-event processes, *Oper. Res.*, 8:446–472, 1960.

[30] E. Kandel, J. Schwartz & T. M. Jessel, *Principles of Neural Science*, Elsevier, New York, 1991.

[31] S. Karlin & H. M. Taylor, *A First Course in Stochastic Processes*, Academic Press, New York, 1975.

[32] M. Karsai, K. Kaski, A. L. Barabasi & J. Kertesz, Universal features of correlated bursty behaviour, *Sci. Rep.*, 2:397, 2012.

[33] L. Kostal & P. Lansky, Similarity of interspike interval distributions and information gain, *Biol. Cybern.*, 94:157–167, 2006.

[34] L. Kostal, P. Lansky & O. Pokora, Variability measures of positive random variables, *PLOS ONE*, 6:e21998, 2011.

[35] L. Kostal, P. Lansky & J. P. Rospars, Neuronal coding and spiking randomness, *Eur. J. Neurosci.*, 18:63–75, 2007.

[36] L. Kostal, P. Lansky & C. Zucca, Randomness and variability of the neuronal activity described by the Ornstein-Uhlenbeck model, *Eur. J. Neurosci.*, 26:2693–2701, 2007.

[37] S. Koyama & L. Kostal, The effect of interspike interval statistics on the information gain under the rate coding hypothesis, *Math. Biosci. Eng.*, 11:63–80, 2014.

[38] P. Lansky, On approximations of Stein's neuronal model, *J. Theor. Biol.*, 107:631–647, 1984.

[39] M. Lefebvre & F. Bensalma, An Application of Filtered Renewal Processes in Hydrology, *Int. J. Eng. Math.*, 2014:593243, 2014.

[40] M. Levakova, S. Ditlevsen & P. Lansky, Estimating latency from inhibitory input, *Biol. Cybern.*, 108:475–493, 2014.

[41] B. Lindner, Superposition of many independent spike trains is generally not a Poisson process, *Phys. Rev. E*, 73:022901, 2006.

[42] B. Lindner, M. J. Chacron & A. Longtin A, Integrate-and-fire neurons with threshold noise: A tractable model of how interspike interval correlations affect neuronal signal transmission, *Phys. Rev. E*, 72:021911, 2005.

[43] S. B. Lowen & M. C. Teich, Power Law Shot Noise, *IEEE T. Inform. Theory*, 36:1302–1318, 1990.

[44] C. Ly & D. Tranchina, Spike Train Statistics and Dynamics with Synaptic Input from any Renewal Process: A Population Density Approach, *Neural. Comput.*, 21:360–396, 2009.

[45] A. H. Marcus, Traffic noise as a filtered Markov renewal process, *J. Appl. Probab.*, 10:377–386, 1973.

[46] S. E. Marzen, M. R. DeWeese, M. Chaput & J. P. Crutchfield, Time resolution dependence of information measures for spiking neurons: scaling and universality, *Front. Comput. Neurosci.*, 9:1085, 2015.

[47] M. D. McDonnell, S. Ikeda & J. H. Manton, An introductory review of information theory in the context of computational neuroscience, *Biol. Cybern.*, 105:55–70, 2011.

[48] M. Musila & P. Lansky, Generalized Stein's model for anatomically complex neurons, *Biosystems*, 25:179–191, 1991.

[49] M. P. Nawrot, Analysis and interpretation of interval and count variability in neural spike trains, In: *Analysis of parallel spike trains*, Springer, New York, 2010.

[50] M. P. Nawrot, C. Boucsein, V. R. Molina, A. Riehle, A. Aertsen & S. Rotter, Measurement of variability dynamics in cortical spike trains, *J. Neurosci. Methods*, 169:374–390, 2008.

[51] T. Omi & S. Shinomoto, Optimizing time histograms for non-poissonian spike trains, *Neural. Comput.*, 23:3125–3144, 2011.

[52] S. Ostojic, Interspike interval distributions of spiking neurons driven by fluctuating inputs, *J. Neurophysiol.*, 106:361–373, 2011.

[53] A. Papoulis, *Probability, Random variables, and Stochastic Processes*, McGraw-Hill, New York, 1991.

[54] Z. Pawlas, L. B. Klebanov, M. Prokop & P. Lansky, Parameters of spike trains observed in a short time window, *Neural. Comput.*, 20:1325–1343, 2008.

[55] Q. M. Pei, X. Zhan, L. J. Yang, C. Bao, W. Cao, A. B. Li, A. Rozi & Y. Jia, Fluctuations of cell population in a colonic crypt, *Phys. Rev. E*, 89:032715, 2014.

[56] D. H. Perkel & T. H. Bullock, Neural coding, *Neurosci. Res. Prog. B.*, 6:221–348, 1968.

[57] A. P. Petropulu, J. C. Pesquet, X. Yang & J. Yin, Power-Law Shot Noise and Its Relationship to Long-Memory α-Stable Processes, *IEEE T. Signal Proces.*, 48:1883–1892, 2000.

[58] A. Ponce-Alvarez, B.E. Kilavik & A. Riehle, Comparison of local measures of spike time irregularity and relating variability to firing rate in motor cortical neurons, *J. Comput. Neurosci.*, 29:351–365, 2010.

[59] Z. Praskova & P. Lachout, *Základy náhodných procesů*, Karolinum, Praha, 2005.

[60] L. M. Ricciardi & L. Sacerdote, The Ornstein-Uhlenbeck process as a model for neuronal activity, I. Mean and variance of the firing time, *Biol. Cybern.*, 35:1–9, 1979.

[61] M. J. E. Richardson & W. Gerstner, Synaptic Shot Noise and Conductance Fluctuations Affect the Membrane Voltage with Equal Significance, *Neural. Comput.*, 17:923–947, 2005.

[62] M. J. E. Richardson & W. Gerstner, Statistics of subthreshold neuronal voltage fluctuations due to conductance-based synaptic shot noise, *Chaos*, 16:026106, 2006.

[63] M. J. E. Richardson & R. Swarbrick, Firing-Rate Response of a Neuron Receiving Excitatory and Inhibitory Synaptic Shot Noise, *Phys. Rev. Lett.*, 105:178102, 2010.

[64] F. Rieke, D. Warland, R. de Ruyter van Steveninck & W. Bialek, *Spikes: exploring the neural code*, MIT Press, Cambridge, 1997.

[65] E. Salinas & T. J. Sejnowski, Impact of Correlated Synaptic Input on Output Firing Rate and Variability in Simple Neuronal Models, *J. Neurosci.*, 20:6193–6209, 2000.

[66] T. Schwalger, F. Droste & B. Lindner, Statistical structure of neural spiking under non-Poissonian or other non-white stimulation, *J. Comput. Neurosci.*, 39:29–51, 2015.

[67] C. Shannon & W. Weaver, *The Mathematical Theory of Communication*, University of Illinois Press, Illinois, 1998.

[68] T. Shimokawa & S. Shinomoto, Estimating instantaneous irregularity of neuronal firing, *Neural. Comput.*, 21:1931–1951, 2009.

[69] T. Shimokawa, S. Koyama & S. Shinomoto, A characterization of the time-rescaled gamma process as a model for spike trains, *J. Comput. Neurosci.*, 29:183–193, 2010.

[70] S. Shinomoto & S. Koyama, A solution to the controversy between rate and temporal coding, *Stat. Med.* 26:4032–4038, 2007.

[71] S. Shinomoto, K. Miura & S. Koyama, A measure of local variation of inter-spike intervals, *BioSystems*, 79:67–72, 2005.

[72] P. L. Smith, From Poisson shot noise to the integrated Ornstein-Uhlenbeck process: Neurally principled models of information accumulation in decision-making and response time, *J. Math. Psychol.*, 54:266–283, 2010.

[73] C. E. Smith & M. V. Smith, Moments of Voltage Trajectories for Stein's Model with Synaptic Reversal Potentials, *J. Theor. Neurobiol.*, 3:67–77, 1984.

[74] R. B. Stein, A Theoretical Analysis of Neuronal Variability, *J. Math. Psychol.*, 5:173–194, 1965.

[75] N. G. Stocks, A. P. Nikitin, M. D. McDonnell & R. P. Morse, The role of stochasticity in an information-optimal neural population code, *J. Phys. Conf. Ser.*, 197:012015, 2009.

[76] S. P. Strong, R. Koberle, R. R. de Ruyter van Steveninck & W. Bialek, Entropy and Information in Neural Spike Trains, *Phys. Rev. Let.*, 80:197–200, 1998.

[77] A. Talbi, K. Nanjo, J. Zhuang, K. Satake & M. Hamdache, Interevent times in a new alarm-based earthquake forecasting model, *Geophys. J. Int.*, 194:1823–1835, 2013.

[78] M. C. Teich, D. H. Johnson, A. R. Kumar & R. G. Turcott, Rate fluctuations and fractional power-law noise recorded from cells in the lower auditory pathway of the cat, *Hearing Res.*, 46:41–52, 1990.

[79] L. Telesca, G. Amatulli, R. Lasaponara, M. Lovallo & A. Santulli, Time-scaling properties in forest-fire sequences observed in Gargano area (southern Italy), *Ecol. Model. 185*, 2–4:531–544 2005.

[80] L. Telesca & L. Toth, Analysis of temporal fluctuations in the 1880-1994 seismicity of pannonian basin, *Fluct. Noise Lett.*, 9:157–165, 2010.

[81] H. C. Tuckwell, Synaptic Transmission in a Model for Stochastic Neural Activity, *J. Theor. Biol.*, 77:65–81, 1979.

[82] H. C. Tuckwell, *Introduction to theoretical neurobiology: Nonlinear and stochastic theories*, Cambridge University Press, Cambridge, 1988.

[83] J. B. Walsh, Well-timed diffusion approximations, *Adv. Appl. Probab.*, 13:352–368, 1981.

[84] N. Watters & G. N. Reeke, Neuronal Spike Train Entropy Estimation by History Clustering, *Neural Comput.*, 26:1–33, 2014.

[85] G. H. Weiss, On the noise generated by a stream of vehicles, *Transport Res.*, 4:229–233, 1970.

[86] Y. Yuan, X. Zhuang, Z. Liu & W. Huang, Time-clustering behavior of sharp fluctuation sequences in Chinese stock markets, *Chaos Soliton. Fract.*, 45:838–845, 2012.

PUBLICATIONS

Publication I

MATHEMATICAL BIOSCIENCES
AND ENGINEERING
Volume **11**, Number **1**, February **2014**

doi:10.3934/mbe.2014.11.105

pp. **105–123**

FANO FACTOR ESTIMATION

Kamil Rajdl

Department of Mathematics and Statistics, Faculty of Science
Masaryk University, Kotlarska 2a, 611 37 Brno, Czech Republic
and
Institute of Physiology, Academy of Sciences of the Czech Republic
Videnska 1083, 142 20 Prague, Czech Republic

Petr Lansky

Institute of Physiology, Academy of Sciences of the Czech Republic
Videnska 1083, 142 20 Prague, Czech Republic
and
Department of Mathematics and Statistics, Faculty of Science
Masaryk University, Kotlarska 2a, 611 37 Brno, Czech Republic

Abstract. Fano factor is one of the most widely used measures of variability of spike trains. Its standard estimator is the ratio of sample variance to sample mean of spike counts observed in a time window and the quality of the estimator strongly depends on the length of the window. We investigate this dependence under the assumption that the spike train behaves as an equilibrium renewal process. It is shown what characteristics of the spike train have large effect on the estimator bias. Namely, the effect of refractory period is analytically evaluated. Next, we create an approximate asymptotic formula for the mean square error of the estimator, which can also be used to find minimum of the error in estimation from single spike trains. The accuracy of the Fano factor estimator is compared with the accuracy of the estimator based on the squared coefficient of variation. All the results are illustrated for spike trains with gamma and inverse Gaussian probability distributions of interspike intervals. Finally, we discuss possibilities of how to select a suitable observation window for the Fano factor estimation.

1. **Introduction.** One of the most important open questions in neuroscience is how neurons code transfered information into spike trains. The basic and frequently considered concept is rate coding [11]. It assumes that the information is coded by the spike rate, which is mostly calculated as a spike count average. The spike rate, however, does not fully depend on exact spike times, different spike sequences can yield the same spike rate. So there is the possibility that there is more information in a spike train than what can be coded using the spike rate. A natural extension of the rate coding, which better reflects the specific spike timing, is variability coding [20]. In that case, it is assumed that the variability in spike trains also carries information. The question whether the variability coding is used in real neurons or the variability is caused just by a noise without useful information is still unanswered. However, this issue increases the importance of suitable variance measurement and estimation.

2010 *Mathematics Subject Classification.* Primary: 60K05, 62-07; Secondary: 62P10.

Key words and phrases. Fano factor, estimation, renewal process, mean square error, refractory period.

The spike train variability is usually examined based on one of two following neuronal data types - a single (long) spike train or multiple (short) spike trains. By a single spike train we understand a relatively long record of spike activity, often spontaneous, of one neuron. On the other hand, multiple spike trains often arise from repeated measurements (repeated trials) of the immediate reaction to a stimulus. The reaction is usually of limited duration therefore there is the demand on a short observation window.

There are many possibilities how to measure the variability in spike trains. Often it is assumed that the spike trains satisfy the definition of renewal process and so a measure of variability of continuous positive random variables, which represent the length of interspike intervals (ISIs), can be used [14]. Such a typical and basic measure is coefficient of variation (CV), which is the ratio of the square root of the variance of the length of the ISIs to their mean. Alternatively, the variability of numbers of spikes occurred in an observation window is measured. In that case, mainly the Fano factor (FF), the ratio of the variance of the number of spikes to the mean, is used. Although CV and FF, as defined, represent different types of variability, they are closely related for renewal processes - with increasing length of the observation window FF converges to CV^2 [18]. Thus to measure their common value it is possible to use CV as well as FF.

Modeling of spike trains using renewal processes assumes independent and identically distributed lengths of ISIs which certainly not always apply to real spike trains, often the spike rate changes in time or the ISIs are correlated [10]. However, there are situations when such a description of ISIs can be appropriate. For instance, when we observe the spike train in a short time window then, even if the character of the spike train changes in time, the observed part can be approximately stationary. The second situation where the spike train often seems to be well described by a renewal process is during spontaneous activity. Moreover, it is possible to eliminate rate changes before variability estimation using a time transformation [18]. Let us notice that also some local measures [22, 24], which are less sensitive to spike rate changes, and methods for extracting the firing variability and the firing rate simultaneously [15, 23] were proposed.

Estimation of both CV and FF is not always trivial. For short spike trains (short observation window) the probability of observation of large ISIs is reduced and therefore the standard estimator of CV (square root of sample variance of ISIs divided by sample mean) is biased. In this case, there is a bias also in the standard estimator of the limit value of FF (sample variance of spike counts divided by sample mean). It is caused by the fact that we estimate FF for infinite intervals based on finite, short observation window. In estimation from single spike train, these issues are usually minor, but there is another complication in FF estimation. To be able to use the estimator, we need data in form of spike counts. They are naturally obtained by segmentation of the spike train into intervals of the same length and the accuracy of the estimator surely depends on this length. However, it is not clear how to choose the most suitable one.

In this article, we explore some problematic aspects of estimation of the limit value of FF from repeated trials and from a single spike train and show that there are situations when the estimator of FF is more suitable for estimation of CV (squared) than its commonly used estimator. Firstly, we describe and illustrate the dependency of FF on the length of the observation window and investigate the effect of refractory period on this dependence. In [25], a decrease of FF for short

observation window caused by refractory period is shown, in [7] it is analytically explained for a Poisson process with absolute refractory period. We show this effect analytically also for equilibrium renewal processes with absolute or relative refractory period. Next, an approximate asymptotic formula for the mean square error (MSE) of the estimator is derived and its accuracy verified using simulated spike trains. This formula can be used, among others, to approximate the MSE in estimation from single spike trains and thus also to choose the suitable length of intervals into which the spike train is segmented. Finally, we compare the accuracy of CV and FF estimators based on simulated spike trains and discuss the suitable choice of the observation window for the FF estimator. For numerical illustrations, we use gamma and inverse Gaussian probability distributions of ISIs.

2. **Theory.** Neural spike trains are often described as a renewal process, where it is assumed that the lengths of ISIs are independent and identically distributed continuous positive random variables. We denote this random variable by T, its probability density function (pdf) by $f(t)$ and cumulative distribution function (cdf) by $F(t)$. The process can also be described as a counting process $\{N_t,\, t \geq 0\}$, which represents the number of spikes occurred from time zero to a time t. For the complete description of a spike train, it is also necessary to specify the position of time zero. Commonly, the observation begins either at the moment of a spike (ordinary renewal process) or in a random moment, unrelated to the spike train (equilibrium renewal process).

The coefficient of variation (CV) and the Fano Factor (FF) are defined as

$$\mathrm{CV} = \frac{\sqrt{\mathrm{Var}(T)}}{\mathrm{E}(T)}, \tag{1}$$

$$\mathrm{FF} = \lim_{t\to\infty} \mathrm{FF}_t, \tag{2}$$

where

$$\mathrm{FF}_t = \frac{\mathrm{Var}(N_t)}{\mathrm{E}(N_t)}, \tag{3}$$

$\mathrm{E}(T)$ and $\mathrm{E}(N_t)$ denote means of random variables T, and N_t and $\mathrm{Var}(T)$ and $\mathrm{Var}(N_t)$ denote their variances. While CV describes directly the variability of the random variable T, FF aims at the variability of N_t. Since T represents only ISIs, not the time up to the first spike, in formula (1), and since t tends to infinity in definition (2), it is not necessary to specify the condition for selection of time zero (in other words, the values of CV and FF do not depend on whether the corresponding renewal process is ordinary or equilibrium).

The estimation of CV is straightforward, its standard estimator is the ratio of the square root of the sample variance to the sample mean of ISIs, thus

$$\widehat{\mathrm{CV}} = \frac{\sqrt{s_T^2}}{\overline{T}} = \frac{\sqrt{\frac{1}{n-1}\sum_{i=1}^{n}(T_i - \frac{1}{n}\sum_{i=1}^{n} T_i)^2}}{\frac{1}{n}\sum_{i=1}^{n} T_i}, \tag{4}$$

where $T_1, T_2, \ldots, T_n$ denote the lengths of ISIs. This estimator is biased, however, the problem has been dealt with in [8, 14].

Estimate of FF is commonly calculated based on numbers of spikes occurred in time intervals (in an observation window) of length t. We denote these numbers by

$N_t^1, N_t^2, \ldots, N_t^n$. Then the usual estimator of FF is

$$\widehat{\mathrm{FF}} = \frac{s_{N_t}^2}{\overline{N}_t} = \frac{\frac{1}{n-1}\sum_{i=1}^{n}(N_t^i - \frac{1}{n}\sum_{i=1}^{n} N_t^i)^2}{\frac{1}{n}\sum_{i=1}^{n} N_t^i}. \tag{5}$$

The counts N_t^i, $i = 1, \ldots, n$, are mostly obtained from n trials, but also, not so frequently, by segmentation of a single spike train (of a length τ) into n parts (see Figure 1). However, even if we assume that both the trials and the single spike train correspond to the same equilibrium renewal process, these situations are not completely equivalent from the point of view of properties of N_t^i. Later, this issue will be discussed in more detail.

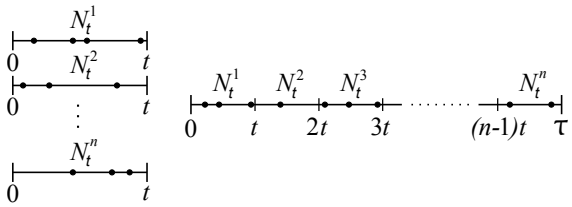

FIGURE 1. Two types of neuronal data for FF estimation, n trials (left) and segmented single spike train of length τ (right).

There is a clear discrepancy between definition (2) and estimator (5). The value of t tends to infinity in the definition of FF, but it is finite and often relatively short in a specific data set. Therefore, formula (5) is more likely an estimator of FF_t. The difference between FF_t and FF causes, for short t, relatively strong bias of $\widehat{\mathrm{FF}}$ [17]. Thus the behavior of FF_t, as a function of t, highly affects the quality of $\widehat{\mathrm{FF}}$. Above all, the rate of convergence to its limit is important. Basic and well known, [5, 13, 17, 19], properties of FF_t which hold for renewal processes are

$$\lim_{t\to 0^+} \mathrm{FF}_t = 1, \tag{6}$$

$$\lim_{t\to\infty} \mathrm{FF}_t = \frac{\mathrm{Var}(T)}{\mathrm{E}(T)^2} = \mathrm{CV}^2, \tag{7}$$

the latter also yields the relationship

$$\mathrm{FF} = \mathrm{CV}^2. \tag{8}$$

Formula (6) can be understood using the fact that the probability distribution of N_t converges, independently of the probability distribution of T, to a Bernoulli distribution as $t \to 0$ (just zero or one spike can occur in $[0, t]$). On the other hand, the probability distribution of N_t is normal for $t \to \infty$ [5], which can be used to justify formula (7).

It follows from relationships (6) and (7) that FF_t goes from one to CV^2 (= FF) as t goes from zero to infinity, but the behavior of FF_t between these two values is not obvious. The simplest situation is for the exponential distribution of T (N_t is the Poisson process), in this case $\mathrm{FF}_t = 1$ for all $t > 0$. For more complex probability distributions of T (e.g., gamma, inverse Gaussian or log-normal) it is possible to approximate FF_t for large t, [5],

$$\mathrm{FF}_t \approx \mathrm{CV}^2 + \frac{1}{t}\left[\frac{\mathrm{E}(T)}{2}\left(1 + \frac{\mathrm{Var}(T)}{\mathrm{E}^2(T)}\right)^2 - \frac{1}{3}\frac{\mathrm{E}(T^3)}{\mathrm{E}^2(T)}\right], \quad \text{for } t \to \infty, \tag{9}$$

however, FF_t itself cannot be exactly expressed in a closed form.

Relationship (8) is an important property of renewal processes, which may be used in various ways. One possibility is estimation of CV^2 instead of FF. However, it is not obvious which estimator is more accurate. Later, we examine this issue using simulated spike trains. Another way how to apply equation (8) is joint analysis of CV^2 and FF estimates, as in [18]. Using this method we can for example test whether the spike train corresponds to a renewal process.

Let us notice that the function FF_t can behave significantly different for non-renewal processes. Mainly, it can diverge for $t \to \infty$. In [25] there is shown a situation when FF_t increases as a power-law function. One of the reasons which can cause such a behavior is ISIs correlation. For example, for equilibrium point processes with correlated ISIs it holds, [17],

$$\lim_{t\to\infty} \mathrm{FF}_t = \mathrm{CV}^2 \left(1 + 2\sum_{i=1}^{\infty} \xi_i\right), \tag{10}$$

where ξ_i is the linear correlation coefficient of ith order of the ISIs. Thus FF is not in general equal to CV^2, however, these situations are out of the scope of this article.

3. Results.

In this section, we present some new properties of FF_t and $\widehat{\mathrm{FF}}$ under the condition that N_t is an equilibrium renewal process.

3.1. Properties of FF_t.

Firstly, we derive a formula which can be used for numerical calculation of FF_t. Let us rewrite definition (3), using the formula, [5],

$$\mathrm{E}(N_t) = \frac{t}{\mathrm{E}(T)}, \tag{11}$$

into the form

$$\mathrm{FF}_t = \frac{\mathrm{E}(T)}{t}\mathrm{E}(N_t^2) - \frac{t}{\mathrm{E}(T)}. \tag{12}$$

There is not a formula similar to equation (11) for $\mathrm{E}(N_t^2)$ so we use its Laplace transform, [13],

$$\mathcal{L}\{\mathrm{E}(N_t^2)\}(s) = \frac{1+\tilde{f}(s)}{\mathrm{E}(T)s^2[1-\tilde{f}(s)]}, \tag{13}$$

where $\tilde{f}(s)$ is the Laplace transform of pdf $f(t)$. Then from equations (12) and (13) we get

$$\mathrm{FF}_t = \frac{1}{t}\mathcal{L}^{-1}\left\{\frac{1+\tilde{f}(s)}{s^2[1-\tilde{f}(s)]}\right\}(t) - \frac{t}{\mathrm{E}(T)}, \tag{14}$$

where $\mathcal{L}^{-1}$ denotes the inverse Laplace transform. Formula (14) allows us to calculate FF_t for any t and any probability distribution of T.

Next, we will specify the behavior of FF_t near zero for a certain situation. Namely, if for pdf $f(t)$ it holds that

$$f(t) \approx at,\ a \geq 0,\ \text{for } t \to 0^+, \tag{15}$$

then (see Appendix A)

$$\lim_{t\to 0^+} \frac{\mathrm{dFF}_t}{\mathrm{d}t} = -\frac{1}{\mathrm{E}(T)}. \tag{16}$$

Condition (15) corresponds to the concept of relative refractory period (very low probability of short ISIs), thus this result can be formulated so that the relative refractory period causes an initial decrease of FF_t independently of the value of FF.

The presence of an absolute refractory period leads to a similar effect. Instead of ISIs of length T we now assume ISIs of length $T + r$, where $r > 0$ represents the length of the absolute refractory period. Then (see Appendix A)

$$\mathrm{FF}_t = 1 - \frac{t}{\mathrm{E}(T) + r}, \quad \text{for } 0 < t \le r. \tag{17}$$

Thus FF_t is just a line with slope $-1/(\mathrm{E}(T) + r)$ in $(0, r]$. Further, it follows from equation (7) that

$$\mathrm{FF} = \frac{\mathrm{Var}(T)}{(\mathrm{E}(T) + r)^2}, \tag{18}$$

so the value of FF is lower than in the situation without a refractory period (because the mean of ISIs is now larger and the variance does not change).

3.2. **Mean square error of $\widehat{\mathrm{FF}}$.** A suitable and often used measure of accuracy of an estimator is the mean square error (MSE). It includes both bias and variance so it is useful in situations when we deal with bias-variance tradeoff. Here we present an approximate asymptotic formula for the MSE of $\widehat{\mathrm{FF}}$ under the assumption that the random variables N_t^i, $i = 1, \dots, n$, describe independent and identical equilibrium renewal processes.

MSE of $\widehat{\mathrm{FF}}$ is defined as

$$\mathrm{MSE}(\widehat{\mathrm{FF}}) = \mathrm{E}(\widehat{\mathrm{FF}} - \mathrm{FF})^2 \tag{19}$$

and it can be rewritten into the form

$$\begin{aligned} \mathrm{MSE}(\widehat{\mathrm{FF}}) &= [\mathrm{E}(\widehat{\mathrm{FF}}) - \mathrm{FF}]^2 + \mathrm{E}[\widehat{\mathrm{FF}} - \mathrm{E}(\widehat{\mathrm{FF}})]^2 \\ &= \mathrm{Bias}^2(\widehat{\mathrm{FF}}) + \mathrm{Var}(\widehat{\mathrm{FF}}). \end{aligned} \tag{20}$$

For large t and n it is possible to approximate $\mathrm{MSE}(\widehat{\mathrm{FF}})$ using formula (see Appendix B)

$$\begin{aligned} \mathrm{MSE}(\widehat{\mathrm{FF}}) \approx{}& \left[\frac{1}{t}\mathrm{E}(T)\mathrm{G}(T)\right]^2 \\ &+ \frac{\mathrm{E}^2(T)}{t^2}\left[\frac{2}{n-1} + \frac{\mathrm{E}^2(T)}{nt^2}\left(\mathrm{G}(T) + \frac{\mathrm{FF}}{\mathrm{E}(T)}t\right)\right] \\ &\cdot \left[\mathrm{G}(T) + \frac{\mathrm{FF}}{\mathrm{E}(T)}t\right]^2, \ \text{for } t \to \infty,\ n \to \infty, \end{aligned} \tag{21}$$

where

$$\mathrm{G}(T) = \frac{1}{2}(1 + \mathrm{FF})^2 - \frac{1}{3}\frac{\mathrm{E}(T^3)}{\mathrm{E}^3(T)}. \tag{22}$$

The first summand in formula (21) represents the squared bias and the second one corresponds to the variance of $\mathrm{MSE}(\widehat{\mathrm{FF}})$.

4. **Examples.** In this section we aim to illustrate properties of FF_t and $\widehat{\mathrm{FF}}$ in some specific situations by using numerical calculations and simulations. As probability distributions of T, we use gamma and inverse Gaussian (IG) distributions. They are probably the most widely used distributions for modeling of lengths of ISIs [8, 17, 19].

The pdf of the gamma distribution is

$$f_G(t;\lambda,k)=\frac{\lambda^k t^{k-1}e^{-\lambda t}}{\Gamma(k)},\quad t\geq 0,\ \lambda>0,\ k>0, \tag{23}$$

where Γ denotes the Gamma function, and the pdf of the IG distribution is

$$f_I(t;\mu,\nu)=\sqrt{\frac{\nu}{2\pi t^3}}\exp\left\{-\frac{\nu(t-\mu)^2}{2\mu^2 t}\right\},\quad t\geq 0,\ \mu>0,\ \nu>0. \tag{24}$$

An advantage of these pdfs is that it is possible to calculate analytically their Laplace transforms, which are necessary for application of formula (14). Note that the pdf (23) with $k=1$ is the exponential distribution and the corresponding counting process N_t is a Poisson process.

Both of these probability distributions (gamma and IG) have two parameters, and their values can be uniquely related to $\mathrm{E}(T)$ and FF. It holds that

$$\lambda=\frac{1}{\mathrm{E}(T)\mathrm{FF}},\ k=\frac{1}{\mathrm{FF}} \tag{25}$$

for the gamma distribution and

$$\mu=\mathrm{E}(T),\ \nu=\frac{\mathrm{E}(T)}{\mathrm{FF}} \tag{26}$$

for the IG distribution.

4.1. **Behavior of** FF_t**.** Here we illustrate the dependency of FF_t on t, calculating (approximating) their values using formula (14).

In Fig. 2, there are displayed the graphs of FF_t and corresponding probability densities for various values of FF. We see that FF_t goes from one to CV^2 and also its initial behavior corresponds to relationship (16), FF_t starts with a decrease at zero if pdf of T satisfies condition (15). This causes relatively large difference between FF_t curves for gamma and IG probability distributions even with the same FF and $\mathrm{E}(T)$ - for IG probability distribution, they can be nonmonotonic and, for $\mathrm{FF}>1$, the convergence to FF is evidently slower than for gamma distribution. It is caused by the presence of relative refractory period for all values of FF. On the other hand, there is no refractory period for gamma distribution with $\mathrm{FF}>1$ so FF_t is, in this case, always monotonic.

Next, we illustrate the effect of the absolute refractory period. We calculate FF_t for the same situations as in Fig. 2 with the difference that we add a refractory period of length $r=0.1$ to T (see Fig. 3). The graph of FF_t is now initially a line, which slope does not depend on the value of FF. Evident consequence is also slower convergence of FF_t to its limit value for $\mathrm{FF}>1$.

Finally, in Fig. 4, there is shown the accuracy of the approximation (9). We see that it is always better for low values of FF and, if $\mathrm{FF}>1$, it is also substantially better for gamma probability distribution of T than for IG distribution.

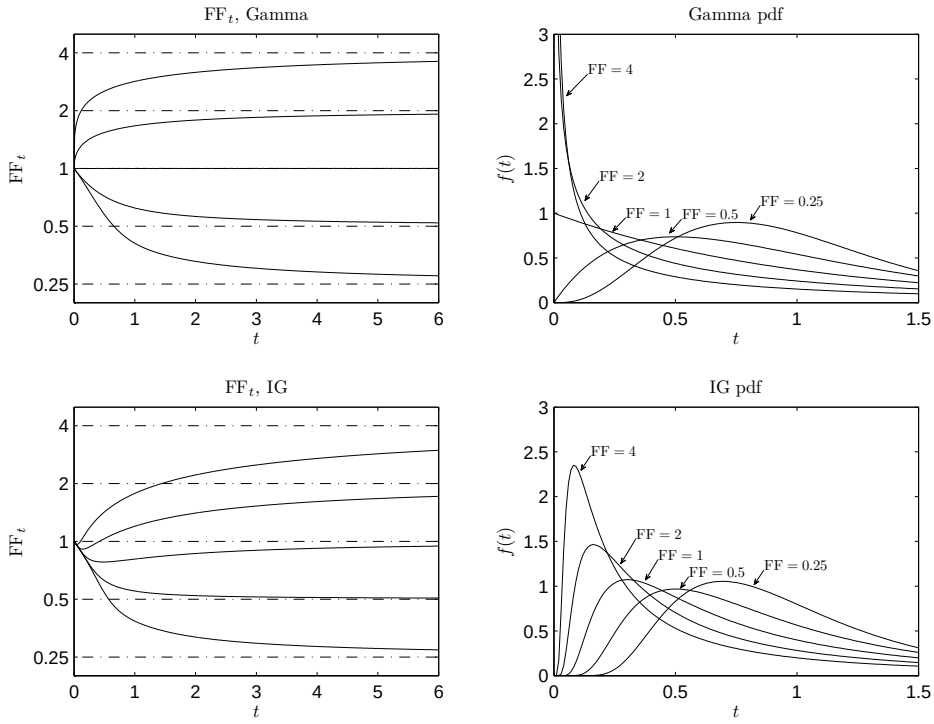

FIGURE 2. Left: Graphs of FF_t for gamma and IG probability distributions of T. Mean of T is always one, values of FF are 0.25, 0.5, 1, 2, 4 (from bottom to top). FF_t-axis is logarithmically scaled. Values of FF_t are calculated numerically using formula (14). Right: Probability density functions of gamma and IG distributions corresponding to the curves on the left.

4.2. **Numerical experiments.** There are some questions we are not able to answer using the analytical results. For example, we do not know the accuracy of asymptotic the approximation (21) or which estimator, (4) or (5), is more suitable to estimate FF. Therefore, these and some other issues are examined here using simulated spike trains.

For measuring the error of the estimators we use sample mean square error which is given by

$$\widehat{\mathrm{MSE}}(\hat{\theta}) = \frac{1}{m}\sum_{i=1}^{m}(\hat{\theta}_i - \theta)^2, \tag{27}$$

where $\hat{\theta}$ is an estimator of θ and $\hat{\theta}_1, \hat{\theta}_2, \ldots, \hat{\theta}_m$ are calculated realizations of $\hat{\theta}$. Definition (27) is a sample analogy (estimator) of formula (19), if it is not confusing we refer to both as MSE only. Their relative square roots in percents are shown in figures.

4.2.1. $\mathrm{MSE}(\widehat{\mathrm{FF}})$ *in estimation from independent trials.* Here we wish to clarify the question for what t and n it is possible to use relationship (21) as a reliable approximation of $\mathrm{MSE}(\widehat{\mathrm{FF}})$ in estimation from repeated trials. To that end, we calculate

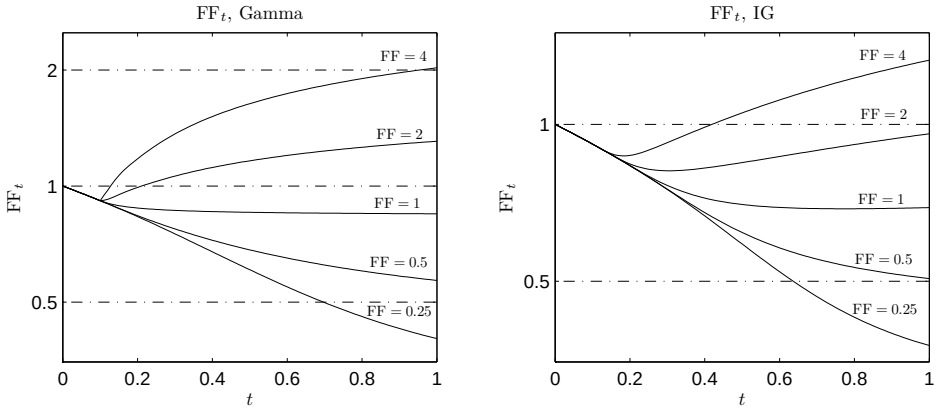

FIGURE 3. Graphs of FF_t for gamma (left) and IG (right) probability distributions of T with absolute refractory period. Mean of T is always 1.1 (of which 0.1 is the absolute refractory period), values of FF are 0.25, 0.5, 1, 2, 4 (from bottom to top). FF_t-axis is logarithmically scaled. Values of FF_t are calculated numerically using formula (14).

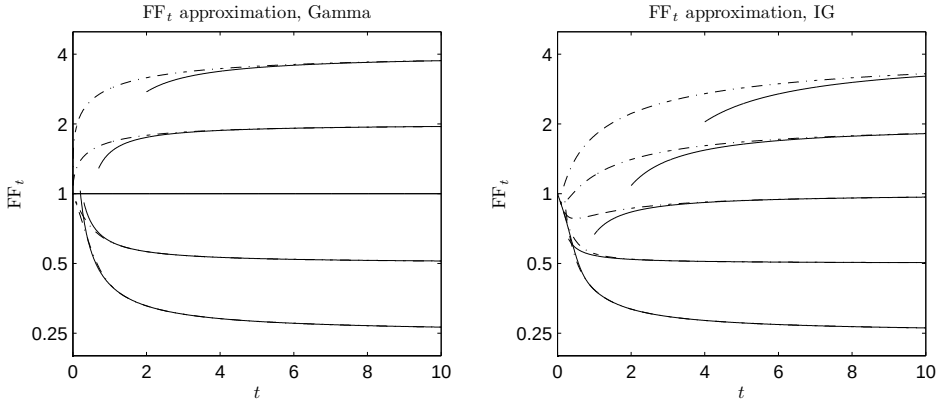

FIGURE 4. Graphs of FF_t (dash-dotted line) and their approximations calculated using formula (9) (solid line) for gamma (left) and IG (right) probability distributions of T. Mean of T is always one, values of FF are 0.25, 0.5, 1, 2, 4 (from bottom to top). FF_t-axis is logarithmically scaled.

MSE based on estimates from simulated spike trains and compare it with values of MSE obtained using approximation (21). This comparison is shown in Fig. 5. We see that the differences between approximated and simulated values of MSE are in considered situations relatively small. It seems that if $\mathrm{FF} < 2$ then formula (21) is a sufficiently accurate approximation of MSE for t about four means of ISIs and n about 25. Moreover, the accuracy quickly improves with decreasing value of FF.

4.2.2. $\mathrm{MSE}(\widehat{\mathrm{FF}})$ *in estimation from single spike train.* In FF estimation from a single spike train it is necessary to segment the spike train into n parts (intervals) of

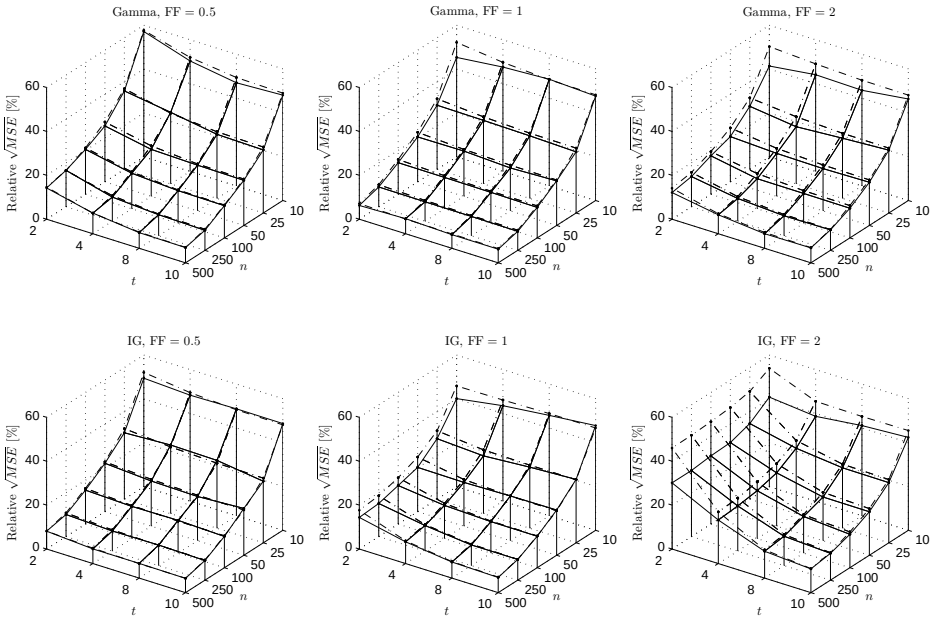

FIGURE 5. Relative $\sqrt{\mathrm{MSE}}$ of $\widehat{\mathrm{FF}}$ in percents obtained using simulations (solid line) and using formula (21) (dashed line). ISIs have gamma (upper panels) and IG (lower panels) probability distributions with mean one and FF $= 0.5, 1, 2$. Simulated values are calculated based on 1000 estimates of FF.

a length t to obtain the spike counts for application of $\widehat{\mathrm{FF}}$ and it is not obvious what t to use. For short intervals, the estimator is strongly biased, but with increasing t the number of intervals decreases (because of fixed length of the spike train) and that leads to an increase of variance of $\widehat{\mathrm{FF}}$. Therefore, here we examine the dependency of $\mathrm{MSE}(\widehat{\mathrm{FF}})$ on t and try to applicate formula (21) to its approximation. However, this formula was derived under the assumption that the spike counts are obtained from independent identical equilibrium renewal processes, which is different situation from one equilibrium renewal process segmented into n parts. For example, the spike counts are not completely independent (except for the Poisson process). However, following simulations indicate that violation of these assumptions does not play any role.

We obtain every estimate of FF based on one simulated spike train, which is segmented into intervals of length t. The length of the whole spike train is always $\tau = 1000$ (mean of ISIs is one), thus $n = [1000/t]$ (integer part of $1000/t$). In this way, we obtain the dependency of MSE of $\widehat{\mathrm{FF}}$ on t and compare it with values obtained using approximation (21) (see Fig. 6). We can conclude that there is a minimum of MSE for a certain value of t. However, if FF $= 1$, this minimum occurs for $t = 0$ (more precisely, MSE $\to 0$ for $t \to 0$). This is obvious because $\mathrm{FF}_t \to 1$ for $t \to 0$. Moreover, for the IG distribution with FF $= 1$, there is another (local) minimum, which is caused by the nonmonocity of FF_t. We also see that the values of MSE and especially their minima are in all situations relatively

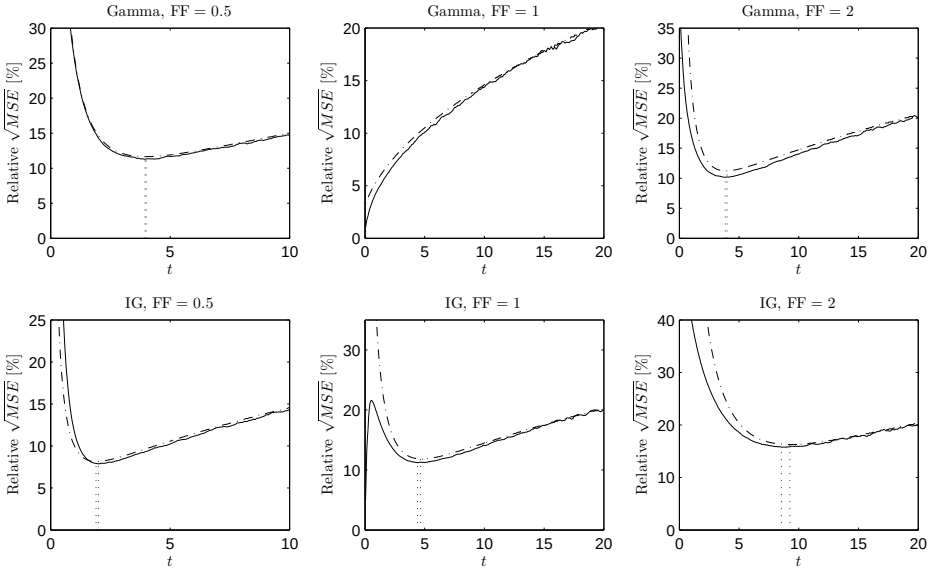

FIGURE 6. Relative $\sqrt{\text{MSE}}$ of $\widehat{\text{FF}}$ in percents in dependence on window size t calculated using formula (21) (dash-dotted line) and using simulations (solid line) in estimation from single spike train. ISIs follow gamma (upper panels) and IG (lower panels) distributions with mean one and $\text{FF} = 0.5, 1, 2$. The length of the spike trains is always $\tau = 1000$. Simulated values are calculated based on 1000 estimates of FF, corresponding curves are smoothed using moving average method.

well approximated by formula (21). One exception is the situation with for the IG distribution with $\text{FF} = 1$, where only the local minimum is approximated.

4.2.3. *Comparison of* $\widehat{\text{FF}}$ *and* $\widehat{\text{CV}}^2$. Due to relationship (8), there is the possibility of estimating FF using estimator of CV and vice versa, therefore, the question which of them is more precise arises. To clarify this issue we calculate and compare their MSE based on simulated spike trains in various situations, short repeated trials and single spike train are distinguished. In the first case, estimation using both estimators is problematic. Mainly, $\widehat{\text{CV}}$ is, as well as $\widehat{\text{FF}}$, strongly biased. We cannot observe ISIs longer than the length of the observation window and thus the variability in ISIs seems to be lower than it is. This problem almost vanishes in estimation from a single spike train, but on the other hand, there is the problem with the spike train segmentation for $\widehat{\text{FF}}$. As was shown, its MSE depends on used length of intervals t and therefore, to obtain "the best possible estimate", we use t which minimizes formula (21). However, it is necessary to avoid situations when this minimum is very low for FF near one (see Fig. 6), thus the minimal t we use is 3 (in mean ISI units). The results of these simulations are in Fig. 7.

Although there are some exceptions, it can be concluded the FF estimator is more suitable for estimation from short repeated trials and CV estimator for estimation from single spike trains. The exception in the first case is for spike trains with low

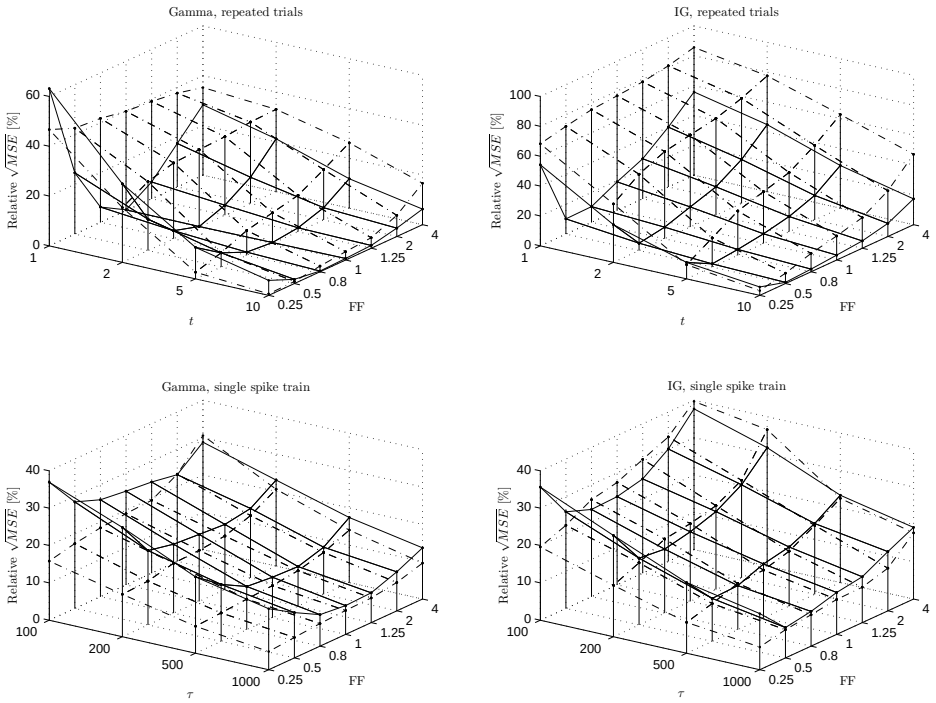

FIGURE 7. Relative $\sqrt{\text{MSE}}$ of $\widehat{\text{FF}}$ (solid line) and of $\widehat{\text{CV}}^2$ (dash-dotted line) in percents in estimating from repeated trials (upper panels) and in estimating from single spike train (lower panels). ISIs follow gamma (left) and IG (right) distributions with mean one and with various values of FF. In estimation from repeated trials, every error is calculated based on 1000 estimates, obtained from 1000 trials. In estimation from a single spike train, the values of the errors are calculated based on 1000 estimates.

variability (approximately for FF < 0.25), when $\widehat{\text{CV}}^2$ seems to be more accurate than $\widehat{\text{FF}}$. In the second case, MSE of $\widehat{\text{FF}}$ is rarely lower than MSE of $\widehat{\text{CV}}^2$. However, this occurs mainly for small τ and FF around one, when the used lower limit for t (3 means of ISIs, which in practice is still too low) is applied.

4.2.4. *Influence of refractory period on* $\widehat{\text{FF}}$. We have shown that both relative and absolute refractory periods have strong influence on the behavior of the function FF_t. Here we explore the practical consequence in FF estimation. We compare MSE of $\widehat{\text{FF}}$ for gamma distribution of T and for IG distribution of T with added absolute refractory period in dependence on the length of the observation window t. These probability distributions are very different from the point of view of refractory period - the first one has no absolute refractory period and, for FF > 1, also no relative refractory period and the second one has always both types of refractory periods. However, their mean and FF (including the refractory period in the case of IG distribution) are set to be the same. The MSE comparison is in Fig. 8. The error is lower for T with "larger" refractory period for FF $= 0.5$ and vice versa

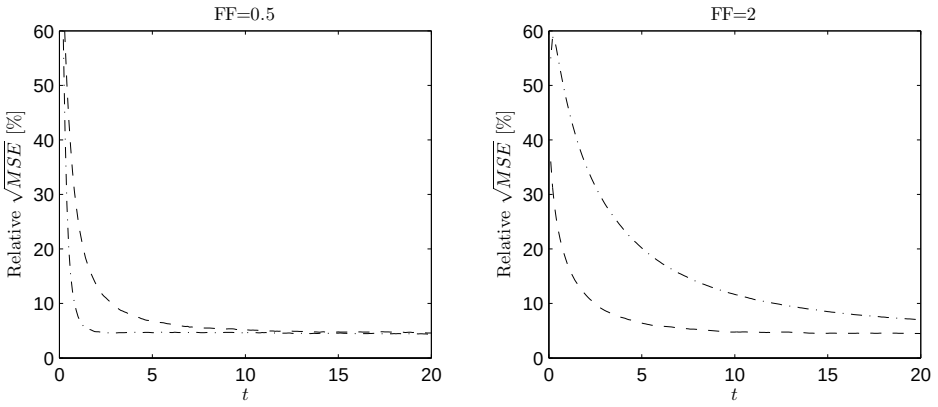

FIGURE 8. Relative $\sqrt{\mathrm{MSE}}$ of $\widehat{\mathrm{FF}}$ in percents for gamma distribution of T without absolute refractory period (dashed) and for IG distribution of T with absolute refractory period (dash-dotted) in dependence on the length of the observation window t. Mean of T is always one and the value of FF is 0.5 (left) and 2 (right) (all including the refractory period of length 0.1 in the case of IG distribution). The errors are calculated based on 1000 values of $\widehat{\mathrm{FF}}$, each estimated from 1000 generated spike trains of relevant length.

for FF = 2. Moreover, in the latter situation, the difference in error is very large. This can be easily understood, refractory period causes an initial decrease of FF_t, thus the convergence to FF is accelerated if FF < 1 (approximately, for FF slightly below one the decrease may be too large) and reduced if FF > 1.

5. **Choice of the observation window.**

5.1. **Estimation from independent trials.** Repeated trials are used mainly in measuring the response to a stimulus. The stimulus causes a change of the character of the spike train, including its variability, which we want to measure. However, this change lasts only for a short time so there is the demand of short observation windows. It of course contradicts with the demand of sufficiently large observation window which is important from the point of view of the accuracy of the FF estimator. Thus, we aim mainly to answer the question how short the observation window can be so that the estimator is still sufficiently accurate.

In this situation, the problem of the estimator is its strong bias for short window length t. It may be approximately expressed as the difference $\mathrm{FF}_t - \mathrm{FF}$, therefore the behavior of the function FF_t is crucial. A theoretical possibility how to measure the bias and select a suitable t is to use the bias approximation from formula (21). However, in practice we do not have the necessary information about the spike trains (e.g., $\mathrm{E}(T^3)$ and of course FF) and thus the observation window must be chosen only heuristically based on general knowledge of FF_t.

From presented illustrations of FF_t, it is obvious that very short trials (e.g., shorter than the mean of the ISIs) are clearly almost always inappropriate. However, this problem complicates in the presence of a refractory period. As was shown, both relative and absolute refractory periods causes the FF_t to be initially lower than one independently of FF. Moreover, if FF > 1 then, even for relatively large observation

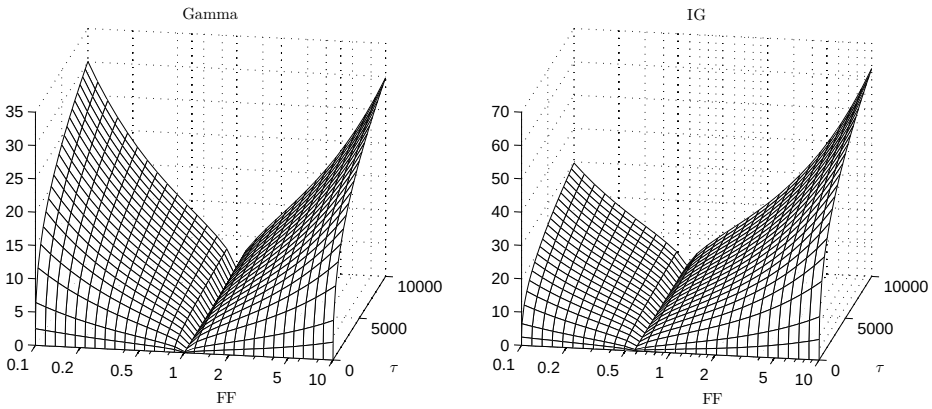

FIGURE 9. Values of t which minimize formula (21) in dependence on FF and length of the spike train τ. ISIs follow gamma (left) and IG (right) distributions with mean one. The FF-axis is logarithmically scaled.

windows, presence of the refractory period, while preserving the value of FF, causes a very large increase of the error of $\widehat{\mathrm{FF}}$ (see Fig. 8). Thus, in selection of window size, absence or presence of the refractory period should be taken into account.

The second characteristic of the spike trains which has large influence on FF_t is the value of FF itself. For $\mathrm{FF} \leq 1$, the length of the observation window about $5 - 10$ means of ISIs, as suggested in [18], can be mostly appropriate. The same value of t seems to be sufficient for $\mathrm{FF} > 1$, if there is no refractory period (as for the gamma distribution, see Fig. 2). The most problematic situation is for $\mathrm{FF} > 1$ in presence of a refractory period. The observation window should be larger than in the previous cases. However, its length cannot be specified more precisely.

5.2. **Estimation from single spike train.** In this situation, the selection of a suitable t for spike train segmentation is the compromise between larger bias and larger variance of $\widehat{\mathrm{FF}}$. We have shown that there is some t which minimizes $\mathrm{MSE}(\widehat{\mathrm{FF}})$ (we denote it by t_o) and this minimum can be approximated using formula (21). For illustration, we approximate t_o for spike trains with various length τ and various values of FF (see Fig. 9).

Again, we see that some values of t_o are too small for practical use. It is caused by the fact that MSE is minimized just for a specific value of FF. In practice, we do not know, of course, the value of FF and thus it is not possible to use direct minimization of relationship (21). However, we can find such a window that $\mathrm{MSE}(\widehat{\mathrm{FF}})$ is acceptable for a range of possible values of FF. This range may be deduced from a preliminary estimate of FF obtained using estimator (5) with a heuristically chosen value of t. We also do not know the values of $\mathrm{E}(T)$ and $\mathrm{E}(T^3)$ for formula (21), but it is now possible to estimate them.

Let us illustrate the described procedure on an example. Suppose that we have a spike train with the following estimates: $\widehat{\mathrm{E}}(T) = 1$, $\widehat{\mathrm{E}}(T^3) = 6$ and $\widehat{\mathrm{FF}} = 1$ and we want to find t which would provide more precise estimate of FF (more precise estimator). It should hold that $\mathrm{MSE}(\widehat{\mathrm{FF}})$ is low for $\mathrm{FF} = 1$ and also for sufficiently wide range of values around one (e.g. for interval $[0.5, 2]$). We plot this situation

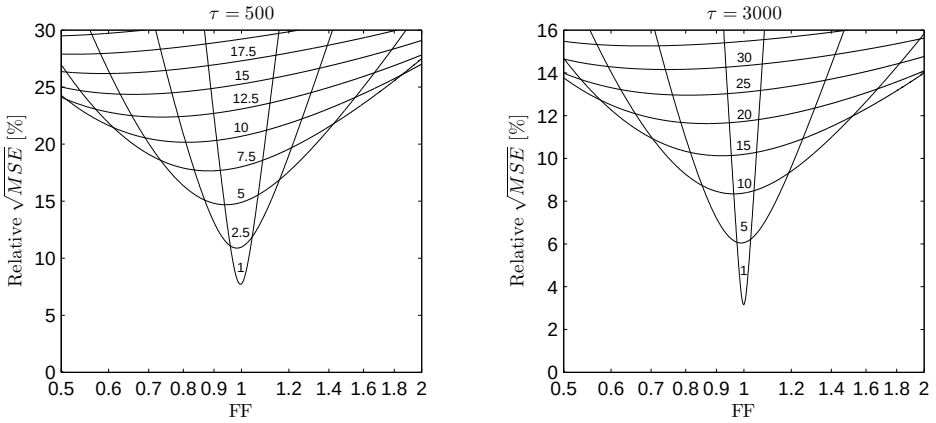

FIGURE 10. Relative $\sqrt{\mathrm{MSE}}$ of $\widehat{\mathrm{FF}}$ in percents in dependence on FF in estimation from single spike train with fixed length τ for various window length t, calculated using (21) ($\mathrm{E}(T) = 1$, $\mathrm{E}(T^3) = 6$, $\tau = 500$ (left) and 3000 (right)). Every curve corresponds to a value of t, these values are displayed in the figures. FF-axis is logarithmically scaled.

for two values of τ, and various values of t (see Fig. 10). The choice of a suitable t now depends on what properties of the estimator $\widehat{\mathrm{FF}}$ we expect. For example, for $\tau = 500$ and $t < 5$, MSE is for many values of FF too large. On the other hand, MSE is unnecessarily large for most likely values of FF (around one) when $t > 10$. Thus, t about 7.5 seems to be a suitable compromise. Analogously, a good choice for $\tau = 3000$ could be $t = 15$.

6. **Conclusions.** We have focused on Fano factor estimation using the standard estimator under the assumption that the spike train satisfies the definition of equilibrium renewal process. Two usual types of neuronal data, repeated trials and single spike train, were considered. In both situations, the accuracy of the estimator strongly depends on the length of the observation window t and so its right choice is important.

In estimating from independent trials, the main problem is the bias of the estimator for short t. We have shown that, beside the value of FF, also refractory period has crucial effect on its value. To be able to avoid the bias, it is important to know the behavior of the function FF_t. However, this information is in practice limited, so it is necessary at least to assume a range of possible values of FF and whether or not the refractory period plays a role. In estimating from a single spike train, we have to take into account also the variance, thus there is a window size t which is optimal from the point of view of the mean square error. This optimal t can be approximated using derived MSE formula.

Because of the property $\mathrm{CV}^2 = \mathrm{FF}$, which holds for renewal processes, we have also compared the accuracy of the estimator of FF with the standard estimator of CV^2. There is no systematic preference, however, in estimation from repeated trials, $\widehat{\mathrm{FF}}$ is mostly more precise than $\widehat{\mathrm{CV}}^2$ and vice versa in estimation from single spike trains.

There is still a possibility to extend this work using different models of spike train, more general or realistic than a renewal process. For example, correlation of ISIs, which is not included in renewal processes, is often observed in experiments [10] and, as was shown in [1, 2], it has a large effect on the dependency of the FF estimate on the length of the observation window.

Appendix A. Proof of properties (16) and (17).

Proof. Here we prove properties (16) and (17). To that end, we modify formula (12), using (11), into the form

$$\begin{aligned} \mathrm{FF}_t &= 1 + \frac{\mathrm{E}(T)}{t}\mathrm{E}[N_t(N_t-1)] - \frac{t}{\mathrm{E}(T)} \\ &= 1 + \frac{\mathrm{E}(T)}{t}\sum_{n=2}^{\infty} n(n-1)P_n(t) - \frac{t}{\mathrm{E}(T)}, \end{aligned} \tag{28}$$

where $P_n(t)$ denotes the probability that n spikes occur in an interval of length t. Then

$$\begin{aligned} \frac{\mathrm{dFF}_t}{\mathrm{d}t} &= -\frac{\mathrm{E}(T)}{t^2}\sum_{n=2}^{\infty} n(n-1)P_n(t) \\ &\quad + \frac{\mathrm{E}(T)}{t}\sum_{n=2}^{\infty} n(n-1)\frac{\mathrm{d}P_n(t)}{\mathrm{d}t} - \frac{1}{\mathrm{E}(T)} \qquad (29) \\ &= \frac{\mathrm{E}(T)}{t}\sum_{n=2}^{\infty} n(n-1)\left(\frac{\mathrm{d}P_n(t)}{\mathrm{d}t} - \frac{P_n(t)}{t}\right) - \frac{1}{\mathrm{E}(T)}. \qquad (30) \end{aligned}$$

Next we use the Laplace transform. It holds, [13],

$$\mathcal{L}\{P_n\}(s) = \frac{(1-\tilde{f}(s))^2(\tilde{f}(s))^{n-1}}{s^2\mathrm{E}(T)} \tag{31}$$

and

$$\mathcal{L}\left\{\frac{\mathrm{d}P_n(t)}{\mathrm{d}t}\right\}(s) = s\mathcal{L}\{P_n\}(s), \tag{32}$$

where equation (32) can be directly derived from the definition of the Laplace transform.

From relationships (15), (31), (32) and using one of Abel and Tauber theorems, which expresses the similarity of behavior of

$$\frac{h(t)}{t^m}, \text{ for } t \to 0^+$$

and

$$\frac{s^{m+1}\mathcal{L}\{h\}(s)}{m!}, \text{ for } s \to \infty,\ m \in \mathbb{N}_0,$$

[13, 21], where as the function $h(t)$ we use $P_n(t)$ and $f(t)$, we further obtain

$$\lim_{t\to 0^+} \frac{\mathrm{E}(T)}{t}\sum_{n=2}^{\infty} n(n-1)\left(\frac{\mathrm{d}P_n(t)}{\mathrm{d}t} - \frac{P_n(t)}{t}\right) = 0,$$

which with formula (30) yields (16).

Finally, in presence of a refractory period of length $r > 0$, it holds $P_n(t) = 0$ for $t \le r$, $n \ge 2$, thus using (28) we get (17). □

Appendix B. Proof of relationship (21).

Proof. In this appendix we derive relationship (21). We use formula (20) and derive firstly formulas for the bias and the variance. We start with bias, thus we need a formula for $\mathrm{E}(\widehat{\mathrm{FF}})$. Estimators $s^2_{N_t}$ and $\overline{N}_t$ in definition (5) are unbiased estimators of $\mathrm{Var}(N_t)$ and $\mathrm{E}(N_t)$, thus

$$\mathrm{E}(s^2_{N_t}) = \mathrm{Var}(N_t),\ \mathrm{E}(\overline{N}_t) = \mathrm{E}(N_t) \tag{33}$$

and using the law of large numbers

$$s^2_{N_t} \to \mathrm{Var}(N_t),\ \overline{N}_t \to \mathrm{E}(N_t),\ \text{for } n \to \infty. \tag{34}$$

That implies

$$\mathrm{E}(\widehat{\mathrm{FF}}) \approx \mathrm{FF}_t,\ \text{for } n \to \infty. \tag{35}$$

Then from formulas (9) and (35) we get

$$\mathrm{Bias}(\widehat{\mathrm{FF}}) \approx \frac{1}{t}\left[\frac{\mathrm{E}(T)}{2}\left(1+\frac{\mathrm{Var}(T)}{\mathrm{E}^2(T)}\right)^2 - \frac{1}{3}\frac{\mathrm{E}(T^3)}{\mathrm{E}^2(T)}\right], \quad \text{for } t\to\infty,\ n\to\infty. \tag{36}$$

Formula for the variance of $\widehat{\mathrm{FF}}$ we find assuming normality of N_t, which holds for $t \to \infty$. Then, [16],

$$\frac{n-1}{\mathrm{Var}(N_t)}s^2_{N_t} \sim \chi^2(n-1), \quad \overline{N}_t \sim N\left(\mathrm{E}(N_t), \frac{\mathrm{Var}(N_t)}{n}\right),$$

where $N(\mathrm{E}(N_t), \mathrm{Var}(N_t)/n)$ denotes the Gaussian (normal) distribution with mean $\mathrm{E}(N_t)$ and variance $\mathrm{Var}(N_t)/n$ and $\chi^2(n-1)$ denotes the Chi-squared distribution with $n-1$ degrees of freedom. Therefore

$$\mathrm{Var}(\overline{N}_t) = \frac{\mathrm{Var}(N_t)}{n},\ \mathrm{Var}(s^2_{N_t}) = \frac{2\mathrm{Var}^2(N_t)}{n-1}. \tag{37}$$

Next, from relationships (33), (37) and from independence of $s^2_{N_t}$ and $\overline{N_t}$ (from normality of N_t) we get

$$\begin{aligned}\mathrm{Var}(\widehat{\mathrm{FF}}) = \mathrm{Var}\left(\frac{s^2_{N_t}}{\overline{N}_t}\right) &\approx \frac{\mathrm{E}^2(s^2_{N_t})}{\mathrm{E}^2(\overline{N}_t)}\left[\frac{\mathrm{Var}(s^2_{N_t})}{\mathrm{E}^2(s^2_{N_t})} + \frac{\mathrm{Var}(\overline{N}_t)}{\mathrm{E}^2(\overline{N}_t)}\right] = \\ &= \frac{\mathrm{Var}^2(N_t)}{\mathrm{E}^2(N_t)}\left[\frac{2}{n-1} + \frac{\mathrm{Var}(N_t)}{n\mathrm{E}^2(N_t)}\right], \quad \text{for } t\to\infty, n\to\infty,\end{aligned} \tag{38}$$

where we used approximation (first order Taylor expansion)

$$\mathrm{Var}\left(\frac{R}{S}\right) \approx \frac{\mathrm{E}^2(R)}{\mathrm{E}^2(S)}\left[\frac{\mathrm{Var}(R)}{\mathrm{E}^2(R)} - \frac{2(\mathrm{Cov}(R,S))}{\mathrm{E}(R)\mathrm{E}(S)} + \frac{\mathrm{Var}(S)}{E^2(S)}\right], \tag{39}$$

where S and R are arbitrary positive continuous random variables.

Now we have formulas for both bias (36) and variance (38) and thus we can put them into relationship (20),

$$\begin{aligned}\mathrm{MSE}(\widehat{\mathrm{FF}}) \approx \frac{1}{t^2}&\left[\frac{\mathrm{E}(T)}{2}\left(1+\frac{\mathrm{Var}(T)}{\mathrm{E}^2(T)}\right)^2 - \frac{1}{3}\frac{\mathrm{E}(T^3)}{\mathrm{E}^2(T)}\right]^2 \\ &+ \frac{\mathrm{Var}^2(N_t)}{\mathrm{E}^2(N_t)}\left[\frac{2}{n-1} + \frac{\mathrm{Var}(N_t)}{n\mathrm{E}^2(N_t)}\right], \quad \text{for } t\to\infty,\ n\to\infty.\end{aligned} \tag{40}$$

Further, $\mathrm{E}(N_t)$ we replace with (11) and for $\mathrm{Var}(N_t)$ we use another asymptotic relationship, [5],

$$\mathrm{Var}(N_t) \approx \frac{\mathrm{Var}(T)}{\mathrm{E}^3(T)}t + \frac{1}{2}\left(1 + \frac{\mathrm{Var}(T)}{\mathrm{E}^2(T)}\right)^2 - \frac{1}{3}\frac{\mathrm{E}(T^3)}{\mathrm{E}^3(T)}, \quad \text{for } t \to \infty. \tag{41}$$

So we obtain the final formula (instead of $\mathrm{Var}(T)/\mathrm{E}^2(T) = \mathrm{CV}^2$ we write FF)

$$\begin{aligned}\mathrm{MSE}(\widehat{\mathrm{FF}}) \approx{}& \left[\frac{1}{t}\mathrm{E}(T)\mathrm{G}(T)\right]^2 \\ &+ \frac{\mathrm{E}^2(T)}{t^2}\left[\frac{2}{n-1} + \frac{\mathrm{E}^2(T)}{nt^2}\left(\mathrm{G}(T) + \frac{\mathrm{FF}}{\mathrm{E}(T)}t\right)\right] \\ &\cdot \left[\mathrm{G}(T) + \frac{\mathrm{FF}}{\mathrm{E}(T)}t\right]^2, \ \text{for } t \to \infty,\ n \to \infty,\end{aligned} \tag{42}$$

where

$$\mathrm{G}(T) = \frac{1}{2}(1 + \mathrm{FF})^2 - \frac{1}{3}\frac{\mathrm{E}(T^3)}{\mathrm{E}^3(T)}. \tag{43}$$

□

Acknowledgments. This work was supported by the Institute of Physiology RVO: 67985823, the Centre for Neuroscience P304/12/G069 and by the Grant Agency of the Czech Republic P103/11/0282.

REFERENCES

[1] O. Avila-Akerberg and M. J. Chacron, *Nonrenewal spike train statistics: Causes and functional consequences on neural coding*, Exp. Brain Res., **210** (2011), 353–371.

[2] M. J. Chacron, A. Longtin and L. Maler, *Negative interspike interval correlations increase the neuronal capacity for encoding time-dependent stimuli*, J. Neurosci., **21** (2001), 5328–5343.

[3] M. H. Chang, K. M. Armstrong and T. Moore, *Dissociation of response variability from firing rate effects in frontal eye field neurons during visual stimulation, working memory, and attention*, J. Neurosci. Methods, **32** (2012), 2204–2216.

[4] M. M. Churchland, B. M. Yu, J. P. Cunningham, L. P. Sugrue, M. R. Cohen, G. S. Corrado, W. T. Newsome, A. M. Clark, P. Hosseini, B. B. Scott, D. C. Bradley, M. A. Smith, A. Kohn, J. A. Movshon, K. M. Armstrong, T. Moore, S. W. Chang, L. H. Snyder, S. G. Lisberger, N. J. Priebe, I. M. Finn, D. Ferster, S. I. Ryu, G. Santhanam, M. Sahani and K. V. Shenoy, *Stimulus onset quenches neural variability: A widespread cortical phenomenon*, Nat. Neurosci., **13** (2010), 369–378.

[5] D. R. Cox, "Renewal Theory," Methuen & Co., Ltd., London; John Wiley & Sons, Inc., New York, 1962.

[6] O. Darbin, J. Soares and T. Wichmann, *Nonlinear analysis of discharge patterns in monkey basal ganglia*, Brain Res., **1118** (2006), 84–93.

[7] M. Deger, M. Helias, C. Boucsein and S. Rotter, *Statistical properties of superimposed stationary spike trains*, J. Comput. Neurosci., **32** (2012), 443–463.

[8] S. Ditlevsen and P. Lansky, *Firing variability is higher than deduced from the empirical coefficient of variation*, Neural. Comput., **23** (2011), 1944–1966.

[9] U. T. Eden and M. A. Kramer, *Drawing inferences from fano factor calculations*, J. Neurosci. Methods, **190** (2010), 149–152.

[10] F. Farkhooi, M. F. Strube-Bloss and M. P. Nawrot, *Serial correlation in neural spike trains: Experimental evidence, stochastic modeling, and single neuron variability*, Phys. Rev. E, **79** (2009), 021905.

[11] W. Gerstner and W. M. Kistler, "Spiking Neuron Models. Single Neurons, Populations, Plasticity," Cambridge University Press, Cambridge, 2002.

[12] C. Hussar and T. Pasternak, *Trial-to-trial variability of the prefrontal neurons reveals the nature of their engagement in a motion discrimination task*, P. Natl. Acad. Sci. USA, **107** (2010), 21842–21847.

[13] W. S. Jewell, *The properties of recurrent-event processes*, Oper. Res., **8** (1960), 446–472.
[14] L. Kostal, P. Lansky and O. Pokora, *Variability measures of positive random variables*, PLOS ONE, **6** (2011), e21998.
[15] S. Koyama and S. Shinomoto, *Inference of intrinsic spiking irregularity based on the Kullback-Leibler information*, BioSystems, **89** (2007), 69–73.
[16] A. M. Mood, F. A. Graybill and D. C. Boes, "Introduction to the Theory of Statistics," McGraw-Hill, Inc., 1974.
[17] M. P. Nawrot, *Analysis and interpretation of interval and count variability in neural spike trains*, in "Analysis of Parallel Spike Trains," Springer, Inc., New York, (2010), 37–58.
[18] M. P. Nawrot, C. Boucsein, V. R. Molina, A. Riehle, A. Aertsen and S. Rotter, *Measurement of variability dynamics in cortical spike trains*, J. Neurosci. Methods, **169** (2008), 374–390.
[19] T. Omi and S. Shinomoto, *Optimizing time histograms for non-Poissonian spike trains*, Neural. Comput., **23** (2011), 3125–3144.
[20] Z. Pawlas, L. B. Klebanov, M. Prokop and P. Lansky, *Parameters of spike trains observed in a short time window*, Neural. Comput., **20** (2008), 1325–1343.
[21] B. V. D. Pol and H. Bremmer, "Operational Calculus Based on the Two-Sided Laplace Integral," Cambridge University Press, Cambridge, 1950.
[22] A. Ponce-Alvarez, B. E. Kilavik and A. Riehle, *Comparison of local measures of spike time irregularity and relating variability to firing rate in motor cortical neurons*, J. Comput. Neurosci., **29** (2010), 351–365.
[23] T. Shimokawa and S. Shinomoto, *Estimating instantaneous irregularity of neuronal firing*, Neural. Comput., **21** (2009), 1931–1951.
[24] S. Shinomoto, K. Miura and S. Koyama, *A measure of local variation of inter-spike intervals*, BioSystems, **79** (2005), 67–72.
[25] M. C. Teich, D. H. Johnson, A. R. Kumar and R. G. Turcott, *Rate fluctuations and fractional power-law noise recorded from cells in the lower auditory pathway of the cat*, Hearing Res., **46** (1990), 41–52.

Received December 23, 2012; Accepted December 26, 2012.

E-mail address: xrajdl@math.muni.cz
E-mail address: lansky@biomed.cas.cz

Publication II

Biol Cybern
DOI 10.1007/s00422-015-0650-x

ORIGINAL PAPER

Biological Cybernetics

Stein's neuronal model with pooled renewal input

Kamil Rajdl[1] · **Petr Lansky**[1,2]

Received: 14 November 2014 / Accepted: 8 April 2015

Abstract The input of Stein's model of a single neuron is usually described by using a Poisson process, which is assumed to represent the behaviour of spikes pooled from a large number of presynaptic spike trains. However, such a description of the input is not always appropriate as the variability cannot be separated from the intensity. Therefore, we create and study Stein's model with a more general input, a sum of equilibrium renewal processes. The mean and variance of the membrane potential are derived for this model. Using these formulas and numerical simulations, the model is analyzed to study the influence of the input variability on the properties of the membrane potential and the output spike trains. The generalized Stein's model is compared with the original Stein's model with Poissonian input using the relative difference of variances of membrane potential at steady state and the integral square error of output interspike intervals. Both of the criteria show large differences between the models for input with high variability.

Keywords Stein's model · Neural input · Poisson process · Pooled renewal processes · First-passage time

1 Introduction

Stein's model is a well-known and often-used tool for the description of neuronal membrane potential and spike generation (Stein 1965; Smith and Smith 1984; Tuckwell 1988; Hohn and Burkitt 2001; Burkitt 2006a; Smith 2010). It belongs to the wide group of leaky integrator models that have two main common features—they transform the input signal into the membrane potential by its integration and assume that the potential spontaneously returns to a resting value, usually by rate of an exponential decay. The leaky integrator mechanism is consistent with current injection experiments (Gerstner and Kistler 2002). In Stein's model, the input is directly formed by discrete spikes (their arrival times), so the corresponding amplitudes of excitatory or inhibitory postsynaptic potentials (EPSPs, IPSPs) are integrated. The membrane potential trajectory is thus a piecewise exponential curve with discontinuities (jumps) at times at which the input spikes arrive. The primary aim of Stein's model is not the direct description of the membrane potential, but the description of the output sequence of spikes. This sequence consists of spikes which are generated as soon as the potential reaches a given threshold. At these first-passage times (FPTs), the membrane potential is instantaneously reset to the resting (reset) level and the integration of input starts over again, sometimes after a refractory period. In this form, the model was introduced in Stein (1965); however, since then various modifications have been proposed. For example, random amplitudes of PSPs are sometimes considered (Musila and Lansky 1991; Richardson and Swarbrick 2010; Smith 2010). Well-known and often-studied modification in the direction of closer biological relevance is Stein's model with reversal potentials (Tuckwell 1979; Burkitt 2001; Di Crescenzo and Martinucci 2007; Jahn et al. 2011). The frequently employed diffusion approximations of the Stein's model, in which the character of stochasticity changes to the Gaussian white noise (Ricciardi and Sacerdote 1979; Lansky 1984; Richardson and Gerstner 2005, 2006; Benedetto and Sacerdote 2013; Cupera

Kamil Rajdl
xrajdl@math.muni.cz

[1] Department of Mathematics and Statistics, Faculty of Science, Masaryk University, Kotlarska 2, 611 37 Brno, Czech Republic

[2] Institute of Physiology, Academy of Sciences of the Czech Republic, Videnska 1083, 142 20 Prague 4, Czech Republic

Published online: 25 April 2015

2014; Giorno and Spina 2014), stem out from the Poissonian character of the input.

Although there are numerous variants of Stein's model, one feature mostly prevails—the input spikes are described using a Poisson process (Gaussian white noise in the case of the diffusion approximations), more complex models of neuronal input are less frequent (Salinas and Sejnowski 2000; Gomez et al. 2005; Lindner et al. 2005; Burkitt 2006b; Ly and Tranchina 2009; Droste and Lindner 2014). One reason for this choice is surely simplicity; a lot of properties can be easily derived and analyzed. However, the more important reason is that a Poisson process can often be a suitable approximation of the real neuronal input. This is because the incoming spikes originate from many presynaptic neurons, and thus they can be viewed as pooled from multiple parallel spike trains (see Fig. 1). This causes their behaviour to appear to be near to a Poisson process even if the behaviour of the individual spike trains is not. This assumption is based on the well-known property of renewal processes, such that their sum converges to a Poisson process (Cox 1962). This convergence is important as the output of Stein's model with Poissonian input is generally a renewal process. Thus, in a homogeneous network of such neurons, the pooled input of every neuron can be theoretically approximated by a Poisson process. Let us stress that the proof of the convergence theorem requires scaling of time which fixes total intensity with increasing number of pooled processes. Otherwise, it was shown that without the scaling, the sum preserves some non-Poissonian characteristics (Lindner 2006).

Despite the above reasons, restriction to a Poisson process might not always be appropriate. Even if the pooled input converges to a Poisson process, it is not clear what the rate of the convergence is and, consequently, whether the standard (Poissonian) Stein's model is sufficiently accurate for a given number of inputs. Moreover, with the Poissonian input, we cannot explore the influence of changing variability on Stein's model. In such a case the variability and frequency coding cannot be separated (Kostal et al. 2007a,b; Shinomoto and Koyama 2007). This is because all properties of a Poisson process are uniquely determined by its intensity, and thus it is not possible to model variously variable spike trains. As a result, variability of the membrane potential is also limited.

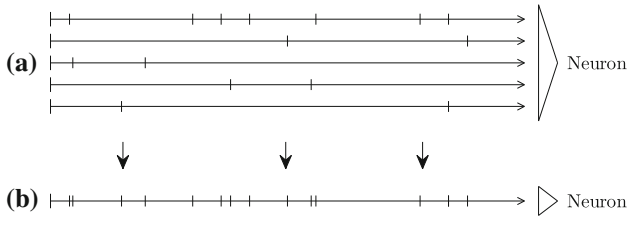

Fig. 1 Pooling of neuronal input. **a** Parallel spike trains which create input of a neuron. **b** Single spike train representing pooled input

To overcome these limitations and to explore the question of the Poissonian input adequacy, we study Stein's model with a more flexible input, a sum of equilibrium renewal processes. Thus, instead of exponentially distributed interspike intervals (ISIs), which are associated with a Poisson process, we assume that the input spike trains can have arbitrary distribution of ISIs. We focus especially on gamma distribution, probably the most often used probability distribution for the modeling of ISIs (Nawrot et al. 2008; Shimokawa et al. 2010; Ditlevsen and Lansky 2011; Omi and Shinomoto 2011; Ostojic 2011; Koyama and Kostal 2014; Levakova et al. 2014). This distribution can be parameterized using intensity and variability represented by the coefficient of variation (CV, ratio of the standard deviation of lengths of ISIs to their mean). It is, therefore, suitable for exploring the influence of input variability independent of intensity. A significant insufficiency of the Poissonian approximation for pooled in vivo data was observed in Deger et al. (2012). It is shown that the match of the model with the data can be largely increased by using a Poisson processes with dead-time. This process is also a simple renewal process, thus these findings indicate potential suitability of the more general model we consider.

In this paper, we firstly derive the formulas for the mean and variance of membrane potential of the generalized Stein's model. Using them, we analyze the model from the point of view of the influence of input variability on the membrane potential and compare it with the corresponding properties of the standard Stein's model. This comparison is based on two criteria, similarity of the membrane potential variances at the steady state and similarity of the distributions of output ISIs. The similarity of the output ISIs is measured by using the integral square error of their distribution functions obtained from numerical simulations. Both of the criteria show that the approximation of pooled input using a Poisson process is not always suitable, mainly if the variability of the single inputs is high.

2 Model of input individual spike trains

As it was mentioned, we assume that every input spike train can be described as an equilibrium renewal process. It means that the lengths of ISIs are independent and identically distributed continuous random variables denoted by T with probability density function (pdf) $f(t)$. The term "equilibrium" specifies that the time zero is unrelated to the sequence of spikes. In such a situation, the time up to the first input spike is called forward recurrence time and it has generally different probability distribution from T (Cox 1962). This assumption is reasonable for a neuron with several inputs, but must be taken with care for a few inputs only. There, time zero coincides with the spike at one of the input trains.

To quantify the variability of T we use a standard measure called coefficient of variation, which is defined as

$$\mathrm{CV} = \frac{\sqrt{\mathrm{Var}(T)}}{\mathrm{E}(T)}, \tag{1}$$

where $\mathrm{E}(T)$ and $\mathrm{Var}(T)$ denote the mean and variance of T.

The random (counting) process which describes the number of spikes in an interval $(0, t]$, $t > 0$, is denoted $N(t)$. Hence, $N(t)$ represents the number of spikes in an interval which is "randomly positioned" with respect to the sequence of spikes. However, we also define the random process $N_o(t)$ representing the number of spikes in $(0, t]$ under the condition that the time zero is identified with a spike (the corresponding renewal process is called ordinary). In this situation, the time up to the first spike has the same probability distribution as the other ISIs. Asymptotically, for a large t, the position of zero plays no role.

Next, we denote

$$\lambda(t) = \frac{\mathrm{dE}(N(t))}{\mathrm{d}t}, \quad \lambda_o(t) = \frac{\mathrm{dE}(N_o(t))}{\mathrm{d}t}, \tag{2}$$

these functions represent the intensities of the renewal processes at time t. Then, since (Cox 1962)

$$\mathrm{E}(N(t)) = \frac{t}{\mathrm{E}(T)}, \tag{3}$$

it holds

$$\lambda(t) = \lambda = \frac{1}{\mathrm{E}(T)}, \tag{4}$$

which is also the mean number of spikes in an interval of length one. Intensity $\lambda_o(t)$ cannot be generally expressed so easily. One possibility is relationship (Cox 1962)

$$\lambda_o(t) = \sum_{k=1}^{\infty} f_k(t), \tag{5}$$

where $f_k(t)$, $k = 1, 2, \ldots$, is the pdf of the sum of k random variables with density $f(t)$. Using the Laplace transform ($\mathscr{L}$), one can rewrite equation (5) into form

$$\mathscr{L}\{\lambda_o\}(s) = \frac{\mathscr{L}\{f\}(s)}{1 - \mathscr{L}\{f\}(s)}. \tag{6}$$

Note that asymptotically $\lambda(t)$ and $\lambda_o(t)$ coincide, $\lim_{t\to\infty} \lambda_o(t) = \lambda$, and that the only renewal process for which $\lambda_o(t) = \lambda$ for all $t > 0$ is the Poisson process.

Although we work with the assumption that the spike trains behave as a general equilibrium renewal process, we focus mainly on the situation when the ISIs have gamma probability distribution (gamma process). This distribution can be parameterized using λ and CV, the pdf of the ISIs has the form

$$f(t) = \frac{t^{1/\mathrm{CV}^2-1}\mathrm{e}^{-\lambda t/\mathrm{CV}^2}}{\Gamma(1/\mathrm{CV}^2)(\mathrm{CV}^2/\lambda)^{1/\mathrm{CV}^2}}, \quad t \geq 0, \tag{7}$$

where Γ denotes the gamma function. Let us note that for the $\mathrm{CV} = 1$ function (7) is the pdf of exponential distribution and the corresponding renewal process is a Poisson process. The value of CV in Eq. (7) indicates how much the gamma process differs from the Poisson process. For CV close to zero, there is a tendency towards regularity, whereas for CV significantly larger than one the process gets clustered (bursting input activity).

3 Stein's model with pooled renewal input

One of the most commonly used descriptions of the membrane potential behavior is the leaky integration mechanism, which can be deduced from the complete Hodgkin–Huxley model (Kistler et al. 1997). The incoming signals, either in the form of the postsynaptic potentials or others, for sensory neurons, move the membrane potential, $S(t)$, towards the spike threshold (depolarization) or away from it (hyperpolarization). In the absence of the input, the potential decays proportionally to its value to the resting potential (S_R). Spiking is not an intrinsic part of the model and thus a firing threshold has to be imposed. If the threshold is reached, the neuron fires and the potential is instantaneously reset to a level (S_0), usually the resting potential. Many variants of the model described above exists (Burkitt 2006a,b). Formally, for the voltage holds

$$\frac{\mathrm{d}S}{\mathrm{d}t} = -\frac{S - S_R}{\tau} + (\text{input}), \quad S(0) = S_0, \tag{8}$$

where time zero coincides with the moment of voltage reset after the last spike and $\tau > 0$ is the membrane time constant. With a stochastic input, the solution of Eq. (8) is a random process $S(t)$. Basic information about the process in the absence of the threshold can be obtained from its properties at steady state, $S = \lim_{t\to\infty} S(t)$.

Equation (8) describes the membrane potential only until it reaches the threshold $\theta > S_0$. The time of its first passage can be defined as

$$T_\theta = \inf\{t \geq 0; \quad S(t) \geq \theta\}. \tag{9}$$

As mentioned, we assume that at time T_θ the value of $S(t)$ is reset to level S_0. Comparing θ and $\mathrm{E}(S)$, two regimes are distinguished, suprathreshold for $\theta < \mathrm{E}(S)$ and subthreshold for $\theta > \mathrm{E}(S)$. The main difference between them is that in the subthreshold regime a random noise is necessary for reaching the threshold. This noise may originate, for example, from randomness in the input ISIs or PSPs. For completeness, note

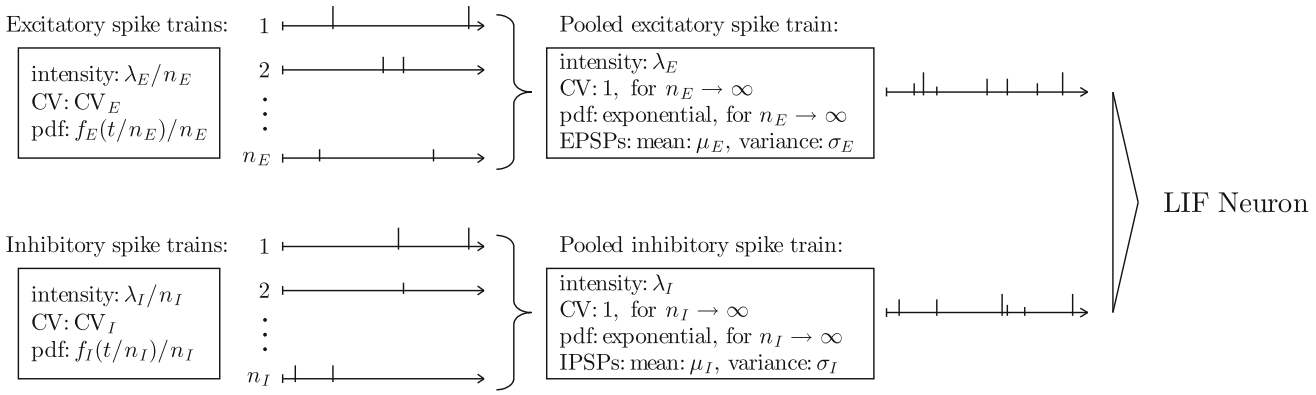

Fig. 2 Model of neuronal input and its properties

that the remaining possible situation when $\theta = \mathrm{E}(S)$ is called the threshold regime.

To obtain a specific model it is necessary to characterize the input in Eq. (8). The standard Stein's model describes it using two mutually independent Poisson processes $N^E(t)$ and $N^I(t)$ representing the arrival times of excitatory and inhibitory pulses. The corresponding stochastic differential equation for the voltage can be written in the form

$$\mathrm{d}S = -\frac{S - S_R}{\tau}\,\mathrm{d}t + A\mathrm{d}N^E(t) + B\mathrm{d}N^I(t), \quad S(0) = S_0, \tag{10}$$

where A, B are (generally random) values of PSPs amplitudes. For simplicity, as model (10) is space homogeneous, we assume that $S_R = S_0 = 0$. Then, Eq. (10) has explicit solution

$$S(t) = \sum_{i=1}^{N^E(t)} A_i \mathrm{e}^{-\frac{t-X_i}{\tau}} - \sum_{i=1}^{N^I(t)} B_i \mathrm{e}^{-\frac{t-Y_i}{\tau}}, \tag{11}$$

where X_i, $i = 1, \ldots, N^E(t)$, and Y_i, $i = 1, \ldots, N^I(t)$, are the arrival times of input spikes and A_i, B_i are corresponding values of PSP amplitudes.

This model is simple and thus contains some aspects which might be too large simplifications of reality; two of them are as follows. Firstly, in reality, the input spikes originate from many presynaptic neurons. However, model (11) directly describes the pooled spikes, using two Poisson processes, and so it ignores the specific character and number of the individual inputs. Secondly, in a more precise description, the sizes of amplitudes of PSPs, in the standard Stein's model taken to be constant, would depend on the presynaptic neuron they originate from; in other words, on the location of the synapse.

We remove the first simplification and, instead of working directly with the pooled input, we take into account the character of the individual spike trains. To that purpose, we model the input using n_E excitatory renewal processes $N_j^E(t)$, $j = 1, \ldots, n_E$, and n_I inhibitory renewal processes $N_j^I(t)$, $j = 1, \ldots, n_I$. The model is illustrated in Fig. 2 and more specific details are as follows. All processes N_j^E correspond to one type of equilibrium renewal process and the same holds for processes $N_j^I(t)$. Next, the sum of intensities is fixed even with changing n_E and n_I. It is ensured by suitable scaling of time in the single inputs. Denote the pdfs of ISIs in the spike trains on the condition that there are n_E and n_I of them as $f_E(t; n_E)$ and $f_I(t; n_I)$, then we set

$$f_E(t; n_E) = \frac{1}{n_E} f_E\left(\frac{t}{n_E}\right), \quad f_I(t; n_I) = \frac{1}{n_I} f_I\left(\frac{t}{n_I}\right), \tag{12}$$

where $f_E(t) = f_E(t; 1)$ and $f_I(t) = f_I(t; 1)$. Because of this scaling, the pooled input converges with increasing n_E and n_I to two Poisson processes for arbitrary distribution of ISIs (Cox 1962). The intensities and CVs corresponding to $f_E(t)$ and $f_I(t)$ are denoted as λ_E, λ_I, CV_E and CV_I. With increasing n_E and n_I, the intensities of the individual spike trains decrease to λ_E/n_E and λ_I/n_I, but the CVs remain constant. Let us mention that, for a fixed n_E and n_I, the pooled input is not a renewal process (except for pooled Poisson processes), mainly because the ISIs are not independent (Câteau and Reyes 2006; Lindner 2006).

With such a description of input, it is possible to model more realistically the sizes of amplitudes of PSPs, e.g., to assign a (constant) value to every input spike train. Starting from this idea, however, for simplification, we follow the standard approach (Tuckwell 1988) and assume that in the pooled input the values of amplitudes are mutually independent and identically distributed random variables (generally different for EPSPs and IPSPs). This can be explained so that after pooling there is no information about the presynaptic neurons the PSPs originate from, so their values appear to be random. Note that the amplitudes are defined as random variables already in the individual spike trains. It does not change the properties of the model, but simplifies its mathe-

matical description. The size of amplitude of ith PSP in jth excitatory spike train we denote as $A_{i,j}$ and analogously $B_{i,j}$ denotes the amplitudes of IPSPs. Next, it is assumed that

$$\mathrm{E}(A_{i,j}) = \mu_E, \quad \mathrm{Var}(A_{i,j}) = \sigma_E^2, \tag{13}$$

$$\mathrm{E}(B_{i,j}) = \mu_I, \quad \mathrm{Var}(B_{i,j}) = \sigma_I^2, \tag{14}$$

for all indexes i and j. Later, we will often consider situations when some characteristics of the excitatory and inhibitory inputs are equal. In such a case we denote $n = n_E = n_I$, $\mu = \mu_E = \mu_I$, $\sigma = \sigma_E = \sigma_I$ and $\mathrm{CV} = \mathrm{CV}_E = \mathrm{CV}_I$.

To reflect the described model, Eq. (11) can be rewritten into form

$$S(t) = \sum_{j=1}^{n_E} \sum_{i=1}^{N_j^E(t)} A_{i,j} \mathrm{e}^{-\frac{t-X_{i,j}}{\tau}} - \sum_{j=1}^{n_I} \sum_{i=1}^{N_j^I(t)} B_{i,j} \mathrm{e}^{-\frac{t-Y_{i,j}}{\tau}}, \tag{15}$$

where $X_{i,j}$, $j = 1, \ldots, n_E$, $i = 1, \ldots, N_j^E(t)$, and $Y_{i,j}$, $j = 1, \ldots, n_I$, $i = 1, \ldots, N_j^I(t)$, are the arrival times of the input spikes. This model can be seen as a generalization of the standard Stein's model (11), they coincide for $n_E = n_I = 1$ and Poissonian arrival times. The main question is how the more complex description of input changes the behaviour of $S(t)$. Of course, it is necessary to compare the behaviour of the membrane potential under the condition that the intensities of the (pooled) excitatory and inhibitory spike trains are the same for both of the models. In such a situation, the membrane potential of the standard Stein's model with Poissonian input is denoted as $S_P(t)$.

4 Mean and variance of the membrane potential

Here, formulas for mean and variance of $S(t)$ defined by Eq. (15) are presented; for details, see "Appendix". The following holds,

$$\mathrm{E}(S(t)) = \tau(\mu_E\lambda_E - \mu_I\lambda_I)\left(1 - \mathrm{e}^{-\frac{t}{\tau}}\right), \tag{16}$$

$$\mathrm{E}(S) = \tau(\mu_E\lambda_E - \mu_I\lambda_I), \tag{17}$$

$$\begin{aligned}\mathrm{Var}(S(t)) = {} & \mu_E^2 \frac{\lambda_E}{n_E} \int_0^t \int_0^t \mathrm{e}^{-\frac{x+y}{\tau}} \left(\lambda_o^E\left(\frac{|y-x|}{n_E}\right) - \lambda_E\right) \mathrm{d}x\,\mathrm{d}y \\ & + \mu_I^2 \frac{\lambda_I}{n_I} \int_0^t \int_0^t \mathrm{e}^{-\frac{x+y}{\tau}} \left(\lambda_o^I\left(\frac{|y-x|}{n_I}\right) - \lambda_I\right) \mathrm{d}x\,\mathrm{d}y \\ & + \frac{1}{2}\tau\left(\mu_E^2\lambda_E + \mu_I^2\lambda_I\right)\left(1 - \mathrm{e}^{-\frac{2t}{\tau}}\right) \\ & + \frac{1}{2}\tau\left(\sigma_E^2\lambda_E + \sigma_I^2\lambda_I\right)\left(1 - \mathrm{e}^{-\frac{2t}{\tau}}\right),\end{aligned} \tag{18}$$

where $\lambda_o^E(t)$ and $\lambda_o^I(t)$ are intensities (5) corresponding to excitatory and inhibitory spike trains, and

$$\begin{aligned}\mathrm{Var}(S) = {} & \frac{\mu_E^2\lambda_E\tau}{1 - \mathscr{L}\{f_E\}(n_E/\tau)} + \frac{\mu_I^2\lambda_I\tau}{1 - \mathscr{L}\{f_I\}(n_I/\tau)} \\ & - \tau^2\left(\mu_E^2\frac{\lambda_E^2}{n_E} + \mu_I^2\frac{\lambda_I^2}{n_I}\right) - \frac{1}{2}\tau\left(\mu_E^2\lambda_E + \mu_I^2\lambda_I\right) \\ & + \frac{1}{2}\tau\left(\sigma_E^2\lambda_E + \sigma_I^2\lambda_I\right).\end{aligned} \tag{19}$$

The formulas for mean (16) and (17) are very simple, independent of both pdfs of ISIs (except for the intensities) and the number of input spike trains. Hence, they coincide with the corresponding formulas for the standard Stein's model. In other words, $S(t)$ and $S_P(t)$ are equivalent from the point of view of the mean. On the other hand, the variance given by relationship (18) is more complex than the standard form (20). The limit value described by formula (19) can be obtained easily, the only problematic part there could be the Laplace transforms of pdfs of ISIs, but for many probability distributions they exist in closed form.

For Poissonian input the relationships (18) and (19) simplify into known formulas

$$\begin{aligned}\mathrm{Var}(S_P(t)) = {} & \frac{1}{2}\tau\left(\mu_E^2\lambda_E + \mu_I^2\lambda_I\right)\left(1 - \mathrm{e}^{-\frac{2t}{\tau}}\right) \\ & + \frac{1}{2}\tau\left(\sigma_E^2\lambda_E + \sigma_I^2\lambda_I\right)\left(1 - \mathrm{e}^{-\frac{2t}{\tau}}\right)\end{aligned} \tag{20}$$

and

$$\mathrm{Var}(S_P) = \frac{1}{2}\tau\left(\lambda_E\left(\mu_E^2 + \sigma_E^2\right) + \lambda_I\left(\mu_I^2 + \sigma_I^2\right)\right). \tag{21}$$

For gamma input, the relationship (18) is still complicated; however, from Eq. (19) relatively simple expression of the limit variance is obtained

$$\begin{aligned}\mathrm{Var}(S) = {} & \frac{\mu_E^2\lambda_E\tau}{1 - \left(1 + \frac{n_E\mathrm{CV}_E^2}{\lambda_E\tau}\right)^{-\frac{1}{\mathrm{CV}_E^2}}} + \frac{\mu_I^2\lambda_I\tau}{1 - \left(1 + \frac{n_I\mathrm{CV}_I^2}{\lambda_I\tau}\right)^{-\frac{1}{\mathrm{CV}_I^2}}} \\ & - \tau^2\left(\mu_E^2\frac{\lambda_E^2}{n_E} + \mu_I^2\frac{\lambda_I^2}{n_I}\right) - \frac{1}{2}\tau\left(\mu_E^2\lambda_E + \mu_I^2\lambda_I\right) \\ & + \frac{1}{2}\tau\left(\sigma_E^2\lambda_E + \sigma_I^2\lambda_I\right).\end{aligned} \tag{22}$$

In Fig. 3, there are illustrations of the variance of $S(t)$ for gamma input in dependence on t for various values of CV. We can see, that $\mathrm{Var}(S(t))$ converges relatively quickly to the limit value (22). The speed of the convergence depends on τ, the exact general dependence is not clear, but formula (20) implies that the rate is approximately exponential with rate constant $2/\tau$.

5 Analysis of variance of asymptotic membrane potential

The generalized Stein's model can be analyzed and compared to the standard variant from the point of view of various aspects. A simple but useful one seems to be the variance of the membrane potential at the steady state, $\mathrm{Var}(S)$. Its main advantage is that it suitably reflects the variability of the input ISIs, and for the gamma distribution it can be easily calculated using formula (22).

First, notice the influence of variance of PSPs amplitudes on $\mathrm{Var}(S)$. It is very simple as σ_E^2 and σ_I^2 affect only the last member of formula (19) and increase $\mathrm{Var}(S)$ linearly.

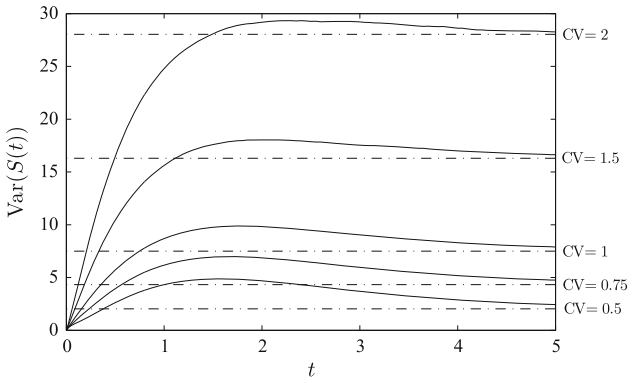

Fig. 3 Variance of the membrane potential for gamma distribution of input ISIs in dependency on time. *Full lines* $\mathrm{Var}(S(t))$ for various values of $\mathrm{CV} = \mathrm{CV}_E = \mathrm{CV}_I$ (0.5, 0.75, 1, 1.5, 2). Values of other parameters, common for all the curves, are $n_E = n_I = 1$, $\lambda_E = 10$, $\lambda_I = 5$, $\mu_E = \mu_I = 1, \sigma_E = \sigma_I = 0$, $\tau = 1$. *Dash-dotted lines* corresponding values of $\mathrm{Var}(S)$

The influence of CV of input, n_E and n_I on $\mathrm{Var}(S)$ is separated from the variance of PSPs, thus next it is assumed that $\sigma_E = \sigma_I = 0$.

The dependency of $\mathrm{Var}(S)$ on CV of input ISIs is more complicated, its illustration for various inputs is shown in Fig. 4a. We can see that the variability of ISIs strongly influences the variability of the steady state membrane potential, namely for small numbers of input spike trains. Note that for $n = 1$ and $\mathrm{CV} \to 0$ $\mathrm{Var}(S)$ is small but nonzero, although the input ISIs are constant. The remaining variability is caused by the randomness of time to the first input spike. The $\mathrm{Var}(S)$ curves resemble power law relationships; however, with increasing n they converge to the constant variance of the standard Stein's model. To explore the rate of this convergence more precisely, relative deviation is defined

$$\rho(n_E, n_I) = \frac{\mathrm{Var}(S) - \mathrm{Var}(S_P)}{\mathrm{Var}(S_P)} \tag{23}$$

and illustrated (see Fig. 4b). The value of $\rho(n_E, n_I)$ and its convergence to zero strongly depends on CV, for $\mathrm{CV} < 1$ the deviation can be low enough from about 100 pooled spike trains. On the other hand, the rate of the convergence quickly decreases with increasing CV and for high CV many more inputs are necessary to obtain low value of $\rho(n_E, n_I)$.

6 Analysis of output ISIs distribution

Until now we focused only on the value of $S(t)$ without its restriction by a threshold, excess of which causes firing. However, the main purpose of Stein's model is to describe

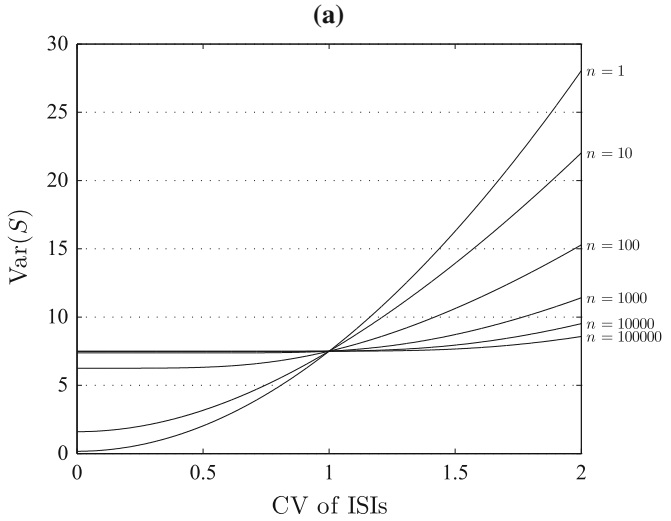

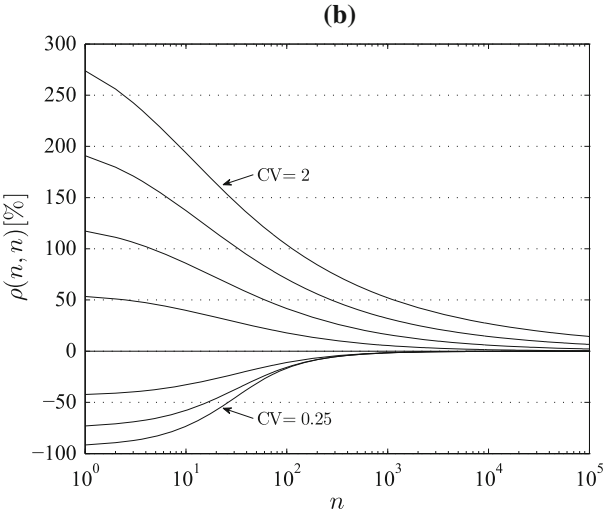

Fig. 4 Comparison of variance of asymptotic membrane potential. Values of parameters used in all panels are: $\tau = 1$, $\mu_E = \mu_I = 1$, $\sigma_E = \sigma_I = 0$, $\lambda_E = 10$ and $\lambda_I = 5$. **a** Values of $\mathrm{Var}(S)$ in dependence on CV of input ISIs for various values of $n = n_E = n_I$. **b** Function $\rho(n, n)$ for various values of CV of input ISIs (from bottom to top: 0.25, 0.5, 0.75, 1, 1.25, 1.5, 1.75, 2), n-axis is logarithmically scaled

properties of the output sequence of spikes. This sequence is not generally a renewal process; for example, the output ISIs may not be independent. Thus, the distribution of the random variable T_θ, representing the FPT, does not fully determine the properties of the output spike train. It lacks any information about the ISIs correlations, which may be an important property of the spike train (Dummer et al. 2014). Nevertheless, we use T_θ for a simple comparison of the standard and generalized Stein's model. There are no theoretical formulas for the properties of T_θ (e.g., the moments), hence we judge them from numerical simulations. In the following experiments, every illustrated value was calculated based on 10,000 realizations of T_θ corresponding to Steins's model with gamma or Poissonian input. For the parameters we use the following values, $\tau = 1$, $\mu_E = \mu_I = 1$, $\lambda_E = 10$, $\lambda_I = 5$, $\sigma_E = \sigma_I = 0$ and $\theta \in \{4, 6\}$. The purpose of the two values of θ, 4 and 6, is to simulate both the suprathreshold and subthreshold regime, as in this setting $\mathrm{E}(S) = 5$.

Firstly, in Fig. 5a, b, the dependencies of mean and CV of T_θ on CV of input ISIs for various values of n in the suprathreshold regime are shown. For $n = 1$ we can see the known behaviour of the output of leaky-integrator models, with increasing variability of the input, both the intensity and variability of output increase. With increasing n, all the values converge to values which correspond to Poissonian input. The rate of convergence decreases with increasing CV. For $\mathrm{CV} < 1$, 100 pooled inputs yield similar results to Poissonian input. On the other hand, for large CV, even 1000 inputs do not provide such precision.

Next, in Fig. 5c, d, the same characteristics of T_θ are presented but in the subthreshold regime. The behaviour of T_θ is relatively similar to the one in the suprathreshold regime, but the higher importance of noise in the input ISIs for reaching the threshold is apparent. Both the values of $\mathrm{E}(T_\theta)$ and their range for given CVs are significantly larger than in the corresponding situation in the suprathreshold regime.

In the previous illustrations, we can see the rate of convergence of the first two moments of T_θ to the corresponding values of Stein's model with Poissonian input. However, we would like also to compare the whole distributions of T_θ. For that purpose, we use the integral square error defined as

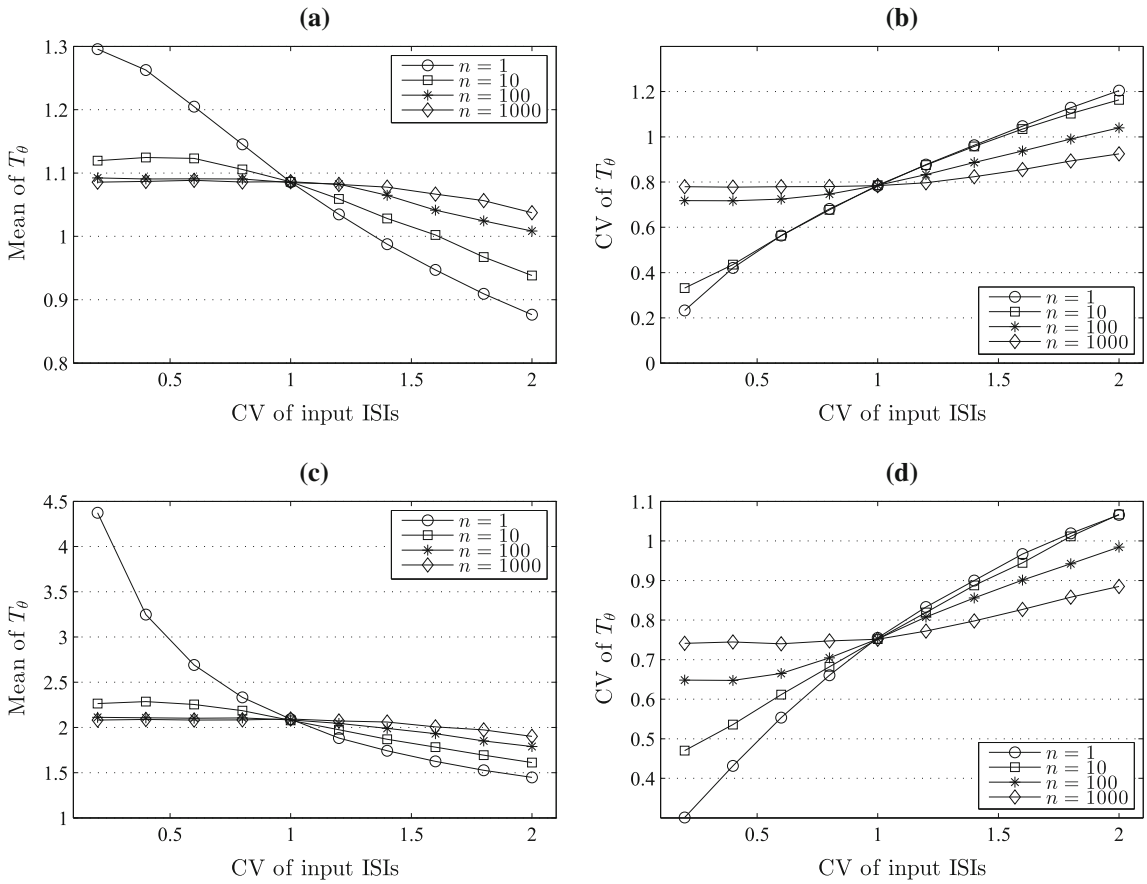

Fig. 5 Mean and CV of output ISIs. Values of parameters used in all panels are: $\tau = 1$, $\mu_E = \mu_I = 1$, $\lambda_E = 10$, $\lambda_I = 5$, $\sigma_E = \sigma_I = 0$ and $\theta = 4$ for the suprathreshold regime and $\theta = 6$ for the subthreshold regime. **a**, **b** Mean and CV of T_θ in dependence on CV of input ISIs for various values of $n = n_E = n_I$ for the suprathreshold regime. **c**, **d** Mean and CV of T_θ in dependence on CV of input ISIs for various values of $n = n_E = n_I$ for the subthreshold regime

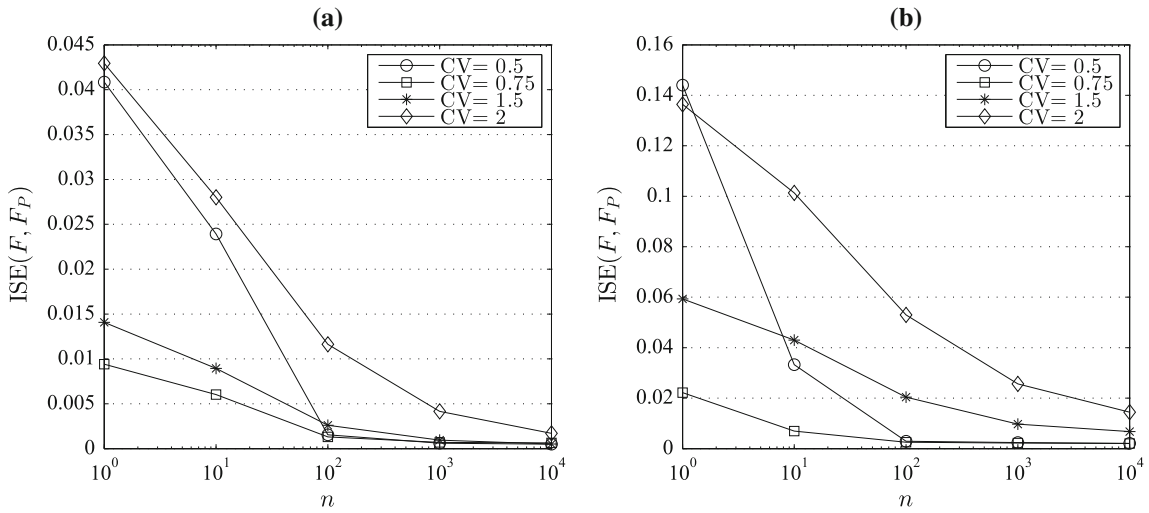

Fig. 6 Integral square error of distribution functions of output ISIs of standard and generalized Stein's model dependent on $n = n_E = n_I$ for various CV of input ISIs (0.5, 0.75, 1.5, 2) in subthreshold (**a**) and suprathreshold (**b**) regime. Values of other parameters panels are: $\tau = 1$, $\mu_E = \mu_I = 1$, $\lambda_E = 10$, $\lambda_I = 5$, $\sigma_E = \sigma_I = 0$ and $\theta = 4$ for the suprathreshold regime and $\theta = 6$ for the subthreshold regime

$$\mathrm{ISE}(F, F_P) = \int_0^\infty (F(t) - F_P(t))^2 \,\mathrm{d}t, \tag{24}$$

where $F(t)$ and $F_P(t)$ are distribution functions of FPT of the generalized Stein's model and of its standard variant. This error is illustrated in Fig. 6a (suprathreshold regime) and Fig. 6b (subthreshold regime). Similar results were already obtained using the variance of S. Initially, for low n, the farther the CV is from one the larger the error is. With increasing n the error decreases, although much faster for CV < 1 than for high CV (which causes intersection of the error curves), e.g., for CV $= 2$ some differences between the models are apparent even for $n = 10{,}000$.

7 Discussion and conclusions

We examined the appropriateness of the often used assumption that pooled neuronal input can be approximated using a Poisson process. To that purpose, we defined a more general model of input, consisting of time-scaled equilibrium renewal processes, and studied its influence on a variant of Stein's model. We focused mainly on input created by pooled gamma processes, which is a suitable extension of the Poissonian input, allowing to change variability independently of intensity.

Firstly, note that we presented the results by using some specific "dimensionless" sets of parameters of the model. The time parameters were in units of the time constant and the voltage parameters in units of the size of the PSPs. As an example of the time parameters in real time units, consider the following situation. Let us set $\tau = 10$ ms, then from the used values of λ_E and λ_I (10 and 5) we obtain that the mean of ISIs in the excitatory spike trains is n_E ms and in the inhibitory spike trains $2n_I$ ms. This, considering 1000 excitatory inputs and 500 inhibitory inputs, implies that each of the individual inputs has an average rate 1 Hz.

The scaling is an important part of our results. It ensures the convergence of the input to a Poisson process; however, there is also the question of realism of such an approach. The main issue emerges when examining the input–output relationship, as in Sect. 6. There, with increasing n, the mean of output ISIs varies relatively little, but the mean of ISIs in the single input spike trains grows to infinity. Then even for realistic values of n, e.g., 10,000, the ratio of the mean of the input ISIs to the mean of the output ISIs reaches very large values. Assuming the above example ($\tau = 10$ ms) and situations from Fig. 5, we obtain the output ISIs on the order of tens of milliseconds, but lengths of the ISIs in the individual inputs on the order of tens of seconds. Such a difference is not usual for a typical neuron, and thus the results have to be interpreted carefully. The model precisely corresponds to the convergence theorem, which is often used to justify the description of the neuronal input by using a Poisson process (Burkitt 2006a). Hence, any discrepancies between this model and the standard Stein's model indicate a fundamental insufficiency of the approximation. It is probably even increased for models in some way differing from these assumptions, in order to achieve larger realism. The alternative possibility how to study pooled spike trains, directly without the scaling, is also problematic because of the increasing total intensity of input, causing increasing output firing rate. The basic problem is also the fact that the intensity changes complicate the comparison of such a model to a fixed Stein's model with

Poissonian input. Some studies which consider other models of neural spike trains, more complex than a Poisson process, or assess the suitability of the Poisson approximation can be found e.g., Salinas and Sejnowski (2000), Moreno et al. (2002), Rocha et al. (2004), Câteau and Reyes (2006), Lindner (2006), Ly and Tranchina (2009) and Avila-Akerberg and Chacron (2011).

Let us emphasize that there are some other aspects of this study which should be taken into account before making any conclusions. Mainly, only a simple variant of Stein's model was used, and thus there is a possibility that the effect of the generalized input would be different for a more complex model. For example, in the presence of the reversal potentials the influence of the additional variability might be distinct. Note also that after neuron fires, one of the input spike trains would be better described as an ordinary renewal process than as a process in equilibrium. For a small number of inputs, this might cause some inaccuracies; however, for more inputs these inaccuracies should be negligible.

In the paper, the mean and variance of the membrane potential for the generalized model were derived. From the point of view of mean, Poisson input and pooled renewal input are equivalent. The complete formula for the time-dependent variance is relatively complicated, but a simple expression was found for its steady state. Based on the expression, it was shown that large discrepancies emerge for the variances. Stein's model with gamma input can yield, in dependence on CV of input ISIs, membrane potential with very distinct variance from the corresponding version of the model with Poissonian input. The Poisson process can be a suitable model if the differences are sufficiently small for a large number of pooled inputs. We showed that this seems to hold for CV ≤ 1, the differences in this case almost vanish from about 100 inputs. Nevertheless, for high variable ISIs (CV > 1), more inputs are necessary to obtain small deviation. For example, for CV about two, even tens of thousands of pooled inputs yield a relatively large difference in the variances.

Although the variance of the membrane potential is an important characteristic of the models, the more important criterion for their comparison is the probability distribution of the output ISIs. We studied its mean, variance and measured the differences between the distributions using the integral square error. The results we obtained are similar to those based on the variance of the membrane potential, values of deviations highly depend on CV and for large CV the error decreases with increasing number of inputs more slowly than for CV < 1.

To summarize, the presented results imply that a Poisson process cannot be always taken as a sufficiently accurate model of pooled neuronal input. Mainly, if the single inputs exhibit large variability, the results obtained based on Stein's model with Poissonian input could be misleading even if the number of pooled inputs is high. In such a situation, some model which allows changing the variability independently of intensity, e.g., the model presented here, should be used.

Acknowledgments This work was supported by the Czech Science Foundation 15-06991S and by the Institute of Physiology RVO: 67985823.

Appendix

Here we derive formulas for mean and variance of $S(t)$ and S. It is clearly sufficient to derive mean and variance of quantity

$$\tilde{S}(t) = \sum_{i=1}^{N(t)} A_i \mathrm{e}^{-\frac{t-X_i}{\tau}}, \tag{25}$$

where $N(t)$ and X_i, $i = 1, \ldots, N(t)$, correspond to an equilibrium renewal process with intensity λ and A_i, $i = 1, \ldots, N(t)$, are positive independent and identically distributed random variables with mean μ and variance σ^2. The formulas (16), (17), (18) and (19) will be simple consequences.

Firstly, let us denote,

$$\tilde{S}_0(t) = \sum_{i=1}^{N(t)} \mathrm{e}^{-\frac{t-X_i}{\tau}} \tag{26}$$

and have $\Delta t > 0$ and points $t_i = i\Delta t$, $i = 0, \ldots, \lfloor t/\Delta t \rfloor$. The number of events in interval $[t_{i-1}, t_i)$ is denoted as N_i, $i = 1, \ldots, \lfloor t/\Delta t \rfloor$. Then

$$\tilde{S}_0(t) = \lim_{\Delta t \to 0} \sum_{i=1}^{\lfloor t/\Delta t \rfloor} N_i \mathrm{e}^{-\frac{t-t_i}{\tau}}, \tag{27}$$

and thus

$$\begin{aligned} \mathrm{E}(\tilde{S}_0(t)) &= \lim_{\Delta t \to 0} \sum_{i=1}^{\lfloor t/\Delta t \rfloor} \mathrm{E}(N_i) \mathrm{e}^{-\frac{t-t_i}{\tau}} = \lim_{\Delta t \to 0} \sum_{i=1}^{\lfloor t/\Delta t \rfloor} \lambda \Delta t \mathrm{e}^{-\frac{t-t_i}{\tau}} \\ &= \lambda \int_0^t \mathrm{e}^{-\frac{t-x}{\tau}} \, \mathrm{d}x = \lambda\tau \left(1 - \mathrm{e}^{-\frac{t}{\tau}}\right), \end{aligned} \tag{28}$$

which simply yields

$$\mathrm{E}(\tilde{S}(t)) = \mu\lambda\tau \left(1 - \mathrm{e}^{-\frac{t}{\tau}}\right). \tag{29}$$

Before deriving the formulas for variance, a necessary relationship is presented. It holds (Cox and Lewis 1966)

$$\lim_{\Delta t \to 0} \frac{\mathrm{Cov}(\Delta N_t, \Delta N_{t+x})}{\Delta t^2} = \lambda(\lambda_o(x) - \lambda + \delta(x)), \tag{30}$$

where ΔN_t denotes the number of events in interval $[t, t+\Delta t]$ and $\delta(x)$ is the Dirac delta function. Note that in neuronal modeling the function (30) is known as correlation function of the spike train (Gerstner and Kistler 2002). Then

$$\begin{aligned}\mathrm{Var}(\tilde{S}_0(t)) &= \lim_{\Delta t\to 0}\sum_{i=1}^{\lfloor t/\Delta t\rfloor}\sum_{j=1}^{\lfloor t/\Delta t\rfloor} \mathrm{e}^{-\frac{t-t_i}{\tau}}\mathrm{e}^{-\frac{t-t_j}{\tau}}\,\mathrm{Cov}(N_i,N_j)\\ &= \lim_{\Delta t\to 0}\sum_{i=1}^{\lfloor t/\Delta t\rfloor}\Delta t\,\mathrm{e}^{-\frac{t-t_i}{\tau}}\sum_{j=1}^{\lfloor t/\Delta t\rfloor}\Delta t\,\mathrm{e}^{-\frac{t-t_j}{\tau}}\,\frac{\mathrm{Cov}(N_i,N_j)}{\Delta t^2}\\ &= \lambda\int_0^t\int_0^t \mathrm{e}^{-\frac{x+y}{\tau}}(\lambda_o(|y-x|)-\lambda)\,\mathrm{d}x\,\mathrm{d}y\\ &\quad+\frac{1}{2}\lambda\tau(1-\mathrm{e}^{-\frac{2t}{\tau}}).\end{aligned} \tag{31}$$

Next,

$$\begin{aligned}\mathrm{Var}(\tilde{S}(t)) &= \mathrm{Var}\left(\sum_{i=1}^{N(t)}A_i\mathrm{e}^{-\frac{t-X_i}{\tau}}\right)=\sum_{i=1}^{N(t)}\mathrm{Var}\left(A_i\mathrm{e}^{-\frac{t-X_i}{\tau}}\right)\\ &\quad+\sum_{i=1}^{N(t)}\sum_{\substack{j=1\\ j\neq i}}^{N(t)}\mathrm{Cov}\left(A_i\mathrm{e}^{-\frac{t-X_i}{\tau}},A_j\mathrm{e}^{-\frac{t-X_j}{\tau}}\right)\\ &= \mu^2\mathrm{Var}(\tilde{S}_0(t))+\sigma^2\mathrm{E}\left(\sum_{i=1}^{N(t)}\mathrm{e}^{-2\frac{t-X_i}{\tau}}\right)\\ &= \mu^2\lambda\int_0^t\int_0^t\mathrm{e}^{-\frac{x+y}{\tau}}(\lambda_o(|y-x|)-\lambda)\,\mathrm{d}x\,\mathrm{d}y\\ &\quad+\frac{1}{2}\mu^2\lambda\tau\left(1-\mathrm{e}^{-\frac{2t}{\tau}}\right)+\frac{1}{2}\sigma^2\lambda\tau\left(1-\mathrm{e}^{-\frac{2t}{\tau}}\right).\end{aligned} \tag{32}$$

Finally, we derive the limit of the previous relationship for $t\to\infty$. Using formula (5) we obtain

$$\begin{aligned}\lim_{t\to\infty}\mathrm{Var}(\tilde{S}(t)) &= 2\mu^2\lambda\tau\int_0^\infty\mathrm{e}^{-\frac{2x}{\tau}}\sum_{k=1}^{\infty}\int_0^\infty\mathrm{e}^{-\frac{y}{\tau}}f_k(y)\,\mathrm{d}y\,\mathrm{d}x\\ &\quad-\mu^2\lambda^2\tau^2+\frac{1}{2}\mu^2\lambda\tau+\frac{1}{2}\sigma^2\lambda\tau\\ &= \frac{\mu^2\lambda\tau}{1-\mathscr{L}\{f\}(1/\tau)}-\mu^2\lambda^2\tau^2-\frac{1}{2}\mu^2\lambda\tau\\ &\quad+\frac{1}{2}\sigma^2\lambda\tau.\end{aligned} \tag{33}$$

References

Avila-Akerberg O, Chacron MJ (2011) Nonrenewal spike train statistics: causes and functional consequences on neural coding. Exp Brain Res 210:353–371

Benedetto E, Sacerdote L (2013) On dependency properties of the ISIs generated by a two-compartmental neuronal model. Biol Cybern 107:95–106

Burkitt AN (2001) Balanced neurons: analysis of leaky integrate-and-fire neurons with reversal potentials. Biol Cybern 85:247–255

Burkitt AN (2006a) A review of the integrate-and-fire neuron model: I. Homogeneous synaptic input. Biol Cybern 95:1–19

Burkitt AN (2006b) A review of the integrate-and-fire neuron model: II. Inhomogeneous synaptic input and network properties. Biol Cybern 95:97–112

Câteau H, Reyes AD (2006) Relation between single neuron and population spiking statistics and effects on network activity. Phys Rev Lett 96:058101

Cox DR (1962) Renewal theory. Methuen & Co., London

Cox DR, Lewis PAW (1966) The statistical analysis of series of events. Chapman & Hall, London

Cupera J (2014) Diffusion approximation of neuronal models revisited. Math Biosci Eng 11:11–25

de la Rocha J, Moreno R, Parga N (2004) Correlations modulate the non-monotonic response of a neuron with short-term plasticity. Neurocomputing 58–60:313–319

Deger M, Helias M, Boucsein C, Rotter S (2012) Statistical properties of superimposed stationary spike trains. J Comput Neurosci 32:443–463

Di Crescenzo A, Martinucci B (2007) Analysis of a stochastic neuronal model with excitatory inputs and state-dependent effects. Math Biosci 209:547–563

Ditlevsen S, Lansky P (2011) Firing variability is higher than deduced from the empirical coefficient of variation. Neural Comput 23:1944–1966

Droste F, Lindner B (2014) Integrate-and-fire neurons driven by asymmetric dichotomous noise. Biol Cybern 108:825–843

Dummer B, Wieland S, Lindner B (2014) Self-consistent determination of the spike-train power spectrum in a neural network with sparse connectivity. Front Comp Neurosci 8:104

Gerstner W, Kistler WM (2002) Spiking neuron models. Cambridge University Press, Cambridge

Giorno W, Spina S (2014) On the return process with refractoriness for a non-homogeneous Ornstein–Uhlenbeck neuronal model. Math Biosci Eng 11:285–302

Gomez L, Budelli R, Saa R, Stiber M, Segundo JP (2005) Pooled spike trains of correlated presynaptic inputs as realizations of cluster point processes. Biol Cybern 92:110–127

Hohn N, Burkitt AN (2001) Shot noise in the leaky integrate-and-fire neuron. Phys Rev E 63:031902

Jahn P, Berg RW, Hounsgaard J, Ditlevsen S (2011) Motoneuron membrane potentials follow a time inhomogeneous jump diffusion process. J Comput Neurosci 31:563–579

Kistler WM, Gerstner W, van Hemmen JL (1997) Reduction of the Hodgkin–Huxley equations to a single-variable threshold model. Neural Comput 9:1015–1045

Kostal L, Lansky P, Rospars JP (2007a) Neuronal coding and spiking randomness. Eur J Neurosci 26:2693–2701

Kostal L, Lansky P, Zucca C (2007b) Randomness and variability of the neuronal activity described by the Ornstein–Uhlenbeck model. Netw Comput Neural 18:63–75

Koyama S, Kostal L (2014) The effect of interspike interval statistics on the information gain under the rate coding hypothesis. Math Biosci Eng 11:63–80

Lansky P (1984) On approximations of Stein's neuronal model. J Theor Biol 107:631–647

Levakova M, Ditlevsen S, Lansky P (2014) Estimating latency from inhibitory input. Biol Cybern 108:475–493

Lindner B (2006) Superposition of many independent spike trains is generally not a Poisson process. Phys Rev E 73:022901

Lindner B, Chacron MJ, Longtin A (2005) Integrate-and-fire neurons with threshold noise: a tractable model of how interspike interval correlations affect neuronal signal transmission. Phys Rev E 72:021911

Ly C, Tranchina D (2009) Spike train statistics and dynamics with synaptic input from any renewal process: a population density approach. Neural Comput 21:360–396

Moreno R, de la Rocha J, Renart A, Parga N (2002) Response of spiking neurons to correlated inputs. Phys Rev Lett 89:288101

Musila M, Lansky P (1991) Generalized Stein's model for anatomically complex neurons. Biosystems 25:179–191

Nawrot MP, Boucsein C, Molina VR, Riehle A, Aertsen A, Rotter S (2008) Measurement of variability dynamics in cortical spike trains. J Neurosci Meth 169:374–390

Omi T, Shinomoto S (2011) Optimizing time histograms for non-poissonian spike trains. Neural Comput 23:3125–3144

Ostojic S (2011) Interspike interval distributions of spiking neurons driven by fluctuating inputs. J Neurophysiol 106:361–373

Ricciardi LM, Sacerdote L (1979) The Ornstein–Uhlenbeck process as a model for neuronal activity, I. Mean and variance of the firing time. Biol Cybern 35:1–9

Richardson MJE, Gerstner W (2005) Synaptic shot noise and conductance fluctuations affect the membrane voltage with equal significance. Neural Comput 17:923–947

Richardson MJE, Gerstner W (2006) Statistics of subthreshold neuronal voltage fluctuations due to conductance-based synaptic shot noise. Chaos 16:026106

Richardson MJE, Swarbrick R (2010) Firing-rate response of a neuron receiving excitatory and inhibitory synaptic shot noise. Phys Rev Lett 105:178102

Salinas E, Sejnowski TJ (2000) Impact of correlated synaptic input on output firing rate and variability in simple neuronal models. J Neurosci 20:6193–6209

Shimokawa T, Koyama S, Shinomoto S (2010) A characterization of the time-rescaled gamma process as a model for spike trains. J Comput Neurosci 29:183–193

Shinomoto S, Koyama S (2007) A solution to the controversy between rate and temporal coding. Stat Med 26:4032–4038

Smith CE, Smith MV (1984) Moments of voltage trajectories for Stein's model with synaptic reversal potentials. J Theor Neurobiol 3:67–77

Smith PL (2010) From Poisson shot noise to the integrated Ornstein–Uhlenbeck process: neurally principled models of information accumulation in decision-making and response time. J Math Psychol 54:266–283

Stein RB (1965) A theoretical analysis of neuronal variability. Biophys J 5:173–194

Tuckwell HC (1979) Synaptic transmission in a model for stochastic neural activity. J Theor Biol 77:65–81

Tuckwell HC (1988) Introduction to theoretical neurobiology: volume 2, nonlinear and stochastic theories. University Press, Cambridge

Publication III

PHYSICAL REVIEW E **92**, 052135 (2015)

Shot-noise Fano factor

Kamil Rajdl* and Petr Lansky
Department of Mathematics and Statistics, Faculty of Science, Masaryk University, Kotlarska 2, 611 37 Brno, Czech Republic
and Institute of Physiology, Academy of Sciences of the Czech Republic, Videnska 1083, 142 20 Prague 4, Czech Republic
(Received 15 June 2015; revised manuscript received 12 October 2015; published 24 November 2015)

A variability measure of the times of uniform events based on a shot-noise process is proposed and studied. The measure is inspired by the Fano factor, which we generalize by considering the time-weighted influence of the events given by a shot-noise response function. The sequence of events is assumed to be an equilibrium renewal process, and based on this assumption we present formulas describing the behavior of the variability measure. The formulas are derived for a general response function, restricted only by some natural conditions, but the main focus is given to the shot noise with exponential decrease. The proposed measure is analyzed and compared with the Fano factor.

DOI: 10.1103/PhysRevE.92.052135 PACS number(s): 02.50.Ey, 05.45.Tp

I. INTRODUCTION

From many experiments or observations, data arise in the form of sequences of times of occurrence of identical events (e.g., radioactive particles emission, accidents, earthquakes, neuronal spikes, arrivals of customers or cars, etc.). The numbers of events in time intervals of a certain length are often examined when analyzing these sequences. For example, the very frequently used variability measure, the Fano factor, is defined as the variance to the mean ratio of numbers of events that occurred up to a time t. The Fano factor was first defined and used in [1] for a slightly different purpose—as a measure of fluctuations of the produced number of ion pairs in a volume of gas. Nevertheless, since then it has been commonly used as a variability measure in many situations, where discrete identical events occur in time. For example, the Fano factor is useful in analysis of natural disasters (earthquakes, fires) [2–4], neural spike trains [5–7], chemical reactions [8,9], or many other phenomena [10–13].

The Fano factor implicitly assumes that all the events have the same effect independently of the times of their occurrence, which may not always be valid. Sometimes, it is more convenient to give a greater influence to the more recent events or to distribute their weights depending on time in some other way. This can be done by employing a function representing the dependence of the weights on time and summing the values of weights corresponding to the single events.

As an example of a scientific field where weighting the events has a transparent empirical reason, let us mention the analysis of neural spike trains. In such an analysis, the Fano factor calculated based on events that occurred in a time window is often supposed to represent the variability that a neuron "registers" at the time corresponding to the end of the window. Nevertheless, a standard property of neurons is that they constantly lose information about the received spikes (the accumulated membrane potential spontaneously decreases). It seems natural, therefore, to improve the Fano factor so that the recent spikes have a larger influence. Most of the standard neuronal models (leaky integrator) describe the "forgetting" using an exponential decay [14], thus a natural choice for the weighting function is a decreasing exponential.

We believe that weighting the events can be convenient in any situation in which the Fano factor is used to measure the instantaneous variability of a series of events, mainly when some "effect" of the events decreases in time. There might not always be a rigorous theoretical justification resulting from the character of the sequences of events, but intuitively the events nearer the time at which the variability is studied should have a larger influence on the measure than the more distant events.

The proposed measure can be formally described as follows. Assuming m time intervals of a length t in which some identical events occur, the "counting" approach yields numbers of events $n_1, \ldots, n_m$ in the individual intervals. On the other hand, the "weighting" approach assesses the occurrence of the events by values $s_1, \ldots, s_m$. Every value $s_i, i = 1, \ldots, m$, is created by summing the weights of the events in every interval. We define the weights using a weighting function w so that the weight $w(t - x)$ is assigned to an event that occurred at a time $x > 0$. A simple example of the weighting function can be a decreasing exponential function, yielding weights $e^{-(t-x)/\tau}$, where $\tau > 0$ is a time constant (for illustration, see Fig. 1).

Using the terminology of filtering theory, the values of s_i arise as the times of the events filtered by a response function $w(x)$, thus as convolution of the (stochastic) counting process describing the events with the function $w(x)$. In this specific case, where the filtered process is created by discrete values, the resulting process is often called shot noise [15]. We define the proposed variability measure analogously to the Fano factor using the values s_i, thus as the variance-to-mean ratio of a shot-noise process. Shot noise has a wide range of applications in many fields [16–22], while it is mostly considered with an exponential distribution of events [23], i.e., the Poisson process. This assumption is too restrictive for our purposes, so we use a more general model, namely an equilibrium renewal process. Two situations are studied: the shot-noise process with an exponential response function, which is the most often used case, and the shot-noise process with a general response function. The renewal shot-noise process was also studied recently in [24,25].

Note that there are also other variability measures of sequences of uniform events such as the very often used coefficient of variation, measures based on entropy or Fisher information [26], or a measure reducing the influence of rate

*xrajdl@math.muni.cz

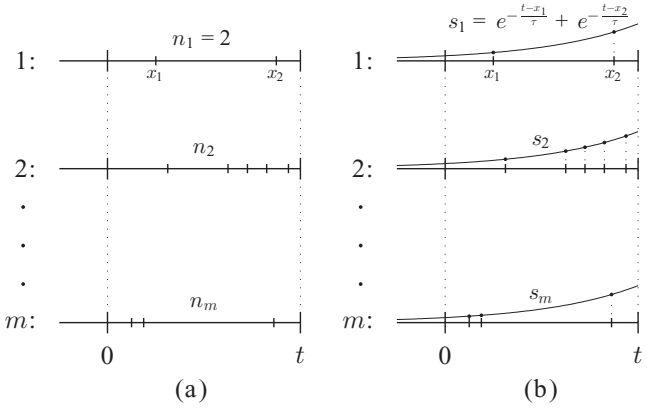

FIG. 1. Data construction based on events that occurred in m time intervals of a length $t > 0$. (a) The events are counted and their numbers $n_1, \ldots, n_m$ obtained. (b) To every event a value is assigned using a weighting (exponential) function, and these values are summed. The individual sums are denoted as $s_1, \ldots, s_m$.

changes [27]. Nevertheless, they all differ from the approach proposed in this article.

II. MODEL OF OCCURRENCE OF EVENTS

First, we specify the considered model of occurrence of events, and we present its properties. The time at which the observation of the events starts is denoted as zero, and the random times at which the events occur are denoted as $X_1, X_2, X_3, \ldots$ [see Fig. 2(a)]. Next, we assume that this sequence can be described as an equilibrium renewal process. Thus, the lengths of intervals between the events [interevent intervals (IEIs)] are independent and identically distributed continuous random variables, denoted by T with the probability density function $f(t)$. The term "equilibrium" moreover specifies that the time zero is unrelated to the sequence of events. In such a situation, the time up to the first event (X_1), i.e., the forward recurrence time, generally has a different probability distribution from T.

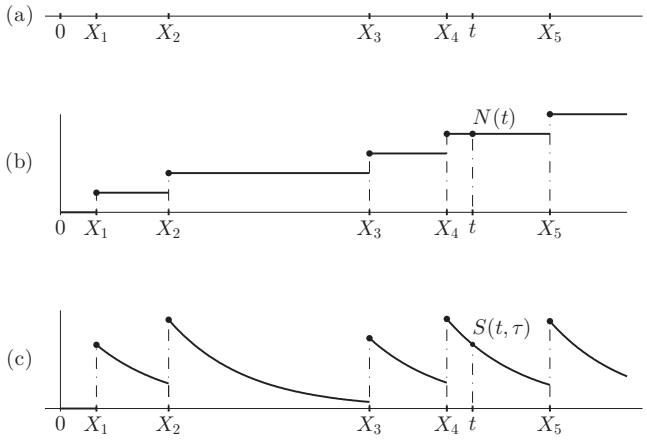

FIG. 2. (a) Illustration of times of events that occurred after time zero. (b) Illustration of the counting process $N(t)$. (c) Illustration of the shot-noise process $S(t,\tau)$ with an exponential response function.

The random process $N(t)$ describes the number of events in an interval $(0, t], t > 0$, where time zero is "randomly positioned" with respect to the sequence of times [see Fig. 2(b)]. The process $N_o(t)$ representing the number of events in $(0, t]$ on the condition that an event occurred at time zero is called an ordinary renewal process. The time up to the first event has, in this situation, the same probability distribution as the IEIs.

Next, we denote the intensity of the renewal process at time t as

$$\mu(t) = \frac{dE(N(t))}{dt}, \quad \mu_o(t) = \frac{dE(N_o(t))}{dt}. \tag{1}$$

Then, since [28]

$$E(N(t)) = \frac{t}{E(T)}, \tag{2}$$

it holds that

$$\mu(t) = \mu = \frac{1}{E(T)}, \tag{3}$$

which is also the mean number of events in an interval of unit length. The function $\mu_o(t)$ cannot be generally expressed so easily. One possibility is the relationship [28]

$$\mu_o(t) = \sum_{k=1}^{\infty} f_k(t), \tag{4}$$

where $f_k(t)$, $k = 1, 2, \ldots$, is the probability density of the sum of k random variables with density $f(t)$. Using the Laplace transform ($\mathcal{L}$), one can rewrite Eq. (4) in the form

$$\mathcal{L}\{\mu_o\}(s) = \frac{\mathcal{L}\{f\}(s)}{1 - \mathcal{L}\{f\}(s)}. \tag{5}$$

Note that

$$\lim_{t\to\infty} \mu_o(t) = \mu \tag{6}$$

and that the only renewal process for which $\mu_o(t) = \mu$ for all $t > 0$ is the Poisson process (the renewal process with exponentially distributed T).

The Fano factor is defined as

$$F(t) = \frac{\mathrm{var}(N(t))}{E(N(t))}, \tag{7}$$

and sometimes the term "Fano factor" also denotes the limit

$$F = \lim_{t\to\infty} F(t). \tag{8}$$

Note that it holds [28] that

$$\lim_{t\to 0} F(t) = 1, \tag{9}$$

$$\lim_{t\to\infty} F(t) = C_v^2, \tag{10}$$

where C_v, the coefficient of variation, is defined as

$$C_v = \frac{\sqrt{\mathrm{var}(T)}}{E(T)}. \tag{11}$$

For a specific t and the known probability distribution of T, $F(t)$ has to be mostly calculated numerically, e.g., using the

formula [29]

$$F(t) = \frac{1}{t}\mathcal{L}^{-1}\left\{\frac{1+\mathcal{L}\{f\}(s)}{s^2[1-\mathcal{L}\{f\}(s)]}\right\}(t) - \frac{t}{E(T)}. \quad (12)$$

On the other hand, empirical values are evaluated using estimates of quantities in Eq. (7). As was mentioned, next we generalize the Fano factor assuming the shot-noise process instead of $N(t)$.

III. SHOT-NOISE PROCESS WITH AN EXPONENTIAL RESPONSE FUNCTION

The shot-noise process is a random process wherein the value is increased when an event occurs but otherwise decreases in time—the events are being "forgotten." The forgetting is given by a response function that represents the time effect of one event on the process [23]. Let us note that the function does not need to be (monotonously) decreasing, however that is the most natural case. First, we assume that this response function is exponentially decreasing [see Fig. 2(c) for an illustration]. The definition of such a process is

$$S_E(t,\tau) = \sum_{i=1}^{N(t)} e^{-\frac{t-X_i}{\tau}}, \quad (13)$$

where $\tau > 0$ is the time constant. Equation (13) represents the process $S_E(t,\tau)$ from the discrete-time point of view. Using the Dirac delta function, $\delta(x)$, it is possible to rewrite it into a continuous-time form,

$$S_E(t,\tau) = \int_0^t u(s)e^{-\frac{t-s}{\tau}}\,ds, \quad (14)$$

where

$$u(t) = \sum_{i=1}^{\infty}\delta(t-X_i). \quad (15)$$

This form is often used in filtering theory, however in this paper we prefer to represent it by the discrete formula (13), which is more intuitive for our purposes.

In analogy to the Fano factor, we define

$$G_E(t,\tau) = \frac{\mathrm{var}(S_E(t,\tau))}{E(S_E(t,\tau))}, \quad (16)$$

$$G_E(\tau) = \lim_{t\to\infty} G_E(t,\tau). \quad (17)$$

To be able to study this measure, first we need the mean and variance of $S_E(t,\tau)$. For the mean, there are very simple formulas (see the Appendix),

$$E(S_E(t,\tau)) = \mu\tau(1-e^{-t/\tau}), \quad (18)$$

$$E(S_E(\tau)) = \lim_{t\to\infty} E(S_E(t,\tau)) = \mu\tau. \quad (19)$$

Thus, taking into account Eq. (3), we do not need more information about T than its mean value. On the other hand, the variance of $S_E(t,\tau)$ depends fully on the distribution of T (see the Appendix),

$$\mathrm{var}(S_E(t,\tau)) = \mu\int_0^t\int_0^t e^{-\frac{x+y}{\tau}}[\mu_o(|y-x|)-\mu]\,dx\,dy + \frac{1}{2}\mu\tau(1-e^{-2t/\tau}). \quad (20)$$

This formula shows that the variance is highly dependent on the difference of $\mu_o(x)$ and μ; the smaller the difference is, the closer the variance is to $\mu\tau(1-e^{-2t/\tau})/2$, which is the variance of shot noise with Poisson-distributed events.

Next, we explore the limit properties of $G_E(t,\tau)$ for $t\to 0$ and $t\to\infty$. It holds that (see the Appendix)

$$\lim_{t\to 0} G_E(t,\tau) = 1 \quad (21)$$

and

$$G_E(\tau) = \frac{1}{1-\mathcal{L}\{f\}(1/\tau)} - \mu\tau - \frac{1}{2}. \quad (22)$$

The function $G_E(\tau)$ represents $G_E(t,\tau)$ for the shot-noise process at steady state. We can see that with a known Laplace transform of $f(t)$, one can simply calculate $G_E(\tau)$, e.g., we obtain

$$G_E(\tau) = \frac{1}{1-\left(1+\frac{C_v^2}{\mu\tau}\right)^{-\frac{1}{C_v^2}}} - \mu\tau - \frac{1}{2} \quad (23)$$

for the gamma probability distribution of T, and

$$G_E(\tau) = \frac{1}{1-e^{\frac{1}{C_v^2}\left(1-\sqrt{1+2\frac{C_v^2}{\mu\tau}}\right)}} - \mu\tau - \frac{1}{2} \quad (24)$$

for the inverse Gaussian (IG) distribution of T. Both of these probability distributions contain two parameters, e.g., $\mu = 1/E(T)$ and C_v, as in the forms assumed by us. With an unknown distribution of T, formula (22) can be approximated for $\mu\tau\to\infty$ as (see the Appendix)

$$G_E(\tau) \approx \frac{\mu\tau}{1-\frac{1+C_v^2}{2\mu\tau}} - \mu\tau - \frac{1}{2}, \quad (25)$$

which yields

$$C_v^2 \approx \frac{4E(S_E(\tau))G_E(\tau) - 2G_E(\tau) - 1}{2G_E(\tau) + 2E(S_E(\tau)) + 1}. \quad (26)$$

Independently of IEI distribution, it also holds that

$$\lim_{C_v\to 0} G_E(\tau) = \frac{1}{1-e^{-\frac{1}{\mu\tau}}} - \mu\tau - \frac{1}{2}, \quad (27)$$

which expresses the behavior of $G_E(\tau)$ when IEIs are all equal, thus when $f(t) = \delta(t-1/\mu)$, where $\delta(x)$ is the Dirac delta function. We can see that even then $G_E(\tau)$ is not zero, which is caused by the equilibrium property of renewal processes we use for the modeling of the sequences of events.

Finally, we present the limit relationships of quantity (16) with respect to τ (see the Appendix),

$$\lim_{\tau\to 0} G_E(t,\tau) = \tfrac{1}{2}, \quad (28)$$

$$\lim_{\tau\to\infty} G_E(t,\tau) = F(t), \quad (29)$$

$$\lim_{\tau\to 0} G_E(\tau) = \tfrac{1}{2}, \quad (30)$$

$$\lim_{\tau\to\infty} G_E(\tau) = \tfrac{1}{2}C_v^2. \quad (31)$$

The second formula can be intuitively explained so that for $\tau\to\infty$ the value of the shot-noise process does not decrease and thus the process is equal to $N(t)$. Note that Eqs. (10), (29),

and (31) imply that the order of the limits (with respect to τ and t) cannot be changed.

IV. SHOT-NOISE PROCESS WITH THE GENERAL RESPONSE FUNCTION

Although the decreasing exponential is the most important example of the shot-noise response function, sometimes a different type of decrease of the process is assumed, e.g., a decaying power law [30,31]. Thus, we will next consider the shot-noise process with the response function in the general form $w(x)$. Such a process can be defined as

$$S(t,\tau) = \sum_{i=1}^{N(t)} w\left(\frac{t - X_i}{\tau}\right), \tag{32}$$

where $\tau > 0$ is the scale parameter. The parameter τ is not usually part of the definition of the general shot-noise process, nevertheless it provides a universal way to change the rate of forgetting of the events (for a decreasing response function, the larger the τ is, the slower is the forgetting), which is suitable for our purposes. Note that process (13) is obtained for response function $w_E(x) = e^{-x}$, $x \in [0,\infty)$.

It is not necessary to restrict the form of $w(x)$, however we want it to fulfill some natural conditions. We assume that the functions $w(x)$ and $w'(x) = \mathrm{d}w(x)/\,dx$ are continuous and bounded functions defined on $[0, \infty)$ such that

$$\lim_{x\to\infty} w(x) = \lim_{x\to\infty} w'(x) = 0. \tag{33}$$

Moreover, $w(x)$ is non-negative and integrable. For the integrals, we use the notation

$$I_k(t) = \int_0^t w^k(x)\,dx, \quad k = 1,2 \tag{34}$$

and

$$I_k = \lim_{t\to\infty} I_k(t). \tag{35}$$

The stated conditions mainly ensure that $G(t,\tau)$ is not divergent in dependence on t and τ, which is reasonable behavior for a variability measure. However, note that they exclude some standard power-law response functions, which are, for example, unbounded in proximity of zero.

Analogically to $G_E(t,\tau)$ we define the variability measure

$$G(t,\tau) = \frac{\mathrm{var}(S(t,\tau))}{E(S(t,\tau))}, \tag{36}$$

$$G(\tau) = \lim_{t\to\infty} G(t,\tau). \tag{37}$$

The mean and variance of $S(t,\tau)$ can be expressed as (see the Appendix)

$$E(S(t,\tau)) = \mu\tau I_1(t/\tau) \tag{38}$$

and

$$\mathrm{var}(S(t,\tau)) = \mu \int_0^t \int_0^t w\left(\frac{x}{\tau}\right) w\left(\frac{y}{\tau}\right) [\mu_o(|y-x|) - \mu] \times dx\,dy + \mu\tau I_2(t/\tau), \tag{39}$$

which is suitable to rewrite into the form

$$\mathrm{var}(S(t,\tau)) = 2\mu\tau^2 \int_0^{t/\tau} w(x) \int_0^x w(x-y)\mu_o(\tau y)\,dy\,dx - [\mu\tau I_1(t/\tau)]^2 + \mu\tau I_2(t/\tau). \tag{40}$$

The ratio of relationships (39) and (38) gives a general formula for $G(t,\tau)$. At the steady state ($t \to \infty$), it simplifies to the form

$$G(\tau) = 2\frac{\tau}{I_1} \int_0^\infty w(x) \int_0^x w(x-y)\mu_o(\tau y)\,dy\,dx - \mu\tau I_1 + \frac{I_2}{I_1}. \tag{41}$$

On the other hand, for $t \to 0$ (see the Appendix),

$$\lim_{t\to 0} G(t,\tau) = w(0). \tag{42}$$

Finally, the limit relationships with respect to τ are (see the Appendix)

$$\lim_{\tau\to 0} G(t,\tau) = \frac{I_2}{I_1}, \tag{43}$$

$$\lim_{\tau\to\infty} G(t,\tau) = w(0)F(t), \tag{44}$$

$$\lim_{\tau\to 0} G(\tau) = \frac{I_2}{I_1}, \tag{45}$$

$$\lim_{\tau\to\infty} G(\tau) = \frac{I_2}{I_1} C_v^2. \tag{46}$$

Relationships (45) and (46) resemble the well-known limit properties of the Fano factor (9) and (10). Because the Fano factor can be seen as a special case of $G(t,\tau)$, it is possible to obtain it also using formula (36). Let us consider the response function in the form

$$w_R(x) = \begin{cases} 1 & \text{for } x \in [0,1], \\ 0 & \text{otherwise} \end{cases} \tag{47}$$

and denote $G(t,\tau)$ with this response function as $G_R(t,\tau)$. Then clearly $G_R(t,\tau) = F(\min\{t,\tau\})$, thus $G_R(\tau) = F(\tau)$, and formulas (45) and (46) are generalizations of formulas (9) and (10).

V. ILLUSTRATION OF THE BEHAVIOR OF $G_E(t,\tau)$ and $F(t)$

Figure 3 illustrates the dependence of $G_E(t,\tau)$ on t and the dependence of $G_E(\tau)$ on τ for gamma, IG, Weibull, and log-normal probability distributions of T and compared with the Fano factor. These distributions are probably the most often used distributions of interevent times in various processes. Let us mention, for example, that gamma, IG, and log-normal distributions are useful in the analysis of neural spike trains [32], and gamma and Weibull distributions are useful in the analysis of earthquakes or tsunamis [33,34]. All values were calculated based on formulas presented in this paper.

First, we compared $G_E(t,\tau)$ for $\tau = 1$ with $F(t)$. Both of these quantities start at the value 1, but with increasing t their behavior differs. Mainly $G_E(t,1)$ is lower than $F(t)$. According to Eq. (29), the value of $G_E(t,\tau)$ converges to $F(t)$ with increasing τ. Next, we compared $G_E(\tau)$ with $F(\tau)/2$. The purpose is to find out how much these values differ, because

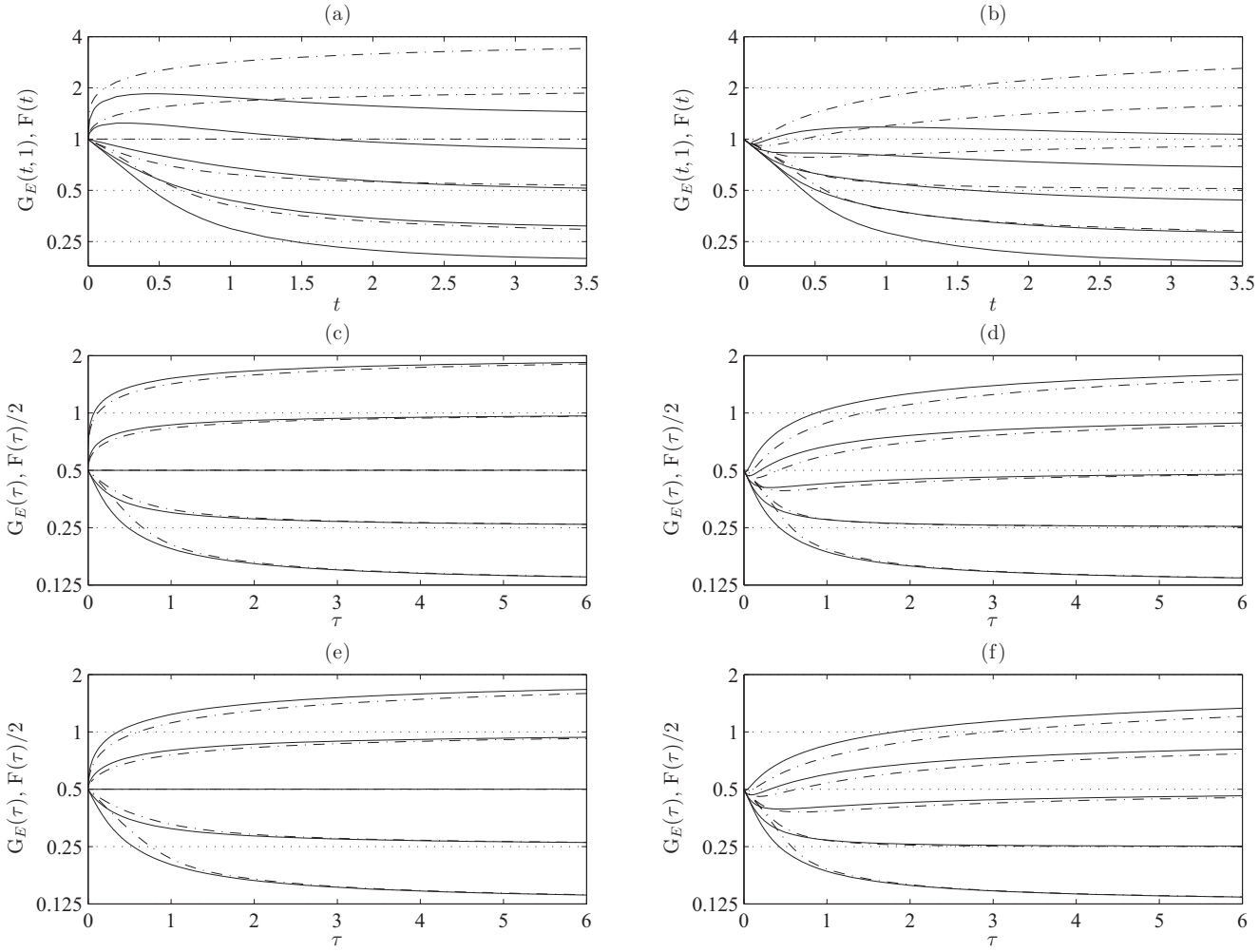

FIG. 3. Illustration of the behavior of $G_E(t,\tau)$ and $F(t)$ for gamma (a),(c), IG (b),(d), Weibull (e), and log-normal (f) probability distributions of IEIs with mean 1 and with various values of C_v^2 (values that correspond to the lines from bottom to top: 0.25, 0.5, 1, 2, 4). The vertical axes are logarithmically scaled. (a),(b) Solid lines: $G_E(t,\tau)$ in dependence on t for $\tau = 1$. Dash-dotted lines: $G(t)$ in dependence on t. (c)–(f) Solid lines: $G_E(\tau)$ in dependence on τ. Dash-dotted lines: $F(\tau)/2$ in dependence on τ. We can see that the behavior in dependence on t of the variability measures differs; however, at the steady state, $G_E(\tau)$ is approximately $G(\tau)/2$.

their limit values for $\tau \to 0$ and $\tau \to \infty$ indicate that $G_E(\tau)$ could be approximately $F(\tau)/2$. We can see that there are some differences, however they are vanishing with increasing τ, as expected.

VI. CONCLUSIONS AND DISCUSSION

The Fano factor, which is a frequently employed measure of the variability of sequences of times of events, was generalized by assuming the time-weighted influence of the events. Such an approach leads to the shot-noise process and variability measure $G(t,\tau)$ defined as its variance-to-mean ratio. Shot noise is almost always considered to be driven by the Poisson process. However, under this assumption, the value of $G(t,\tau)$ depends only on the arguments t and τ, which is clearly too restrictive. Therefore, shot noise with events described by an equilibrium renewal process was assumed. For this process, we presented the mean and variance, yielding formulas for $G(t,\tau)$. Moreover, the limit properties of $G(t,\tau)$ were derived and the behavior of the new variability measure was compared with the Fano factor.

Our results are mainly theoretical, but we also briefly describe some potential applications. They depend on whether we deal with data in the form of times of events or in the form of realizations of a shot-noise process. In the processing of times of events, we suggest $G(t,\tau)$ (its empirical version) as a measure of local variability. For such a purpose, the Fano factor is often used. Specifically, in the situation when we have multiple parallel records of times of events, the variability at time t can be measured using the Fano factor calculated based on events in the time interval $[t-\tau,t]$ for a $\tau > 0$. It corresponds to $G(t,\tau)$, where $w(x)$ is a rectangular function (47). However, if there is no specific reason for the rectangular function, a decreasing smooth function (mainly exponential) might be more suitable—it might reflect the importance of the time-dependent events more naturally. Our theoretical results can be then used to make inferences about the character of the data.

An advantage of $G_E(t,\tau)$ over $F(\tau)$ is also that the theoretical values of $G_E(t,\tau)$ can be more easily calculated. If the data records are long enough with respect to τ (values of the response function outside the interval $[0,t]$ are negligible), the behavior of $G_E(t,\tau)$ can surely be well approximated using $G_E(\tau)$, for which relatively simple formulas exist. Moreover, we have shown that $F(\tau) \approx 2G_E(\tau)$, which can be used to approximate the theoretical values of the Fano factor, mainly for gamma and IG distributions.

The second area of application is in processing data that we assume to be values of a shot-noise process (with an exponential response function). Such data arise in many situations, as shot-noise realizations can be interpreted, for example, in traffic noise [35,36], river flows [37], or neural membrane potential [38]. The presented results describe some theoretical properties of such data and can be used, for example, to construct simple moment estimators of C_v of the underlying renewal process. To deduce the value of C_v with a known sample mean and variance of the shot noise, it is possible to use Eq. (26) directly or, while assuming gamma or IG distribution of IEIs, Eqs. (23) and (24). An assumption about the probability distribution might seem to be too restrictive, however there are two reasons why gamma distribution in particular is often suitable. First, it is relatively flexible and thus it could appropriately approximate a wide range of various distributions. The second reason is its connection with the Poisson process. The gamma distribution with $C_v = 1$ is exponential and the events create the Poisson process. Thus, C_v estimation using the gamma distribution assumption indicates whether the shot-noise events are Poissonian or less or more variable.

ACKNOWLEDGMENT

This work was supported by the Czech Science Foundation project 15-06991S.

APPENDIX

We focus mainly on the case with a general response function $w(x)$. The special formulas are their simple consequences. In the following, we assume that $w(x)$ satisfies the conditions stated in Sec. IV.

First, we derive formulas for the mean and variance of $S(t,\tau)$. Using results from [39], we simply obtain

$$E(S(t,\tau)) = \mu\tau \int_0^{t/\tau} w(x)\,dx \tag{A1}$$

and

$$\begin{aligned}\operatorname{var}(S(t,\tau)) =& \mu \int_0^t \int_0^t w\left(\frac{x}{\tau}\right) w\left(\frac{y}{\tau}\right) [\mu_o(|y-x|) - \mu]\,dx\,dy \\ &+ \mu\tau \int_0^{t/\tau} w^2(x)\,dx.\end{aligned} \tag{A2}$$

Next, we derive the limit properties (45) and (46). Limit (45) can be deduced directly from relationship (41) considering Eq. (4). To derive limit (46), let us first denote

$$H_o(t) = E(N_o(t)) = \int_0^t \mu_o(x)\,dx. \tag{A3}$$

Then it holds [28] that

$$H_o(t) = \mu t + \tfrac{1}{2}\left(C_v^2 - 1\right) + g(t), \tag{A4}$$

where $g(t)$ is a bounded function satisfying

$$\lim_{t\to\infty} g(t) = 0. \tag{A5}$$

Using integration by parts, it is possible to derive

$$\begin{aligned}\int_0^x w(x-y)\mu_o(\tau y)\,dy =& \frac{1}{\tau} w(0) H_o(\tau x) \\ &+ \frac{1}{\tau}\int_0^x w'(x-y) H_o(\tau y)\,dy.\end{aligned} \tag{A6}$$

Now, combining relationships (41), (A4), and (A6), one can obtain

$$\begin{aligned}G(\tau) =& \frac{I_2}{I_1} C_v^2 + \frac{2}{I_1}\int_0^\infty w(x) \int_0^x w'(x-y) g(\tau y)\,dy\,dx \\ &+ \frac{2w(0)}{I_1}\int_0^\infty w(x) g(\tau x)\,dx,\end{aligned} \tag{A7}$$

which yields relationship (46).

Another relationship we derive is (22). Putting formula (4) and $w(x) = e^{-x}$ into (41) gives

$$\begin{aligned}G_E(\tau) =& 2\tau \sum_{k=1}^\infty \int_0^\infty e^{-2x} \int_0^x e^y f_k(\tau y)\,dy\,dx \\ &- \mu\tau + \frac{1}{2}.\end{aligned} \tag{A8}$$

Then, using integration by parts with $u(x) = \int_0^x e^y f_k(\tau y)\,dy$ and $v'(x) = e^{-2x}$, we obtain

$$\begin{aligned}G_E(\tau) &= \tau \sum_{k=1}^\infty \int_0^\infty e^{-x} f_k(\tau x)\,dx - \mu\tau + \frac{1}{2} \\ &= \sum_{k=0}^\infty \mathcal{L}^k\{f\}\left(\frac{1}{\tau}\right) - \mu\tau - \frac{1}{2} \\ &= \frac{1}{1 - \mathcal{L}\{f\}(1/\tau)} - \mu\tau - \frac{1}{2}.\end{aligned} \tag{A9}$$

Approximation (25) can be derived from relationship (A9) using a Taylor expansion of the exponential function in the Laplace transform.

It remains to prove formulas (42), (43), and (44). They are not too complicated, so we present only their rather intuitive explanations. The first formula can be explained using the fact that clearly $\lim_{t\to 0} S(t,\tau) = \lim_{t\to 0} w(0)N(t)$. Next, the second formula holds because for $\tau \to 0$ the process $S(t,\tau)$ converges to a steady state ("most of the response function" will be in the interval $[0,t]$) and thus the limit value is the same as the limit value of $G(\tau)$. Finally, Eq. (44) stems from the obvious relationship $\lim_{\tau\to\infty} S(t,\tau) = w(0)N(t)$.

[1] U. Fano, Phys. Rev. **72**, 26 (1947).
[2] A. Talbi, K. Nanjo, J. C. Zhuang, K. Satake, and M. Hamdache, Geophys. J. Int. **194**, 1823 (2013).
[3] L. Telesca and L. Toth, Fluct. Noise Lett. **09**, 157 (2010).
[4] L. Telesca, G. Amatulli, R. Lasaponara, M. Lovallo, and A. Santulli, Ecol. Model. **185**, 531 (2005).
[5] F. Farkhooi, M. F. Strube-Bloss, and M. P. Nawrot, Phys. Rev. E **79**, 021905 (2009).
[6] M. P. Nawrot, C. Boucsein, V. R. Molina, A. Riehle, A. Aertsen, and S. Rotter, J. Neurosci. Methods **169**, 374 (2008).
[7] T. Omi and S. Shinomoto, Neural Comput. **23**, 3125 (2011).
[8] S. Chaudhury, J. Phys. Chem. B **118**, 10405 (2014).
[9] A. C. Barato and U. Seifert, J. Phys. Chem. B **119**, 6555 (2015).
[10] C. Anteneodo, R. D. Malmgren, and D. R. Chialvo, Eur. Phys. J. B **75**, 389 (2010).
[11] Q. M. Pei, X. Zhan, L. J. Yang, C. Bao, W. Cao, A. B. Li, A. Rozi, and Y. Jia, Phys. Rev. E **89**, 032715 (2014).
[12] Y. Yuan, X. Zhuang, Z. Liu, and W. Huang, Chaos Solitons Fractals **45**, 838 (2012).
[13] M. Karsai, K. Kaski, A. L. Barabsi, and J. Kertsz, Sci. Rep. **2**, 397 (2012).
[14] W. Gerstner and W. M. Kistler, *Spiking Neuron Models* (Cambridge University Press, Cambridge, 2002).
[15] D. R. Cox and V. Isham, *Point Processes* (Chapman & Hall, London, 1980).
[16] D. Vere-Jones, J. Roy. Stat. Soc. B **32**, 1 (1970).
[17] C. Kluppelberg and T. Mikosch, Bernoulli **1**, 125 (1995).
[18] A. J. Lawrance and N. T. Kottegoda, J. R. Stat. Soc. A Sta. **140**, 1 (1977).
[19] P. A. W. Lewis, J. Roy. Stat. Soc. B **26**, 398 (1964).
[20] F. Muller-Hansen, F. Droste, and B. Lindner, Phys. Rev. E **91**, 022718 (2015).
[21] I. Rodriguez-Iturbe, D. R. Cox, and V. Isham, Proc. R. Soc. London **410**, 269 (1987).
[22] G. Samorodnitsky, Lect. Notes Stat. **114**, 332 (1996).
[23] A. Papoulis, *Probability, Random Variables, and Stochastic Processes* (McGraw-Hill, New York, 1991).
[24] A. Iksanov, Stoch. Proc. Appl. **123**, 1987 (2013).
[25] A. Iksanov, A. Marynych, and M. Meiners, Stoch. Proc. Appl. **124**, 2132 (2014).
[26] L. Kostal, P. Lansky, and O. Pokora, PLoS ONE **6**, e21998 (2011).
[27] S. Shinomoto, K. Miura, and S. Koyama, BioSystems **79**, 67 (2005).
[28] D. R. Cox, *Renewal Theory* (Methuen & Co., London, 1962).
[29] K. Rajdl and P. Lansky, Math. Biosci. Eng. **11**, 105 (2014).
[30] S. B. Lowen and M. C. Teich, IEEE Trans. Inf. Theor. **36**, 1302 (1990).
[31] A. P. Petropulu, J.-C. Pesquet, X. Yang, and J. Yin, IEEE Trans. Signal Process. **48**, 1883 (2000).
[32] S. Ditlevsen and P. Lansky, Neural Comput. **23**, 1944 (2011).
[33] S. Pasari and O. Dikshit, Earth Planets Space **67**, 129 (2015).
[34] E. L. Geist and T. Parsons, Geophys. Res. Lett. **35**, L02612 (2008).
[35] A. H. Marcus, J. Appl. Probab. **10**, 377 (1973).
[36] G. H. Weiss, Transport Res. **4**, 229 (1970).
[37] M. Lefebvre and F. Bensalma, Int. J. Eng. Math. **2014**, 1 (2014).
[38] P. L. Smith, J. Math. Psychol. **54**, 266 (2010).
[39] J. Rice, Adv. Appl. Probab. **9**, 553 (1977).

Publication IV

Entropy Factor for Randomness Quantification in Neuronal Data

Rajdl K.[a,*], Lansky P.[b], Kostal L.[b]

[a]*Department of Mathematics and Statistics, Faculty of Science, Masaryk University, Kotlarska 2, 611 37 Brno, Czech Republic*
[b]*Institute of Physiology, Academy of Sciences of the Czech Republic, Videnska 1083, 142 20 Prague 4, Czech Republic*

Abstract

A new measure of randomness of neural spike trains, an entropy factor, is proposed. It is based on the Shannon entropy of the numbers of spikes in a time window and can be seen as an analogy to the Fano factor, where the entropy is employed instead of the variance. We study the theoretical properties of the measure for equilibrium renewal processes and illustrate them for gamma and inverse Gaussian probability distributions of the interspike intervals. Finally, the theoretical behavior of the entropy factor is compared to its properties deduced from the experimental data records of spontaneous firing of olfactory receptor neurons in rats.

Keywords: Variability measure, Shannon entropy, Renewal process, Fano factor

1. Introduction

One of the most important questions in neuroscience is how information is transferred in the nervous system. Some aspects of the mechanism are clear and generally accepted – the information is transferred using spikes which are transmitted by neurons and it is coded only by times of their occurrence, not by their size or shape (Gerstner & Kistler, 2002; Kandel et al., 1991; Rieke et al., 1999). However, more specific details of the mechanism are not obvious, mainly the exact method of coding. The simplest and most often assumed concept is that the coding is realized using the spike rate (defined for example as the number of spikes

*Corresponding author
Email address: rajdlk@mail.muni.cz (Rajdl K.)

fired in a unit of time), called the rate coding. It is a natural idea, as responses of a neuron are usually strongly influenced by the input rate. Nevertheless, the rate reflects only a small part of the character of spike trains and thus a possibility exists that a more complex coding is employed. The codes which assume some rate-independent behavior, given by specific position of the single spikes, are called temporal codes (temporal coding).

There are many possibilities how a temporal code could be created, one of the variants focuses on variability (variability coding). It is a concept in which information is transferred not only by the rate, but also using the variability of spike trains. The crucial question while studying the variability is how to quantify it. The two of the most often used measures are coefficient of variation (CV) and Fano factor, see (Ditlevsen & Lansky, 2011; Rajdl & Lansky, 2014) and other references therein. The CV is defined as the standard deviation to mean of interspike intervals (ISIs) ratio and the Fano factor is defined as the variance to mean of number of spikes in a time window ratio. The number of experimental studies where these two measures were applied is practically countless. The definitions of coefficient of variation and Fano factor also show two main ways how to see neuronal data – as ISIs or numbers of spikes in a time window of a length $w > 0$. A real neuron registers probably more the counts of spikes than the exact lengths of ISIs, nevertheless, both of these variants are useful and provide a different perspective. Another feature of these two variability measures we would like to point out is that they can be seen as variance (of ISIs or counts) in comparison to corresponding variance of Poisson process with the same intensity. As Poisson process has a unique position among the random processes used to model spike trains, it is an important property of these measures, which increases their interpretability.

Variability is usually used as a general term for the rate-independent behavior, nevertheless, it is not fully correct, there is a similar but not equivalent term which should be distinguished – randomness or predictability. Both the variability and randomness describe the character of spike trains which is not fully determined by the intensity, but there is a clear difference between them. It can be seen for example from that fact that even a variable process can be non-random. A very suitable quantity to measure randomness is the Shannon entropy (Shannon & Weaver, 1998), which is widely applied in neuroscience (Marzen et al., 2015; McDonnell et al., 2011; Stocks et al., 2009; Strong et al., 1998; Watters & Reeke, 2014). Some randomness measures based on entropy have been proposed in neural context and thoroughly studied (Kostal et al., 2007, 2011; Kostal & Lansky, 2006). Nevertheless, they focus only on ISIs, creating an alternative to CV. The most suitable way how to measure the randomness of ISIs seems to be usage of the Kullback-Leibler

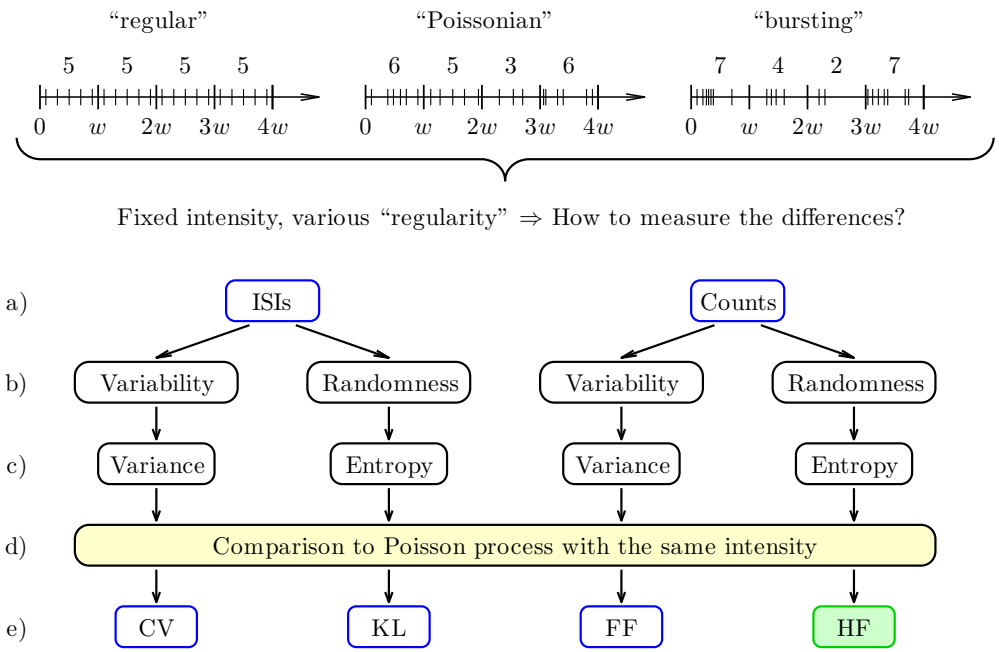

Figure 1: An overview of selected measures of intensity independent behavior of spike trains. (a) Two main ways how to describe spike trains – using ISIs or counts of spikes in a time window. (b) Two concepts how to understand the intensity independent behavior – variability and randomness. (c) Specific characteristics which suitably represent variability and randomness – variance and (Shannon) entropy. (d) Comparison of given characteristics to Poisson process with intensity equal to the examined processes. (e) Resulting measures – coefficient of variation (CV), Kullback-Leibler distance (KL), Fano factor (FF) and entropy factor (HF).

(KL) distance of probability density of ISIs to density of ISIs in a Poisson process with the same intensity, thus to density of an exponential distribution (Kostal & Lansky, 2006).

The KL distance can be seen as an analogy to CV representing randomness instead of variance. It would be thus natural to use the entropy to measure the randomness of numbers of spikes in a time window analogously to Fano factor. We propose such a measure in this paper. It is defined as the ratio of the Shannon entropy of numbers of spikes in a time interval to the Shannon entropy of a Poisson counting process with the same intensity. Due to similarity to the Fano factor, we call the measure an entropy factor (HF). It creates a natural complement to the existing measures, for an overview of selected measures of variability and randomness see Fig. 1. As this figure shows, all the measures compare a charac-

teristic of given spike train to a Poisson process, which is a simple, but efficient way, how to make the results better interpretable and comparable through various experiments. Our aim is mainly to explore properties of entropy factor and compare them with properties of Fano factor, to show that there are some fundamental differences between the measures. Behavior of the Fano factor was studied in various papers, mostly its dependence on the length of the observation window or CV (Nawrot et al., 2008; Rajdl & Lansky, 2014) or its statistical properties (Eden, 2010). For entropy based measures of randomness of ISIs, their relation to variability expressed by CV is of interest (Kostal & Lansky, 2006).

Similarly to the mentioned papers, we study the theoretical properties of the entropy factor and derive some formulas describing its behavior. Firstly, we define the assumed model of spike trains – equilibrium renewal processes. Based on this model the standard variability measures and their basic properties are summarized. Next, the focus if given to the new measure, it is defined and some of its properties are derived and illustrated. We aim mainly on comparing both Fano and entropy factors in dependence on the CV (limit value of Fano factor) and on the length of the observation window. To illustrate the properties, two of the most often assumed models of the lengths of ISIs are used, gamma and inverse Gaussian distributions (Fisch et al., 2012; Koyama & Kostal, 2014; Lansky et al., 2016; Nawrot et al., 2008; Omi & Shinomoto, 2011; Ostojic, 2011; Shimokawa et al., 2010). Finally, entropy factor is compared to Fano factor estimated from experimental data.

2. Model of spike trains

In a formal description, a spike train can be represented as a sequence of times of occurrence of the individual spikes, $X_1, \ldots, X_n$, $n \in \mathbb{N}$, and modeled using a (stochastic) point process. Probably the most often used are renewal processes, which assume that all the ISIs, $T_i = X_{i+1} - X_i, i = 1, \ldots, n-1$, are mutually independent and identically distributed random variables. In this paper, we use this model to describe the neural spike trains. However, note that true character of spike trains can be more complex (Avila-Akerberg & Chacron, 2011; Chacron et al., 2001; Farkhooi et al., 2009; Schwalger et al., 2015).

A renewal process is defined by a continuous positive random variable T, representing the lengths of ISIs, with probability density function $f(t)$, cumulative distribution function $F(t)$ and mean $\mu = \mathrm{E}(T)$. To fully specify the renewal process it is also necessary to state the relationship between the sequence of spikes and the time zero (start of the observation). In a role of an external observer,

we assume that the zero time is random with respect to the spikes (equilibrium renewal process). Note, that the time up to the first spike (T_0) has in this case generally a different probability distribution to T. The only renewal process in which T is equivalent to T_0 is the Poisson process. In that case, the random variables T and T_0 are exponentially distributed.

As follows from a frequency coding approach, neurons are influenced by numbers of spikes received in a time period. This point of view leads to a counting process $N(w)$, which denotes the number of spikes occurred in an interval $(0, w]$, $w > 0$. For a fixed $w > 0$, $N(w)$ is a discrete random variable with probability mass function

$$p_n(w) = P\big(N(w) = n\big),\ n = 0, 1, 2, \ldots. \tag{1}$$

The counting process is an alternative way how to describe a renewal process using ISIs,

$$N(w) \geq n \Leftrightarrow T_0 + \ldots + T_{n-1} \leq w, \tag{2}$$

from which follows, (Jewell, 1960),

$$p_0(w) = \mathcal{L}^{-1}\left\{\frac{1}{s} - \frac{1 - \tilde{f}(s)}{\mathrm{E}(T)s^2}\right\}(w), \tag{3}$$

$$p_n(w) = \mathcal{L}^{-1}\left\{\frac{(1 - \tilde{f}(s))^2\big(\tilde{f}(s)\big)^{n-1}}{s^2\mathrm{E}(T)}\right\}(w),\ n \in \mathbb{N}, \tag{4}$$

where $\mathcal{L}$ denotes the Laplace transform and $\tilde{f}(s) = \mathcal{L}\{f\}(s)$. Evaluation of formulas (3) and (4) is rather complicated, it is mostly difficult to obtain even some basic characteristics of $N(w)$. There is an explicit formula for the mean,

$$\mathrm{E}\big(N(w)\big) = \frac{w}{\mathrm{E}(T)} = \frac{w}{\mu}, \tag{5}$$

but none other exists for higher moments. For approximation of the variance of $N(w)$, the following asymptotic relationship can be used, (Cox, 1962),

$$\mathrm{Var}\big(N(w)\big) \approx \frac{\mathrm{Var}(T)}{\mathrm{E}^3(T)}w + \frac{1}{2}\left(1 + \frac{\mathrm{Var}(T)}{\mathrm{E}^2(T)}\right)^2 - \frac{1}{3}\frac{\mathrm{E}(T^3)}{\mathrm{E}^3(T)}, \quad \text{for } w \to \infty. \tag{6}$$

Relationship (5) also yields a simple formula for the intensity of the process,

$$\lambda = \frac{1}{\mu}, \tag{7}$$

as for a general counting process the definition of intensity is $\lambda(w) = \mathrm{dE}(N(w))/\,\mathrm{d}t$. Note that probably the only non-trivial renewal process for which it is possible to express the probability mass function and many other characteristics of $N(w)$ by simple closed formulas is the Poisson process. Let us denote the corresponding counting process and random variable representing the ISIs as $N_P(w)$ and T_P. It holds that

$$\mathrm{E}(T_P) = \sqrt{\mathrm{Var}(T_P)} = 1/\lambda \tag{8}$$

and

$$\mathrm{E}\big(N_P(w)\big) = \mathrm{Var}\big(N_P(w)\big) = \lambda w. \tag{9}$$

3. Variability

The term variability is standardly used to denote the intensity independent behavior (of spike trains). It is not rigorously defined what this term exactly covers, however, it is mostly related to characteristics based on (second) statistical moments of given quantities. The two of the most often used measures are defined as the second moments of T or $N(w)$ in relation to the Poisson process with the *same intensity*. Specifically, it is the coefficient of variation,

$$\mathrm{CV}^2 = \frac{\mathrm{Var}(T)}{\mathrm{Var}(T_P)}, \tag{10}$$

and Fano factor,

$$\mathrm{FF}(w) = \frac{\mathrm{Var}\big(N(w)\big)}{\mathrm{Var}\big(N_P(w)\big)},\ w > 0. \tag{11}$$

These measures are commonly defined with $\mathrm{E}^2(T)$ and $\mathrm{E}\big(N(w)\big)$ instead of $\mathrm{Var}(T_P)$ and $\mathrm{Var}\big(N_P(w)\big)$. However, due to relationships (5), (8) and (9), such definitions are equivalent to the formulas (10) and (11).

While the CV is a constant, $\mathrm{FF}(w)$ is a function of w, and therefore Fano factor is sometimes defined as the limit

$$\mathrm{FF} = \lim_{w\to\infty} \mathrm{FF}(w), \tag{12}$$

with, (Cox, 1962),

$$\mathrm{FF} = \mathrm{CV}^2. \tag{13}$$

For a general distribution of T, the following formulas hold, (Cox, 1962),

$$\lim_{w\to 0} \mathrm{FF}(w) = 1 \tag{14}$$

and, (Rajdl & Lansky, 2014),

$$\mathrm{FF}(w) = \frac{1}{w}\mathcal{L}^{-1}\left\{\frac{1+\mathcal{L}\{f\}(s)}{s^2[1-\mathcal{L}\{f\}(s)]}\right\}(w) - \frac{w}{\mathrm{E}(T)}, \tag{15}$$

where the latter can be used to numerically calculate $\mathrm{FF}(w)$ for any $w > 0$.

4. Predictability, the new measure and its properties

As it was mentioned, predictability or randomness should be distinguished from variability, it reflects a different type of intensity independent behavior. To measure randomness, it is suitable to use the Shannon entropy. For a discrete random variable $N(w)$ with probabilities $p_n(w)$, $n = 0, 1, \ldots$, it is defined as

$$\mathrm{H}\big(N(w)\big) = -\sum_{n=0}^{\infty} p_n(w) \ln p_n(w). \tag{16}$$

The larger the value of $\mathrm{H}\big(N(w)\big)$ the more difficult it is to predict the value of $N(w)$, and so, the more information we obtain from a realization of $N(w)$ (the variable $N(w)$ is more random).

The randomness of T has been thoroughly studied (Kostal et al., 2011, 2013), however, we are not aware of any similar studies of $N(w)$. We therefore define and study a randomness measure of $N(w)$ based on the Shannon entropy. It would be possible to directly use quantity (16). Nevertheless, for a better interpretation, it is suitable to also relate its value to a Poisson process like in (10) and (11). We suggest to define the entropy factor as

$$\mathrm{HF}(w) = \frac{\mathrm{H}\big(N(w)\big)}{\mathrm{H}\big(N_P(w)\big)}, \tag{17}$$

where $N_P(w)$ denotes the Poisson process with the same intensity as $N(w)$.

Analogously to studies on the Fano factor, we are interested in the behavior of $\mathrm{HF}(w)$ in dependence on w and on properties of T, mainly the CV. Calculation of $\mathrm{HF}(w)$ requires calculation of the entropy of $N(w)$ and entropy of the Poisson process. The entropy of the counting Poisson process with intensity λ is

$$\mathrm{H}\big(N_P(w)\big) = \lambda w[1 - \ln(\lambda w)] + e^{-\lambda w}\sum_{n=0}^{\infty}\frac{(\lambda w)^n \ln(n!)}{n!}. \tag{18}$$

Relationship (18) can be approximated using, (Evans, 1998),

$$\mathrm{H}\big(N_P(w)\big) \approx \frac{1}{2}\ln(2\pi e\lambda w) - \frac{1}{12\lambda w} - \frac{1}{24(\lambda w)^2} - \frac{19}{360(\lambda w)^2}, \text{ for } \lambda w \to \infty. \tag{19}$$

For a general renewal process with intensity λ, it is possible to numerically evaluate the equations (3), (4) and (16) or to use the asymptotic formula

$$\begin{aligned}\mathrm{H}\big(N(w)\big) \approx & \frac{1}{2}\ln(2\pi e) + \\ & \frac{1}{2}\ln\left(\mathrm{CV}^2\lambda w + \frac{1}{2}\left(1+\mathrm{CV}^2\right)^2 - \frac{1}{3}\lambda^3\mathrm{E}(T^3)\right), \\ & \text{for } \lambda w \to \infty. \end{aligned} \tag{20}$$

Relationship (20) was derived using the fact that distribution of $N(w)$ converges for $\lambda t \to \infty$ to a normal distribution, (Cox, 1962). Its mean is λw and the variance can be approximated using formula (6).

Some limit properties of $\mathrm{HF}(w)$ are

$$\lim_{w\to 0} \mathrm{HF}(w) = 1, \tag{21}$$

$$\lim_{w\to \infty} \mathrm{HF}(w) = 1 \tag{22}$$

and

$$\lim_{\mathrm{CV}\to 0} \mathrm{HF}(w) = \frac{-q\ln(q) - (1-q)\ln(1-q)}{\frac{1}{2}\ln(2\pi e\lambda w)}, \tag{23}$$

where $q = \lambda w - \lfloor \lambda w \rfloor$ and $\lfloor \lambda w \rfloor$ is the integer part of λw. Limit (21) is a simple consequence of convergence of distribution of $N(w)$ to Bernoulli distribution with mean λw for $w \to 0$ (Cox, 1962), limit (22) follows from formulas (19) and (20). Derivation of limit (23) uses the fact that for $\mathrm{CV} \to 0$ the distribution of the time up to the first spike converges to uniform distribution on $[0,\, \mu]$ and all the following ISIs to μ .

According to relationship (22), $\mathrm{HF}(w)$ always converges to value one, which substantially differs from the behavior of the Fano factor. Another principal difference between $\mathrm{HF}(w)$ and $\mathrm{FF}(w)$ is that the entropy factor is bounded from above (for fixed w and μ), as there is a maximum value of entropy of $N(w)$, whereas the Fano factor can take arbitrarily large values. The maximum entropy among all the discrete distributions with mean λw has the geometric distribution (Cover &

Thomas, 2006). Its probability mass function is

$$P\big(X(w)=n\big)=\left(1-\frac{1}{1+\lambda w}\right)^{n}\frac{1}{1+\lambda w},\ n=0,1,2,\ldots \tag{24}$$

and its entropy is

$$\mathrm{H}\big(X(w)\big)=(1+\lambda w)\ln(1+\lambda w)-\lambda w\ln(\lambda w). \tag{25}$$

No renewal process has such a distribution of number of spikes and thus no renewal process can reach the value (25). This fact can be easily seen through the limit behavior of $N(w)$ of any renewal process. As it was mentioned, it converges to the normal distribution for $\lambda w\to\infty$, however, the geometric distribution (24) does not. An upper bound of $\mathrm{HF}(w)$ is thus created by the ratio of $\mathrm{H}\big(X(w)\big)$ to $\mathrm{H}\big(N_P(w)\big)$. It holds that

$$\lim_{w\to\infty}\frac{\mathrm{H}\big(X(w)\big)}{\mathrm{H}\big(N_P(w)\big)}=2, \tag{26}$$

which is a direct consequence of relationships (19) and (25).

Finally, note that an analogy for a continuous positive random variable with probability density function $f(t)$ is the differential entropy

$$h(f)=-\int_0^\infty f(t)\ln\big(f(t)\big)\,\mathrm{d}t. \tag{27}$$

Despite formula (27) being similar to formula (16), $h(f)$ is not suitable to quantify the randomness (or information content) of T directly. For example, $h(f)$ can be negative and it is scale dependent. To resolve this problem, it was proposed in (Kostal & Lansky, 2006) to measure the variability of T using the Kullback-Leibler (KL) distance from an exponential distribution. The KL distance is then a non-negative quantity, as a result of the fact that the exponential distribution maximizes entropy among all the distributions with given mean.

5. Examples of entropy factor and comparison with Fano factor

The above presented theoretical properties of $\mathrm{HF}(w)$ give a basic idea about its behavior. However, they do not yield the dependence on w or CV in a simple way. Therefore, we illustrate it for two commonly used distributions of T, gamma and inverse Gaussian (IG). Both of the distributions are parametrized using two

independent parameters. For our purpose it is suitable to use μ and CV. The density of gamma distribution is

$$f_G(t) = \frac{t^{1/\mathrm{CV}^2-1}\exp[-t/(\mu\mathrm{CV}^2)]}{\Gamma(1/\mathrm{CV}^2)(\mu\mathrm{CV}^2)^{1/\mathrm{CV}^2}}, \quad t \geq 0, \tag{28}$$

and the density of IG distribution is

$$f_{IG}(t) = \sqrt{\frac{\mu}{2\pi\mathrm{CV}^2 t^2}}\exp[-(t-\mu)^2/(2\mathrm{CV}^2 t\mu)], \quad t \geq 0. \tag{29}$$

Let us note that the gamma distribution becomes exponential for $\mathrm{CV} = 1$ and thus the corresponding renewal process is a Poisson process. On the contrary, IG distribution never attains the exponential distribution. Without loss of generality, in the following examples we assume that $\mu = 1$, this can be always achieved by using a suitable linear transformation of time. The time is thus shown in mean ISI units. The remaining free parameters are then CV and w.

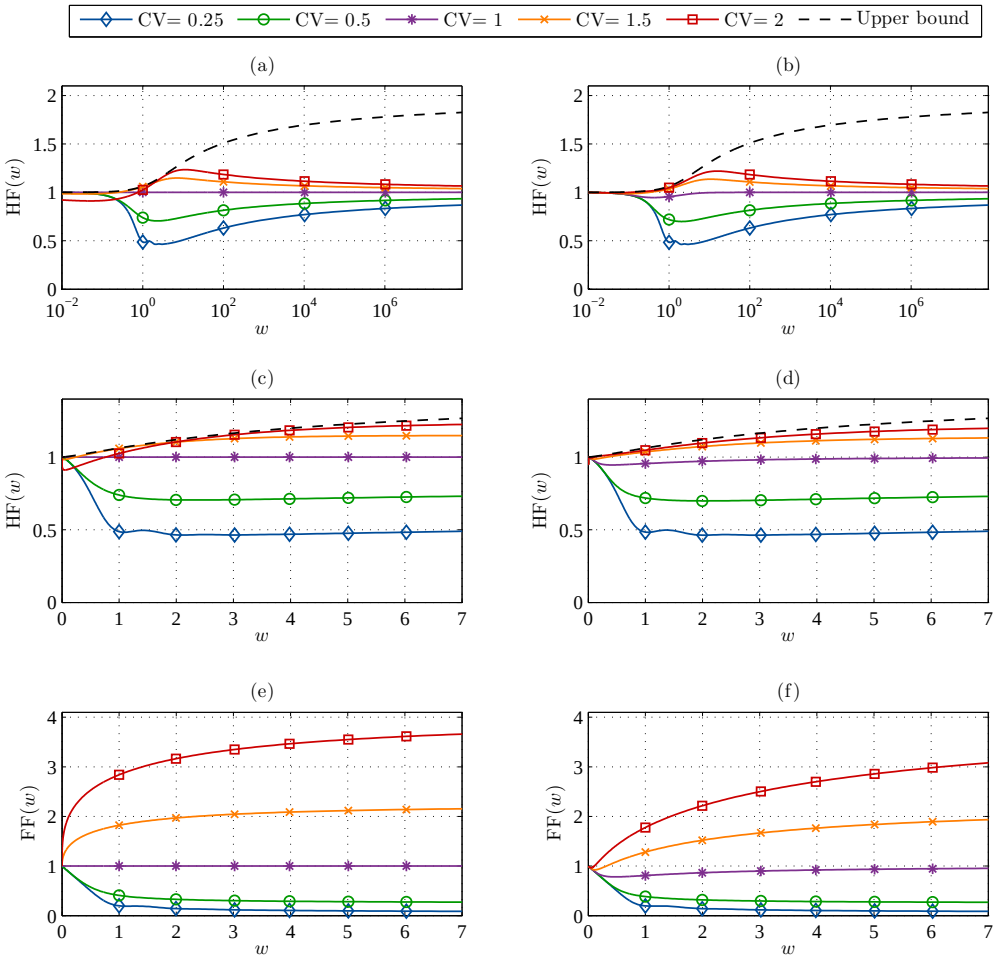

Figure 2: Dependence of $\mathrm{HF}(w)$ (a,b,c,d) and $\mathrm{FF}(w)$ (e,f) on w for various values of CV. The ISIs follow gamma (a,c,e) and IG (b,d,f) probability distributions with $\mu = 1$. The values of CV are $0.25, 0.5, 1, 1.5, 2$ (corresponding to the individual full-line curves from bottom to top on the right sides of the panels). Dashed-lines: An upper boundary for $\mathrm{HF}(w)$, given by geometric distribution $X(w)$, (25), with parameter $\lambda = 1$.

To compare $\mathrm{HF}(w)$ with $\mathrm{FF}(w)$, the necessary values were numerically calculated using formulas (3), (4) and (16). In Fig. 2, the dependence on the length of the time window is illustrated. The common feature of both $\mathrm{HF}(w)$ and $\mathrm{FF}(w)$ is that they start at value one and the following behavior is influenced by the value of CV. For the Fano factor, lower values of CV yield lower values of the measure and vice versa, however, this does not hold for $\mathrm{HF}(w)$. A large difference between

the measures is in their limiting behavior for increasing w, the Fano factor converges to CV^2, and the entropy factor returning back to one. Nevertheless, the rate of convergence of $\mathrm{HF}(w)$ to the value one is exceptionally slow (logarithmic).

A special property of the entropy factor is the upper boundary. We can see that it is relatively low and thus the entropy of $N(w)$ cannot be much larger than the entropy of the Poisson process, at most double – according to relationship (26). Another feature we would like to point out is the sinusoid-like shape for low CV. It is common for both of the measures, but it is more apparent for $\mathrm{HF}(w)$. The reason for this behavior is the equilibrium property of the process we use to model the spike trains. Even for $\mathrm{CV} = 0$, when all the ISIs are same, the time to the first spike is random (due to the random start of the observation), but less or equal to μ. It results, that at times which are multiples of the mean ISI, we know exactly how many spikes there will be and the entropy is zero. At other times, the number of spikes is still influenced by the random beginning and the entropy is thus positive.

For the sake of completeness, the range of w in Fig. 2(a,b) is from 10^{-2} up to 10^{8} while the mean ISI is equal to one. However, we may ask what range is interesting from neural coding point of view. Typical experimental data contains a maximum of thousands of ISIs, the main reason being that current technology does not permit simultaneous observation of thousands of individual neurons and thus parallel observation is replaced by a single spike train. In a real neural network, in which synchrony (coincidence) of spiking plays its role, we can expect that the range of interest for the time window is between fractions of the mean ISI up to several of its multiples. We can see that the extremes of $\mathrm{HF}(w)$ are reached in this range, which supports the importance of randomness evaluation. In Fig. 2(c,d), the behavior of the entropy factor for the most important lengths of the observation window is shown in more detail.

In Fig. 3 and 4, there is shown directly the relation of $\mathrm{FF}(w)$ and $\mathrm{HF}(w)$. In the first case, the values of CV of ISIs are fixed for the single curves and w is going continuously from 0 to ∞. In the second figure, every curve corresponds to a fixed w while CV changes from 0.2 to 2. We can see that the relation of HF to FF is not linear, often not even monotonic. Mainly, the dependence in Fig. 3 is relatively complicated, it is caused by the fact that the course of $\mathrm{HF}(w)$ is non-monotonic, as shown in Fig. 2. In Fig. 4, the curves are simpler, nevertheless, their order and intersections are not intuitive, which is again caused mainly by the non-monotonic dependency of the entropy factor an the length of the observation window.

Another question we were interested in is what CV maximizes $\mathrm{HF}(w)$ for given model of ISIs and w. Such CVs in dependence on w are illustrated in

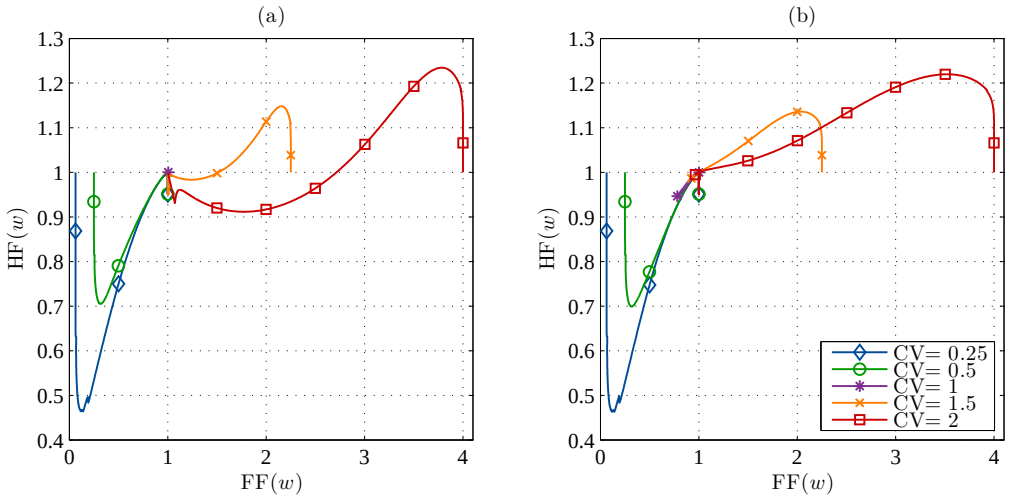

Figure 3: The relation between $\mathrm{FF}(w)$ and $\mathrm{HF}(w)$ for various values of CV $(0.25, 0.5, 1, 1.5, 2)$. The ISIs follow gamma (a) and IG (b) probability distributions with $\mu = 1$. The values of $\mathrm{FF}(w)$ and $\mathrm{HF}(w)$ are shown for $w \in (0, \infty)$.

Fig. 5(a). A larger w mostly requires a larger CV to maximize the entropy factor, however, the opposite holds for IG distribution and short windows. The individual maxima are always lower than the theoretical upper bound given by geometric distribution (25). In Fig. 5(b), the corresponding values of the maximum entropy achieved by gamma and IG distributions in relation to the upper boundary are shown. We can see that for the presented lengths of the observation window ($w \leq 5$) the entropy factor of a renewal process can be relatively near to the upper boundary.

Finally, in Fig. 6 the accuracy of the approximation (20) is explored, using relative error,

$$\varrho(w) = 100 \frac{\widetilde{\mathrm{HF}}(t) - \mathrm{HF}(w)}{\mathrm{HF}(w)}, \tag{30}$$

where $\widetilde{\mathrm{HF}}(w)$ is approximation of entropy factor which uses formula (20) to calculate the entropy. The precision is low mainly for small w and large CV. Very low values of CV are also problematic, as the approximation cannot reflect the sinusoid-like behavior of $\mathrm{HF}(w)$. However, for a standard range of CV (e.g, $[0.5, 1.5]$) the accuracy seems to be sufficient from w around several means of ISIs.

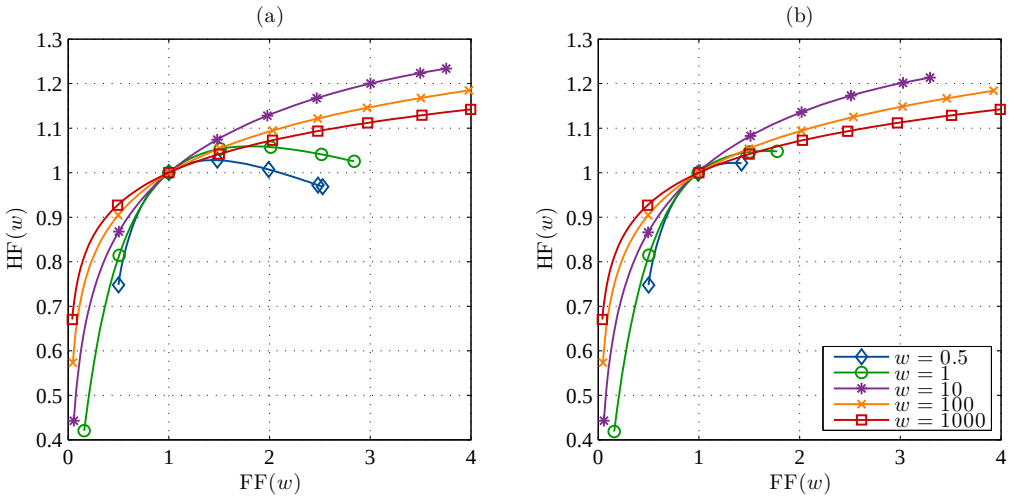

Figure 4: The relation between $\mathrm{FF}(w)$ and $\mathrm{HF}(w)$ for various values of w $(0.5, 1, 10, 100, 1000)$. The ISIs follow gamma (a) and IG (b) probability distributions with $\mu = 1$. The values of $\mathrm{FF}(w)$ and $\mathrm{HF}(w)$ are shown for $\mathrm{CV} \in (0.2, 2)$.

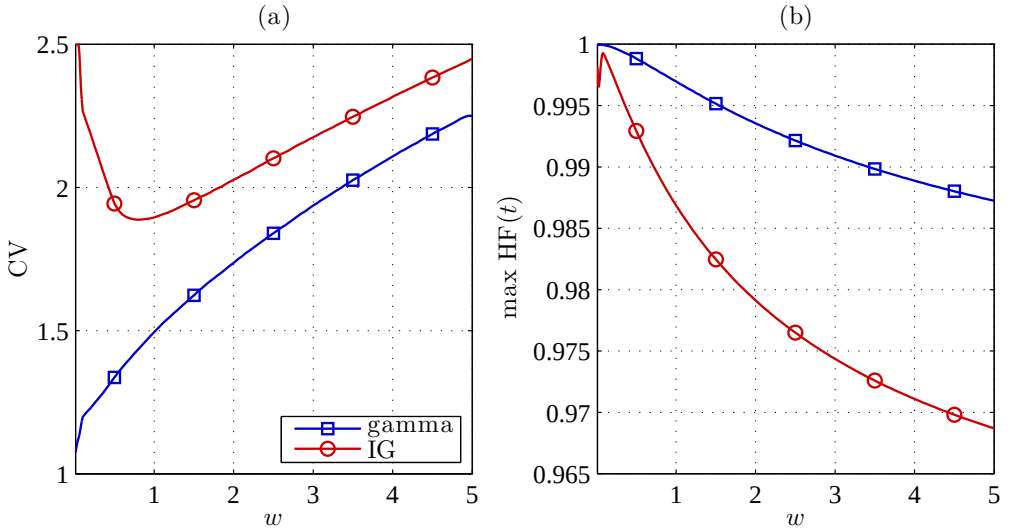

Figure 5: (a) CV which maximizes the entropy of $N(w)$ in dependence on w for gamma and IG distribution of T with $\mu = 1$. (b) Maximum of $\mathrm{H}\big(N(w)\big)$ to $\mathrm{H}\big(N_G(w)\big)$ ratio in dependence on t.

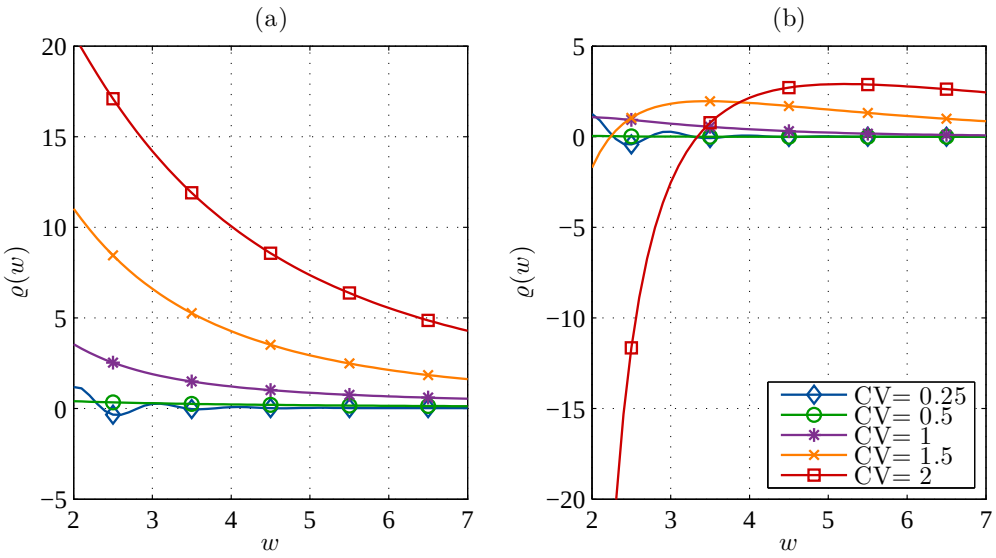

Figure 6: The relative error $\varrho(w)$ [%] of approximation (20) for gamma (a) and IG (b) distribution of T in dependence on CV and w, $\mu = 1$.

6. Entropy factor evaluated from experimental data

In this section, we compare entropy factor to Fano factor estimated from experimental data, records of spontaneous firing of olfactory receptor neurons in rats. The spike trains were recorded under two different conditions. In the first scenario the rats were allowed to breathe freely (FB), in the second they were tracheotomized (TT). More specific details can be found in (Duchamp-Viret et al., 2005). The data consist of multiple neural firing sequences of varying length, from which we selected ten, five each of both types, with sufficient length and with the largest signs of stationarity. The lengths of individual records are approximately from $180\,s$ s to $280\,s$ with mean of ISIs from $0.15\,s$ to $0.33\,s$ for the FB scenario and from $150\,s$ to $210\,s$ with mean of ISIs from $0.19\,s$ to $0.50\,s$ for the TT scenario.

The relation of $\mathrm{FF}(w)$ to $\mathrm{HF}(w)$ in this data is explored. Values of $\mathrm{FF}(w)$ and $\mathrm{HF}(w)$ were estimated for various values of w (from $0.1\,s$ to $5\,s$). Before the estimation, it was necessary to transform the spike trains to numbers of spikes in time intervals of a certain length. For this purpose, the records were divided into segments of the required length so that after each segment an interval of length $0.5\,s$ was discarded to reduce possible dependencies of the segments. Next,

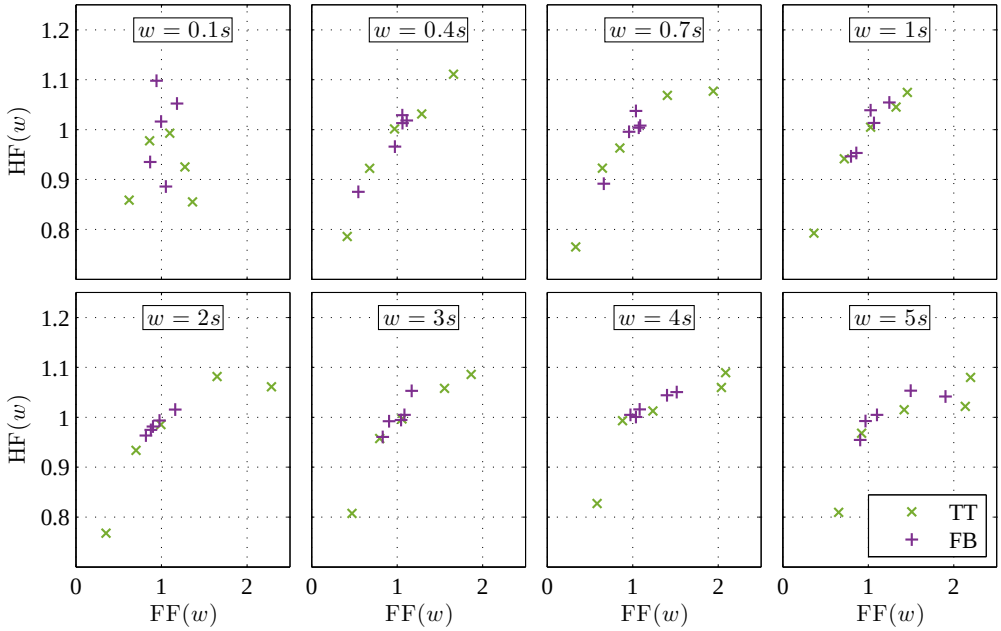

Figure 7: The relation of $\mathrm{HF}(w)$ to $\mathrm{FF}(w)$ in experimental data for the length of the observation window $w \in \{0.1, 0.4, 0.7, 1, 2, 3, 4, 5\}$. The values of w are in seconds. The two types of data are distinguished - TT (with tracheotomy) and FB (freely breathing).

the numbers of spikes in the individual segments were counted. Based on these counts, the entropy was calculated for every spike train by simply using formula (16) with sample probabilities. Note, that this simple method leads to a negative bias of the entropy estimator (Schurmann, 2004). It is caused by the fact that very low probabilities are not observed in the finite samples, leading to underestimation of the true value of quantity (16). To reduce the influence of this issue on the estimated value of $\mathrm{HF}(w)$, we did not use an analytically calculated entropy of the Poisson process in formula (17). We estimated it based on generated data with number of samples equal to the number of samples available in the individual records of the experimental data. The purpose of this procedure was to have a similar bias in both parts of formula (17), which possibly reduced the bias of the ratio. The entropy of the Poisson process was generated 10000 times and averaged to minimize the variance of the estimator.

The results obtained for the data are shown in Fig. 7, with the TT and FB scenarios being distinguished. We can see that there is a certain relation between $\mathrm{FF}(w)$ and $\mathrm{HF}(w)$, larger values of $\mathrm{FF}(w)$ mostly yield larger values of $\mathrm{HF}(w)$,

but not always, in accordance with the theoretic results, there is a tendency to slowing the increase of $\mathrm{HF}(w)$ and potential decreasing with increasing Fano factor. There is no major difference between TT and FB data from the point of view of $\mathrm{HF}(w)$. However, TT data has a smaller range of $\mathrm{HF}(w)$ values than FB. The same holds for CV, as it was also observed already in (Duchamp-Viret et al., 2005).

7. Discussion and conclusions

We have defined and studied an entropy-based measure of randomness of a counting process $N(w)$, with the aim to its application in analysis of neural spike trains. Up to now, mainly three quantities have been used to measure the rate-independent behavior of spike trains – coefficient of variation, Fano factor and KL distance. As CV measures the variability of ISIs, Fano factor the variability of $N(w)$ and KL distance the randomness of ISIs, the entropy factor is a natural complement to these measures.

We have studied the entropy factor based on assumption that the spike trains correspond to a renewal process, which can be seen as a drawback, as real character of spike trains is probably far more complex. This simplification can be justified by the fact, that neurons has to "read" information relatively quickly – bases on short time intervals, in which the stationarity might be (approximately) satisfied. Nevertheless, it could be useful to study the behavior of HF even for some more realistic models, at least for serially dependent ISIs.

Another issue which should be explored in the future is estimation of the entropy factor. To use HF as a randomness measure for data, it has to be estimable with sufficient reliability. There might be a problem with a bias of its estimate, as there is a known problem of bias in estimation of the entropy (Schurmann, 2004). In Sec. 6, we attempted to reduce this bias by creating a similar bias in the numerator and denominator of definition (17), however, character of the bias and efficiency of this method should be theoretically examined.

We have focused mainly on behavior of the entropy factor in dependence on the length of the observation window w and on the relation of $\mathrm{HF}(w)$ to $\mathrm{FF}(w)$. The theoretical formulas cannot be often expressed in closed forms and analyzed easily. Therefore, we illustrated some selected relationships using numerical calculations for two of the most often used probability distributions of ISIs – gamma and inverse Gaussian. The main results can be summed up using the following points.

- The entropy factor can be larger than one – a Poisson process does not maximize the entropy of $N(w)$ among the renewal processes. It is in contrast with the fact that a Poisson process (exponential distribution) maximizes the differential entropy of ISIs.

- The extremes of entropy factor in dependence on w (for standard values of CV) occur for length of the observation window about several mean ISI, which is length of window that might be used by neurons. Because at these extremes the information about randomness is most significant, this supports the possibility of randomness coding and the importance of randomness evaluation.

- One of the main differences of entropy factor from the Fano factor is the existence of an upper bound. The Fano factor (variance) can reach arbitrary large values, yet the entropy of $N(w)$ with a fixed mean is bounded from above by the entropy of geometric distribution.

- The value of $\mathrm{HF}(w)$ is always in the interval $[0, 2)$. The entropy of a counting process cannot be larger than double the entropy of a Poisson process with the same mean. However, it seems that for a renewal process with properties corresponding to a realistic spike train, the values of the entropy factor cannot be much higher than one.

- Both limits of $\mathrm{HF}(w)$ with respect to w (to 0 and ∞) are one. From the point of view of entropy, a renewal process starts to behave as a Poisson process and ends the same. However, the convergence for $w \to \infty$ is very slow.

- The relation of the entropy factor and the Fano factor is not linear and often not even monotonic.

- For a fixed observation window, there is a maximum of the entropy factor in dependence on CV. For a short observation window, this maximum can be relatively near to the upper boundary (e.g., over 98% of the boundary for $w \leq 5\mu$ and gamma distribution of T).

- Except for large values of CV and low values of w, it seems to be possible to approximate $\mathrm{HF}(w)$ using formula (20).

- Values of the entropy factor and the Fano factor estimated from experimental data confirm that there is not a simple relationship between these two characteristics.

These results imply that behavior of the entropy factor significantly differs from behavior of the Fano factor. According to our expectations, HF reflects a different aspect of the intensity independent character of spike trains (randomness) and thus can be seen as a complement to the standardly used measures. We do not claim that the amount of variability (FF) or randomness (HF) in spike firing carries some information, however, if there is some information expressed by randomness, analysis of Fano factor is not sufficient to detect it (and vice versa).

Acknowledgments

This work was supported by the Institute of Physiology RVO:67985823 and by the Czech Science Foundation project 15-08066S.

References

Avila-Akerberg, O., & Chacron, J. (2011). Nonrenewal spike train statistics: causes and functional consequences on neural coding. *Exp Brain Res*, *210*, 353–371.

Chacron, M. J., Longtin, A., & Maler, R. (2001). Negative interspike interval correlations increase the neuronal capacity for encoding time-dependent stimuli. *J Neurosci*, *21*, 5328–5343.

Cover, T. M., & Thomas, J. A. (2006). *Elements of information theory.* New Jersey: John Wiley & Sons.

Cox, D. R. (1962). *Renewal Theory.* London: Methuen & Co.

Ditlevsen, S., & Lansky, P. (2011). Firing Variability Is Higher than Deduced from the Empirical Coefficient of Variation. *Neural Comput*, *23*, 1944–1966.

Duchamp-Viret, P., Kostal, L., Chaput, M., Lansky, P., & Rospars, J. P. (2005). Patterns of Spontaneous Activity in Single Rat Olfactory Receptor Neurons Are Different in Normally Breathing and Tracheotomized Animals. *Eur J Neurosci*, *10*, 2690–2696.

Eden, U. T. (2010). Drawing inferences from Fano factor calculations. *J Neurosci Meth*, *190*, 149–152.

Evans, R. J. (1998). The entropy of a Poisson-distribution. *SIAM Review*, *30*, 314–315.

Farkhooi, M., Strube-Bloss, M. F., & Nawrot, M. P. (2009). Serial correlation in neural spike trains: Experimental evidence, stochastic modeling, and single neuron variability. *Phys Rev E*, *79*, 021905.

Fisch, K., Schwalger, T., Lindner, B., Herz, A. V. M., & Benda, J. (2012). Channel Noise from Both Slow Adaptation Currents and Fast Currents Is Required to Explain Spike-Response Variability in a Sensory Neuron. *J Neurosci*, *32*, 17332–17344.

Gerstner, W., & Kistler, W. M. (2002). *Spiking Neuron Models.* Cambridge: Cambridge University Press.

Jewell, W. S. (1960). The Properties of Recurrent-Event Processes. *Oper Res*, *8*, 446–472.

Kandel, E., Schwartz, J., & Jessel, T. M. (1991). *Principles of Neural Science.* New York: Elsevier.

Kostal, L., & Lansky, P. (2006). Similarity of interspike interval distributions and information gain. *Biol Cybern*, *94*, 157–167.

Kostal, L., Lansky, P., & Pokora, O. (2011). Variability Measures of Positive Random Variables. *Plos One*, *6*, e21998.

Kostal, L., Lansky, P., & Pokora, O. (2013). Measures of statistical dispersion based on Shannon and Fisher information concepts. *Inform Sciences*, *235*, 214–223.

Kostal, L., Lansky, P., & Rospars, J. P. (2007). Neuronal coding and spiking randomness. *Eur J Neurosci*, *26*, 2693–2701.

Koyama, S., & Kostal, L. (2014). The effect of interspike interval statistics on the information gain under the rate coding hypothesis. *Math Biosci Eng*, *11*, 63–80.

Lansky, P., Sacerdote, L., & Zucca, C. (2016). The Gamma renewal process as an output of the diffusion leaky integrate-and-fire neuronal model. *Biol Cybern*, *110*, 193–200.

Marzen, S. E., DeWeese, M. R., Chaput, M., & Crutchfield, J. P. (2015). Time resolution dependence of information measures for spiking neurons: scaling and universality. *Front Comput Neurosci*, *9*, 105.

McDonnell, M. D., Ikeda, S., & Manton, J. H. (2011). An introductory review of information theory in the context of computational neuroscience. *Biol Cybern*, *105*, 55–70.

Nawrot, M. P., Bouscein, C., Molina, V. R., Riehle, A., Aertsen, A., & Rotter S. (2008). Measurement of variability dynamics in cortical spike trains. *J Neurosci Meth*, *169*, 374–390.

Omi, T., & Shinomoto, S. (2011). Optimizing Time Histograms for Non-Poissonian Spike Trains. *Neural Comput*, *23*, 3125–3144.

Ostojic, S. (2011). Interspike interval distributions of spiking neurons driven by fluctuating inputs. *J Neurophysiol*, *106*, 361–373.

Rajdl, K., & Lansky, P. (2014). Fano Factor Estimation. *Math Biosci Eng*, *11*, 105–123.

Rieke, F., Warland, D., de Ruyter van Steveninck, R., & Bialek, W. (1999). *Spikes: exploring the neural code.* Cambridge: MIT Press.

Schurmann, T. (2004). Bias Analysis in Entropy Estimation. *J Phys A: Math Gen*, *37*, 295–301.

Schwalger, T., Droste, F., & Lindner, B. (2015). Statistical structure of neural spiking under non-Poissonian or other non-white stimulation. *J Comput Neurosci*, *39*, 29–51.

Shannon, C., & Weaver, W. (1998). *The Mathematical Theory of Communication.* Illinois: University of Illinois Press.

Shimokawa, T., Koyama, S., & Shinomoto, S. (2010). A characterization of the time-rescaled gamma process as a model for spike trains. *J Comput Neurosci*, *29*, 183–191.

Stocks, N. G., Nikitin, A. P., McDonnell, M. D., & Morse, R. P. (2009). The role of stochasticity in an information-optimal neural population code. *J Phys Conf Ser*, *197*, 012015.

Strong, S. P., Koberle, R., de Ruyter van Steveninck, R. R., & Bialek, W. (1998). Entropy and Information in Neural Spike Trains. *Phys Rev Lett*, *80*, 197–200.

Watters, N., & Reeke, G. N. (2014). Neuronal Spike Train Entropy Estimation by History Clustering. *Neural Comput*, *26*, 1–33.